

**THE ROLE OF VAGINAL SMOOTH MUSCLE IN THE PATHOGENESIS OF  
PELVIC ORGAN PROLAPSE**

by

Zegbeh Claudel Jallah

B.S., Saint Augustine's College, 2006

Submitted to the Graduate Faculty of  
Swanson School of Engineering in partial fulfillment  
of the requirements for the degree of  
Doctor of Philosophy

University of Pittsburgh

2014

UNIVERSITY OF PITTSBURGH  
SWANSON SCHOOL OF ENGINEERING

This dissertation was presented

by

Zegbeh Claudel Jallah

It was defended on

December 1, 2014

and approved by

James H-C. Wang, Ph.D, Professor, Department of Orthopaedic Surgery

Lance Davidson, Ph.D, Professor, Department of Bioengineering

Anne Robertson, Ph.D, Professor, Department of Mechanical Engineering

Naoki Yoshimura, MD, Ph.D, Professor, School of Medicine (Urology)

Pamela Moalli, MD, Ph.D, Professor, Department of Obstetrics, Gynecology & Reproductive  
Sciences

Dissertation Director: Steven Abramowitch, Ph.D, Assistant Professor, Department of  
Bioengineering

Copyright © by Zegbeh Claudel Jallah

2014

# THE ROLE OF VAGINAL SMOOTH MUSCLE INJURY IN THE PATHOGENESIS OF PELVIC ORGAN PROLAPSE

Zegbeh Claudel Jallah, PhD

University of Pittsburgh, 2014

Pelvic organ prolapse (POP) is a life changing condition affecting over 50% of women aged 50 and older. Women with POP typically suffer from sexual, defecatory and urinary dysfunction, resulting from the descent of their unsupported pelvic organs into the vaginal canal. Over one billion dollars in annual costs are associated with surgery to repair POP. In general, surgical repair strategies merely provide an anatomical repair and fail to address the underlying cause of POP, thus increasing the risk of reoccurrence and complications. Vaginal birth injury (VaBI) has been identified as a major risk factor for POP. As such, the study of VaBI provides an opportunity to better understand how POP develops in order to provide improved remedies. To date, the exact mechanism by which vaginal delivery leads to POP remains elusive, as the time lapse between childbirth and POP symptoms (usually 20-30 years) creates multiple confounders that limit the ability to prove causality. Therefore, the goal of this thesis work was to utilize controlled animal models to assess the impact of VaBI on vaginal smooth muscle (VaSM), as a possible mechanism of VaBI in the pathogenesis of POP. In addition, we wished to examine the impact of current surgical mesh repair on VaSM functional outcomes. Specially, this work 1) investigated the impact of a simulated vaginal birth injury on VaSM 2) characterized the impact of a potential loss of smooth muscle function on vaginal biaxial mechanics, and 3) evaluated the ability of surgical mesh, designed to restore the unsupported organs to their anatomical position, on



VaSM function. Our findings indicate that VaBI can cause non-recoverable loss in vaginal function, and that a loss of function alters vaginal mechanics, with the potential to compromise support of the pelvic organs. Additionally, the results showed that surgically implanted meshes have mechanical and textile properties that further promote a loss of VaSM function. Ultimately, we hope that these findings motivate the need for more measures to prevent VaSM injury during delivery, and serve as a guide for the design of *de novo* meshes aiming to improve VaSM function.

## TABLE OF CONTENTS

<b>TABLE OF CONTENTS .....</b>	<b>vi</b>
<b>PREFACE .....</b>	<b>xiv</b>
<b>NOMENCLATURE .....</b>	<b>xv</b>
<b>1.0 INTRODUCTION .....</b>	<b>1</b>
<b>1.1 PELVIC ORGAN PROLAPSE (POP) .....</b>	<b>2</b>
1.1.1 Symptoms and Incidence .....	2
1.1.2 Treatment Methods .....	4
1.1.3 Risk Factors .....	6
<b>1.2 IMPACT OF VAGINAL DELIVERY ON THE PELVIC FLOOR STRUCTURES .....</b>	<b>8</b>
1.2.1 Pudendal Nerves .....	8
1.2.2 Levator Ani Muscles .....	11
1.2.3 Vaginal Supportive Tissue Complex (VSTC) .....	13
<b>1.3 VAGINAL STRUCTURAL ANATOMY.....</b>	<b>14</b>
1.3.1 Anatomical Layers .....	14
1.3.2 Mechanical Constituents .....	16
1.3.3 Innervations.....	19
<b>1.4 MARKERS OF VAGINAL REMODELING.....</b>	<b>20</b>
1.4.1 Biochemical and Immunohistochemical Markers .....	20
1.4.2 Mechanical Parameters .....	25
1.4.3 Animal Models .....	26
<b>1.5 MOTIVATION AND SPECIFIC AIMS.....</b>	<b>30</b>
1.5.1 Motivation .....	30
1.5.2 Specific Aims .....	32
<b>2.0 VAGINAL DELIVERY WITH INJURY ALTERS VaSM FUNCTION .....</b>	<b>36</b>
<b>2.1 BACKGROUND .....</b>	<b>36</b>
<b>2.2 PROTOCOLS.....</b>	<b>38</b>
2.2.1 Birth Injury Model .....	38
2.2.2 Functional Analysis (Organ Bath).....	39
2.2.3 Histochemical and Immunohistochemical Analysis (Nerve Labeling) .....	41
2.2.4 Morphometric Analysis .....	42
2.2.5 Statistical Analysis .....	43
<b>2.3 RESULTS.....</b>	<b>44</b>

2.3.1	Histological Results .....	44
2.3.2	Functional Results .....	46
2.3.3	Immunohistochemical Results.....	54
2.4	<b>DISCUSSION .....</b>	<b>58</b>
3.0	<b>VaSM FUNCTION INFLUENCES VAGINAL BIAxIAL MECHANICS .....</b>	<b>63</b>
3.1	<b>BACKGROUND .....</b>	<b>63</b>
3.2	<b>PROTOCOL.....</b>	<b>66</b>
3.2.1	Animals.....	66
3.2.2	Biaxial Mechanical Tests .....	66
3.2.3	Collagen, Elastin, and Smooth Muscle Imaging.....	69
3.2.4	Statistical Analysis .....	69
3.3	<b>RESULTS.....</b>	<b>70</b>
3.3.1	Functional Results .....	70
3.3.2	Histological Results .....	74
3.4	<b>DISCUSSION .....</b>	<b>75</b>
4.0	<b>PROLAPSE MESHES NEGATIVELY IMPACT VaSM FUNCTION.....</b>	<b>81</b>
4.1	<b>BACKGROUND .....</b>	<b>81</b>
4.2	<b>PROTOCOLS.....</b>	<b>84</b>
4.2.1	Animals.....	84
4.2.2	Surgical Procedure .....	85
4.2.3	Functional Analysis (Organ Bath).....	86
4.2.4	Histochemical and Immunohistochemical Analysis (Nerve Labeling) .....	88
4.2.5	Morphometric Analysis .....	89
4.2.6	Statistical Analysis .....	90
4.3	<b>RESULTS.....</b>	<b>90</b>
4.3.1	Morphological Results .....	93
4.3.2	Functional Results .....	94
4.3.3	Immunohistochemical Results.....	97
4.4	<b>DISCUSSION .....</b>	<b>103</b>
5.0	<b>AFTERWORD.....</b>	<b>109</b>
5.1	<b>SYNOPSIS .....</b>	<b>109</b>
5.2	<b>IMPLICATIONS .....</b>	<b>113</b>
5.3	<b>LIMITATIONS AND FUTURE DIRECTIONS.....</b>	<b>124</b>
	<b>APPENDIX A .....</b>	<b>128</b>
	<b>APPENDIX B .....</b>	<b>143</b>
	<b>BIBLIOGRAPHY.....</b>	<b>147</b>

## LIST OF TABLES

Table 1. Morphometric Analysis .....	44
Table 2. Maximum Contractile (Emax) Response to KCl and EFS .....	50
Table 3. Half-Maximum Concentration (EC <sub>50</sub> ) for KCl, CCh, and PE .....	52
Table 4. Maximum contractile (Emax) response to CCh and PE .....	53
Table 5. Innervation Density (% Fractional Area) .....	57
Table 6. Biaxial Curves - Parameters.....	72
Table 7. Biaxial Coupling - Parameters .....	73
Table 8. Macaques Demographics .....	91
Table 9. Peripheral Nerve Density (%Fractional Area) .....	99
Table 10. Cholinergic and Adrenergic Nerve Density (%Fractional Area).....	102
Table 11. Data Demonstrating the Baseline Number of Fetuses, Weight, GH, and TVL.....	135
Table 12. Comparison of the Mechanical Properties of the VSTC.....	137

## LIST FIGURES

- Figure 1. Schematic Representation of the Pelvic Organs. The role of the pelvic floor is to support the pelvic organs. Failure to support the pelvic organs can result in pelvic organ prolapse (POP), a condition characterized by the decent of the pelvic organs into the vaginal canal.....3
- Figure 2. Fibromuscular Supportive Structures. The vagina is supported by connective tissues and ligamentous attachments through anchoring to muscle or bony structures. Women with POP exhibit a weakening of these structures, for which synthetic mesh may be surgically implanted, as a means to augment support.....4
- Figure 3. Pelvic Organ Prolapse (POP) Mesh for Pelvic Reconstruction. One of common treatment methods of for POP symptom management involves the placement of a graft, similar to one in this figure, to replace the weakened supportive tissues. The use of native tissues grafts or biologics is associated with high failure rates, while synthetic grafts or meshes which provide more long-term anatomical support are associated with complications including erosion.....5
- Figure 4. Risk Factors of POP. Obesity, a predisposition to connective tissue disorders, family history of POP, increasing parity, and increasing age have been identified as factors predisposing women to developing POP. Of the risk factors, parity is known to have the greatest association with the development of POP.....7
- Figure 5. Innervation of the Pelvic Organs. Innervation of the pelvic organs is provided by the hypogastric, pelvic, and pudendal nerves. The pudendal nerve innervates the striated muscle sphincters of the bladder, vagina, and rectum, while the hypogastric and pelvic nerve provides region-specific innervation to the smooth muscle within these organs. .... 10
- Figure 6. Schematic Representation of the Pelvic Floor Musculature. The levator ani muscles are the major muscle supports for the pelvic organs. They provide support in response to downward forces, and are subjected to large magnitudes of force during parturition..... 11
- Figure 7. Cross Section through the Vagina. Shown are the layers of the vagina, which include the epithelium, subepithelium, muscularis, and the adventitia. .... 16
- Figure 8. Mechanical Constituents of the Vagina. The vaginal layers contain collagen (red), elastin (green dots), and smooth muscle (green lines – actinin striations), which collectively, are the main contributors to the mechanical properties of the vagina. 17

- Figure 9. Thesis Paradigm. The goal of the thesis is to provide insight into the association between VaBI, and the development of POP. The focus of which, is on vaginal smooth muscle as a pathogenic factor of POP. Specially, the goal of this thesis is to 1) investigate the impact of a simulated vaginal birth injury on VaSM 2) characterize the impact of a potential loss of smooth muscle function on vaginal biaxial mechanics, and 3) evaluate the ability of surgical mesh, designed to restore the unsupported organs to their anatomical position, on VaSM function. .... 35
- Figure 10. Histological Results of Vaginal Cross-Sections. (I) Representative outlines of the mid vaginal lumen of hematoxylin - and eosin stained cross sections from control (A), 4 WEEK INJ(B), and 8 WEEK INJ(C) groups. Vaginal injury was associated with an increase in the vaginal lumen, observed in the 4 WEEK INJ group ( $P = 0.007$ ), with minimal recovery in the 8 WEEK INJ group ( $P = 0.041$ ). (II) Evaluation of morphology of the corresponding cross sections from control (A), 4 WEEK INJ (B), and 8 WEEK INJ groups showed gross disorganization in the 4 WEEK INJ group (arrows), and increased fibrosis (short arrows) in the 8 WEEK INJ group. (u = urethra, v = vagina, f = fascia) bar = 100  $\mu$ m ..... 45
- Figure 11. Representative Tracings of EFS and KCl Responses. Recordings of the contractile response of mid-vaginal segments to KCl (120 mM) and EFS (1- 64Hz), in control (A), 4 WEEK INJ (B), and 8 WEEK INJ (C) groups showed increased contraction in the control group, relative to the injured groups, with decreasing contractile magnitude with time post injury. There was also evidence of increased fatigue in the injured group as evidence by the oscillations following KCl administration. .... 47
- Figure 12. Functional Response Curves. Evaluation of the 4 WEEK INJ vs 8 WEEK INJ group showed an increase in EC50 ( $P = 0.001$ ,  $P = 0.069$ ) in response to KCl ( $n=7$ ), a decrease in Emax ( $P = 0.002$ ,  $P = 0.005$ ) in response to CCh ( $n=7$ ), a decline in the EC50 in the distal vagina ( $P = 0.011$ ) in response to PE ( $n=7$ ), and no further decline in EFS response following a decline in the 4 WEEK INJ group ( $P = 0.758$ )..... 48
- Figure 13. Peripheral Nerve Labeling. Evaluation of peripheral innervations (A) in addition to more specific evaluations of the cholinergic (B), and adrenergic innervations (C) of mid-vaginal segments from control 4 WEEK INJ and 8 WEEK INJ middle groups, showed a increased paucity of adrenergic nerve innervations with injury. .... 55
- Figure 14. Schematic Representation of the Stretch-Stress Curves. Loading of the axial (A), and the circumferential (B) direction of the vagina resulted in distinct loading patterns when the muscle was at baseline, contracted, or relaxed. Of note, was the observation that contraction of the muscle resulted in a curve synonymous of a more gradual recruitment of collagen fibers in the axial direction. .... 70
- Figure 15. Axial and Circumferential Tensile Modulus. At the low-stiffness region, the vagina was significantly less stiff in the circumferential direction when smooth muscle was at baseline, contracted, and relaxed ( $P = 0.012$ ,  $P = 0.023$ ,  $P = 0.005$ ). (Panel 2) Smooth muscle contraction was associated with a trend toward a decrease in the tensile modulus in the high-stiffness region of the curve ( $P = 0.10$ )..... 71

- Figure 16. Collagen, Elastin and Smooth Muscle Imaging. Multiphoton imaging revealed resident collagen (red), elastin (green), and smooth muscle (green bundles) within the vaginal muscularis (16-A). These structures are intricately connected, and may function synergistically to regulate collagen recruitment in response to applied loads (16-B). ..... 74
- Figure 17. Collagen, Elastin, and Smooth Muscle Imaging of the Injured Vagina. Multiphoton imaging of 8-weeks after VaBi in the rat revealed less visible smooth muscle (green bundles) within the vaginal muscularis, evidenced by the absence of  $\alpha$ -actinin,( an actin binding protein). ..... 75
- Figure 18. Vaginal Explants. 3 months post implantation explants from Gynemesh™ PS, Restorelle®, UltraPro™ perpendicular and UltraPro™ parallel (A-D). The half closest to the cervix, underlying the mesh was defined as the grafted region, and the lower portion adjacent to the mesh was defined as the non-grafted region. At the mesh-tissue interface of each mesh, there was evidence of host tissue ingrowth, with varying degree of incorporation as a function of mesh-type. Less stiff meshes, UltraPro™ perpendicular and Restorelle®, had better incorporation into the tissue, while the stiffer Gynemesh™ PS appeared buckled and surrounded by a connective tissue capsule (A). ..... 92
- Figure 19. Morphological Results. Representative images showing gross smooth muscle morphology following Massons trichrome staining of cross-sections of (A) sham-operated; (B) Gynemesh PS, (C) Restorelle, (D) Ultrapro™ perpendicular, and (E) UltraPro™ parallel tissue biopsies from the grafted region. Compared to Sham and UltraPro™ perpendicular, implantation with the higher stiffness meshes appeared to have more disorganized smooth muscle fibers. Additionally, following implantation with Gynemesh (B), there was increased thinning of the muscle layer relative to all the other meshes. Scale bar = 250  $\mu$ m. .... 93
- Figure 20. Functional Response (Maximum Response). Muscle mediated contraction significantly declined following implantation with Gynemesh PS, UltraPro™ parallel, and Restorelle® in the grafted region ( $P < 0.001$ ,  $P < 0.001$ ,  $P = 0.015$ ) (A), and UltraPro™ perpendicular was greater than UltraPro parallel ( $P = 0.052$ ) in the non-grafted region (B). Nerve mediated contractions significantly declined following Gynemesh™ PS ( $P = 0.008$ ) implantation in the grafted region (C). Cholinergic receptor mediated contractions significantly also declined following Gynemesh™ PS ( $P = 0.007$ ) in the grafted region (E). ..... 96
- Figure 21. Peripheral Nerve Labeling. (Panel 1) PGP 9.5 immunolabeling (arrows: positive labeling) of cross-sections of tissue explants for the sham group, showed high levels of immunoreactivity (IR), indicative of the maintenance of peripheral nerve fibers following sham operation, localized immediately below the epithelial layer (ep) and within the smooth muscle (sm) bundles. Arrows: nerve fibers. Scale bar = 250  $\mu$ m (Panel 2) correspondingly analysis of the smooth muscle layer following (A) Gynemesh™ PS, (B) Restorelle, (C) Ultrapro™ perpendicular, and (D) UltraPro™ parallel showed decrease innervation density and altered innervation morphology, which was significantly different relative to Restorelle®, and UltraPro™

perpendicular ( $P < 0.001$ ,  $P < 0.001$ ,  $P < 0.001$ ), but not UltraPro™ H ( $P = 0.260$ ).  
Scale bar = 100  $\mu\text{m}$ . ..... 98

Figure 22. Theoretical Framework. VaBI can lead to a degenerative remodeling process, due to changes in the loading environment following the compromise of the active mechanics (smooth muscle) (I). The underlying mechanism, of which is governed by the potential for changes in the active mechanics to alter changes in the passive mechanics (II)..... 118

Figure 23. Load-distension curves. Typical curves generated from mechanically evaluating the VSTC in normal and LOX deficient mice (adapted from Alperin et al.), illustrating the potential of the mechanical tests to characterize differences in tissues resulting from pathologic conditions. Highlighted in the figure are the parameters obtained from each curve including maximum load (A), maximum distension (B), maximum stiffness (slope) (C), the energy absorbed (area under the curve). Also highlighted is the yield point or point of permanent deformation (boxed region) occurring in the tissues of LOX deficient mice at a lower load, as LOX deficient mice exhibit mechanically inferior tissues. .... 133

Figure 24. Schematic of the Average Load-distension Curves. The VSTC from Virgin (A), 4-week postpartum (B), and 8-week postpartum (C) control (solid lines) and injured groups (dotted lines). Distinct differences in the impact of injury on the virgin group vs the PP group can be observed. The curves also show increased stiffening of the VSTC with times PP in the absence of injury, but a lack of the recovery mechanism is observed in the presence of an injury. There was evidence of permanent deformation of the tissue occurring at 31% less load than controls in the 4-week postpartum injured group, and at 22% in the 8-week postpartum. This permanent deformation was appeared to be unique to VSTC in the postpartum group, as this did not occur in the virgin group..... 136

Figure 25. Pelvic Cross-Sections. Masson's trichrome staining of paraffin embedded sections of the rat pelvic showing level I (A), level II (B) and level III (C) support. The vagina supportive tissue-complex (VSTC) in the rat are indeed contiguous with the vagina, and appears to be most dense. .... 139

Figure 26. Maximum Axial (E11) & Circumferential (E22) Strain. Strains in the circumferential direction were, on average, greater than strains in the axial direction. Strains in the axial direction did not appear to be a function of the stress, but a function of circumferential strains. Increased strain in the circumferential direction was associated with decreased strain (or a shortening) in the axial direction (*Poisson* effect). Smooth muscle contraction enables the axial direction to maintain its geometry, thus limiting the *Poisson* effect (observed at .75:1 & .5:1 loading regimens). .... 144

Figure 27. Areal Strain. Areal strain exhibited an increasing trend following smooth muscle contraction, relative to baseline and relaxed conditions. This trend is even more evident during .75:1 and .5:1 loading regimens, where smooth muscle contraction resulted in a greater increase in areal strain, likely due to the increase in the axial



strain (Figure 26). As noted above, the observed increase in strain following smooth muscle contraction is likely associated with increased compliance and likely confers protection from vaginal injury. ....	145
28. Anisotropic Index. Smooth muscle appeared to influence the anisotropic index, as previously noted. There was a trend toward decreased anisotropy with smooth muscle contraction, relative to when smooth muscle was at baseline or when relaxed. This decrease in anisotropy was even more evident when there is increased discrepancy between the magnitudes of the load applied to each axes (evident during .75:1 and .5:1 loading regimens). This finding further supports the theory of smooth muscles role in stress distribution [149]. ....	146

## **PREFACE**

I would like to express my sincere gratitude to the many individuals who have significantly impacted my life throughout this journey. This work would not exist, today, without your support and guidance.

## NOMENCLATURE

AI	anisotropic index
ATFP	arcus tendenius fascia pelvis
AR	alpha adreno-receptor
Ca <sup>2+</sup>	calcium
CCh	(2-[(Aminocarbonyl)oxy]- <i>N,N,N</i> -trimethylethanaminium chloride
ECM	extracellular matrix
EC50	half maximum effective concentration
EFS	electrical field stimulation
EGTA	ethylene glycol-bis(2-aminoethylether)- <i>N,N,N',N'</i> -tetraacetic acid
EMAX	maximum effective response
FDA	Food and Drug Administration (US)
GAGS	glycoaminoglycans
K <sup>+</sup>	potassium
KCl	potassium chloride
NaCl	sodium chloride
MgCl <sub>2</sub>	magnesium chloride hexahydrate
MR	muscarinic receptor
MTM	maximum tensile modulus
KH <sub>2</sub> PO <sub>4</sub>	potassium dihydrogen phosphate
NaHCO <sub>3</sub>	sodium bicarbonate
NANC	non-adrenergic non-cholinergic
NHP	non-human primate
IR	immunoreactive
LOX	lysyl oxidase
LOXL1	lysyl oxidase like-1
MMPs	matrix metalloproteinases
PE	phenylephrine
PFDs	pelvic floor dysfunctions
PGs	proteoglycans
PGP 9.5	protein gene product 9.5
POP	pelvic organ prolapse
POP-Q	pelvic organ prolapse quantification
QOL	quality of life

SM	smooth muscle
SMCs	smooth muscle cells
TH	tyrosine hydroxylase
TNF- $\alpha$	tissue necrosis factor alpha
USL	uterosacral ligament
VaBI	vaginal birth injury
VACHT	vesicular acetylcholine transporter
VD	vaginal delivery
VaSM	vaginal smooth muscle
VSTC	vaginal supportive tissue complex

## **1.0 INTRODUCTION**

This introduction begins with a general overview of a condition known as pelvic organ prolapse (POP), including its symptoms, risk factors, and treatment methods, which conveys the severity and prevalence of this condition. Also highlighted are the limitations associated with current methods for symptom management of POP that has prompted the need for studies aimed at elucidating its etiology in order to develop better treatment options. Following is a discussion of vaginal birth injury (VaBI), shown recently to have the greatest association with the development of POP. Specifically discussed, are the inconclusive associations, to date, of how VaBI promotes long-term degeneration of key pelvic supportive structures. The vagina, which has recently emerged as a key pelvic supportive structure, is therefore introduced, with a description of its anatomy, in addition to arguments supporting the need for studies evaluating how VaBI may affect the vagina, and in turn, pelvic organ support. Further support to these assertions is provided as summaries of experimental methods and evidence of changes in the anatomy, structure and constituents of the vagina, in women with POP, relative to the possible onset of these changes occurring as a result of VaBI. However, to date, very few studies have investigated, if and how, VaBI impairs vaginal smooth muscle (VaSM), as it is a common phenomenon that has the potential to alter vaginal supportive function. Hence, this introduction concludes with the motivation and specific aims of this work, which is to investigate the

impact of VaBI on VaSM, and the ability of current treatment methods (specifically, surgical mesh repair) to aid in reversing those changes.

## **1.1 PELVIC ORGAN PROLAPSE (POP)**

### **1.1.1 Symptoms and Incidence**

Pelvic organ prolapse (POP) is a pelvic floor dysfunction characterized by the protrusion and-or eversion of the pelvic organs (bladder, uterus, and rectum) from their anatomical position, into the vaginal canal (**Figure 1**). Women presenting with POP commonly experience difficulty defecating and urinating, in addition to varying levels of sexual dysfunction based on the anatomical site of the prolapse [1]–[3]. This pelvic floor condition, which is highly associated with decreased quality of life (QOL) and depression, affects millions of women in the United States and worldwide [4], [5]. Up to 50% of women, over age 50 are understood to exhibit some degree of POP, the degree of which, is rated in stages that are defined by the POP Quantification Score (POP-Q Score) [6]. The scoring begins at stage zero, and increases with increasing level of decent of the anterior wall, posterior wall, or the vaginal apex, in relation to the hymen. Approximately 40% of women with POP are asymptomatic and experience minimal progression, but women with POP beyond stage II typically require intervention [7], [8]. As reported by Wu et al., the lifetime risk of a woman undergoing a single operation for POP, by the age of 80 years, is 12.6% [9], [10]. This cohort of woman with symptomatic POP requiring intervention is expected to increase to 56% within the next 40 years due to the rise in the population of elderly

women, which is the fastest growing population segment in the United States [9]. This increase is expected to pose a substantial health and economic burden due to increased hospitalization, a factor which accounts for over 70% of the direct annual, and currently exceeds \$1 billion in the United States [11].

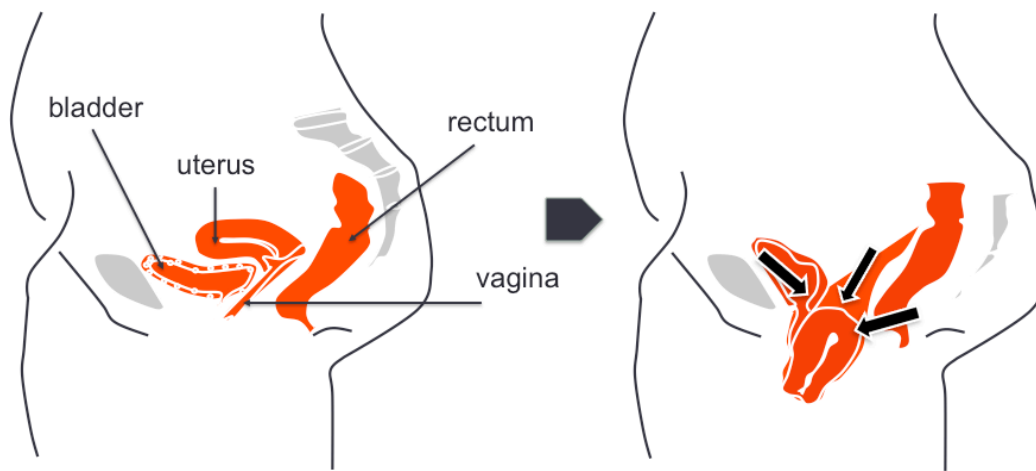


**Figure 1. Schematic Representation of the Pelvic Organs.** The role of the pelvic floor is to support the pelvic organs. Failure to support the pelvic organs can result in pelvic organ prolapse (POP), a condition characterized by the decent of the pelvic organs into the vaginal canal.

### 1.1.2 Treatment Methods

Surgical procedures performed for symptomatic management, generally involve replacement or reinforcement of weakened fibromuscular supports to restore the structural anatomy of the supported pelvic organs, commonly referred to as ligaments (Figure 2).

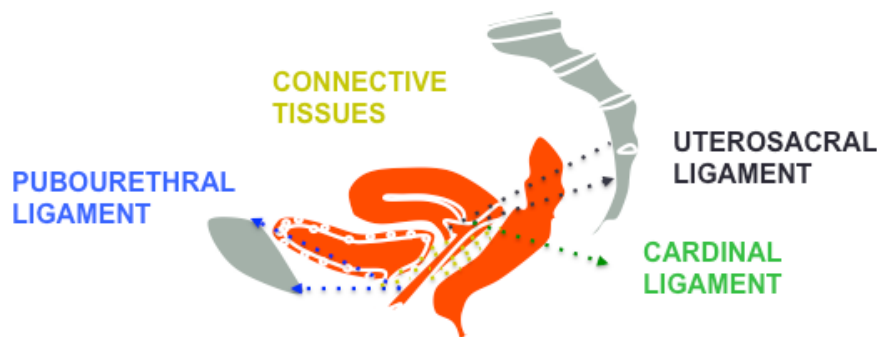


**Figure 2. Fibromuscular Supportive Structures.** The vagina is supported by connective tissues and ligamentous attachments through anchoring to muscle or bony structures. Women with POP exhibit a weakening of these structures, for which synthetic mesh may be surgically implanted, as a means to augment support.

With the focus being anatomical outcomes, non-absorbable synthetic polypropylene mesh use for surgical repair was widely adopted by clinicians because of the long-term anatomical support that it provides to the vagina following failure of its fibromuscular supports [12]. Additionally, with patients presenting with less symptoms during follow-up visits, synthetic mesh use gradually increased relative to other treatment modalities [13].



Synthetic propylene mesh use has continued to be widely used due to the ease of acquisition relative to biologic grafts. In 2010, over 100,000 prolapse surgeries were performed which involved the use of polypropylene mesh, accounting for 30% of cases [14]. With increasing mesh use, the incidence of complications including exposure (**Figure 3**), erosion, rejection, pain, and infection became highly evident, but the etiology of complications eludes many clinicians [15]–[17].

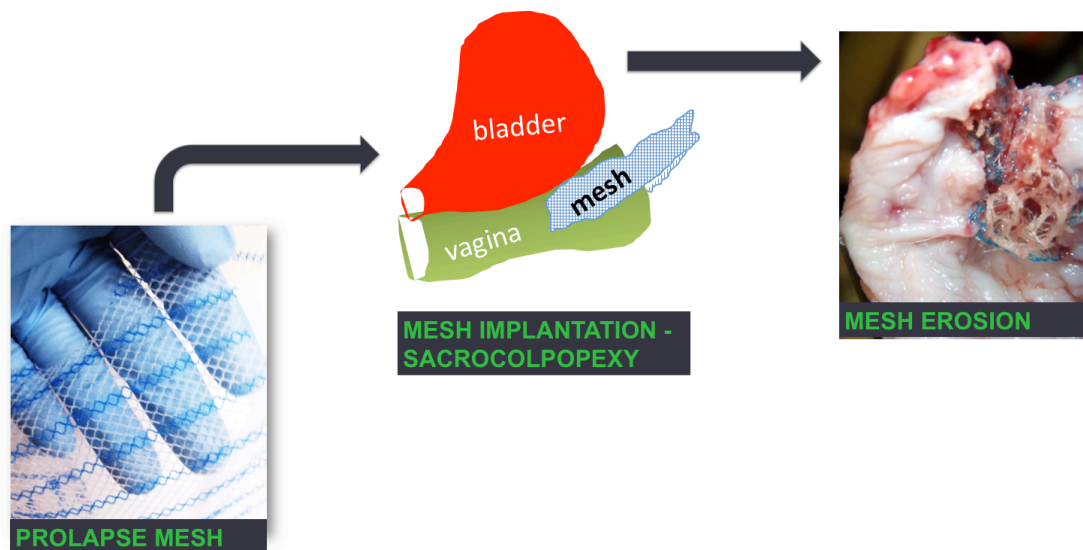


**Figure 3. Pelvic Organ Prolapse (POP) Mesh for Pelvic Reconstruction.** One of common treatment methods of for POP symptom management involves the placement of a graft, similar to one in this figure, to replace the weakened supportive tissues. The use of native tissues grafts or biologics is associated with high failure rates, while synthetic grafts or meshes which provide more long-term anatomical support are associated with complications including erosion.

Possible factors reported to contribute to complications include the host immune response, surgical technique, and mesh properties [18], [19]. Route of surgical procedure can also influence outcomes, with abdominal procedures proving to be associated with less complications relative to transvaginal procedures [17], [20]. However, rigorous pre-market evaluation of these factors only began following a new mandate by the Food and Drug Administration (FDA), as these meshes were previously approved using a 510K process [21], [22]. Longitudinal studies estimate that 30% of surgery for POP will result in failure, which will require a repeat surgery, and that 10 - 25% of surgeries will result in complications with a majority requiring mesh excision [6], [23]–[25]. In order to improve these outcomes and develop improved treatment and preventative strategies, studies aimed at further understanding key pathologic factors of POP are necessary. The development of therapeutics directed toward those factors could potentially obviate the need for surgery and also significantly improve surgical outcomes.

### **1.1.3 Risk Factors**

In an effort to develop preventative and improved treatment strategies for POP, genetics, obesity, age, race, and parity have been identified as important risk factors for the development of POP (**Figure 4**) [26], [27]. Parity, which refers to the number of times a woman has given birth, has been independently shown to have the greatest association with the development of POP [6], [28][29]. In a study evaluating siblings, Buchsbaum et al. reported no indication of prolapse in 82% of nulliparous women, compared to 42.6% of parous women [30]. Subsequent studies have shown that parity capable of increasing one's

risk by over 25%, and doubling with each subsequent delivery. This is not surprising, as vaginal delivery is considered one of the most mechanically taxing events that the pelvic floor undergoes. As the fetus passes through the vaginal canal, which must typically expand to 4 to 5 times its original diameter, this increases the risk of injury to the pelvic supportive structures. More detailed studies show that women undergoing operative vaginal delivery with perineal lacerations are at an even greater risk of developing POP [31]–[33].

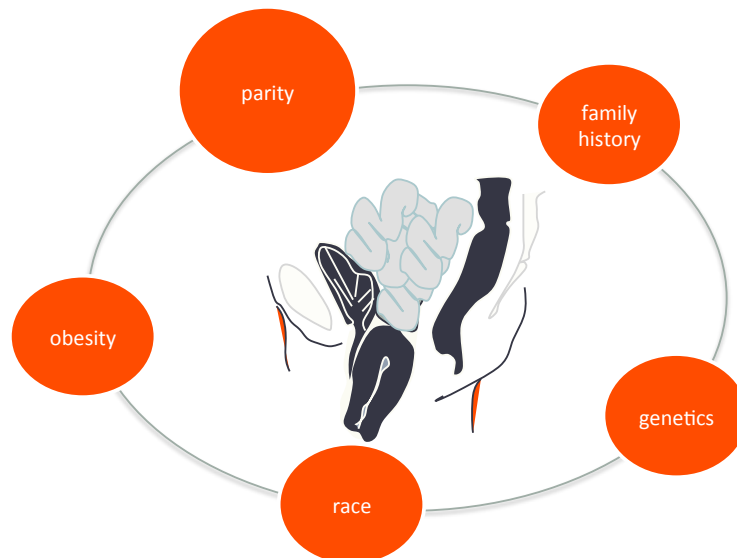


**Figure 4. Risk Factors of POP.** Obesity, a predisposition to connective tissue disorders, family history of POP, increasing parity, and increasing age have been identified as factors predisposing women to developing POP. Of the risk factors, parity is known to have the greatest association with the development of POP.

However, what has been proven to be a major factor for the development of POP is the duration of the second stage of labor, an approximately 90 minute period. This period begins when the fetal head enters the vaginal canal, and ends when it passes the introitus [34], [35]. A prolonged second stage of labor, which results in an extended period of elevated pressure, is usually positively correlated with the use of operative devices used to expedite the process, but their use has also been associated with the development of POP [36], [37]. Interestingly, studies of home labors, which typically exclude the use of operative devices also show an association between a prolonged second stage of labor and the development of POP suggesting that inadequate maternal adaptation to accommodate the passage of the fetus may be the driving the association [38][39]. The resulting extended duration of the fetus in the vaginal canal has been proposed to lead to injury to the nerves, muscles, and connective tissue attachments, which may in turn lead to the development of POP decades later. As discussed below, the impact of vaginal birth injury (VaBI) on these structures has been inconclusive, but nevertheless, essential, as they have provided a foundation for the studies outlined in this work.

## **1.2 IMPACT OF VAGINAL DELIVERY ON THE PELVIC FLOOR STRUCTURES**

### **1.2.1 Pudendal Nerves**

The pudendal nerves supplies most of the anatomic structures responsible for maintaining pelvic support and continence – including the striated muscles in the vagina, perineum, anus, and the levator ani muscles (**Figure 5**). Injury to the pudendal nerves has been

linked to many PFDs including POP[40]–[42]. Rates of nerve injury are known to be increased with forceps delivery, multiparity, longer second-stage labor, third-degree perineal tear, and large fetal size. These findings were supported by a study by Allen et al., who showed pudendal nerve denervation in 80% of women following their first vaginal delivery [32]. In the study, the risk factors also included a prolonged active second stage of labor and heavier babies. Early studies by Snooks et al. reported partially reversible pudendal nerve injury occurring commonly with vaginal birth [43]. Partial reinnervation of surrounding nerves can indeed occur, but muscle function is usually permanently lost. They subsequently showed that partial denervation in some structures do persist and worsens with the passage of time from delivery, suggesting a higher risk of pelvic floor dysfunctions (PFDs) [44]. Clinical studies have corroborated these results, showing denervation, following a prolong second stage of labor, which has been associated with the development of many PFDs, a finding that is not surprising as evidence of neuropathy leading to PFDs has also been shown in women with chronic constipation associated with increased pressure on the pelvic floor [32], [45], [46]. Elective cesarean but not caesarean performed after the onset of labor appears to be protective against denervation, which would suggest that the presence of the fetus in the vaginal canal for an extended period may be inducing the reported nerve compression and transection [47][48]. These studies also suggest that inadequate maternal adaptation during pregnancy may, therefore increase the risk of partial denervation of the supporting pelvic structures. To date, denervation in the key pelvic supportive structures does not appear to be predictive of all cases of POP development. More studies looking at the impact to the hypogastric and pelvic nerves are also warranted, as innervation integrity of the pudendal nerves may be a poor

indicator of the integrity of the hypogastric and pelvic nerves. The impact of VaBI on the pudendal nerves, but not the hypogastric or pelvic nerves that carry autonomic nerves (sympathetic and parasympathetic) innervating the vagina has been more rigorously evaluated due to the ease of in-vivo analysis of striated vs smooth muscle innervation function. It is also likely that a loss of pudendal nerve innervation to the striated muscles, as well as hypogastric and pelvic nerve innervation of the smooth muscle may prove more predictive of the onset of POP. Additionally, due to most studies' use of retrospective data, it remains to be clearly proven whether the changes in innervation are pathogenic factors or the result of POP.

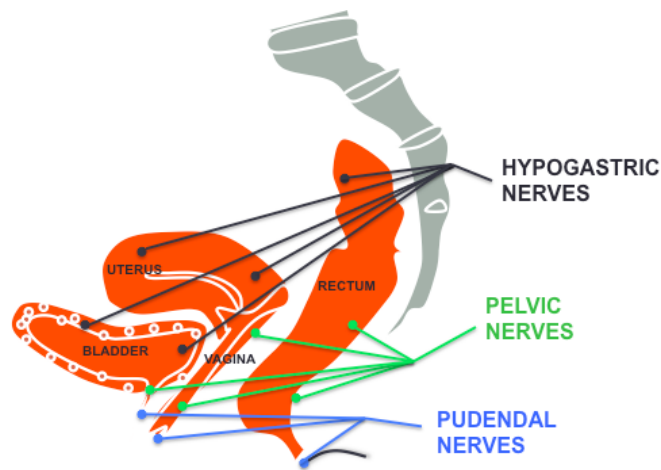


**Figure 5. Innervation of the Pelvic Organs.** Innervation of the pelvic organs is provided by the hypogastric, pelvic, and pudendal nerves. The pudendal nerve innervates the striated muscle sphincters of the bladder, vagina, and rectum, while the hypogastric and pelvic nerve provides region-specific innervation to the smooth muscle within these organs.

### 1.2.2 Levator Ani Muscles

Of the key pelvic supportive structures, the levator ani muscles have received the most focus due to their major role in pelvic organ support, and their high risk of injury during vaginal delivery [18], [33], [49]–[51].

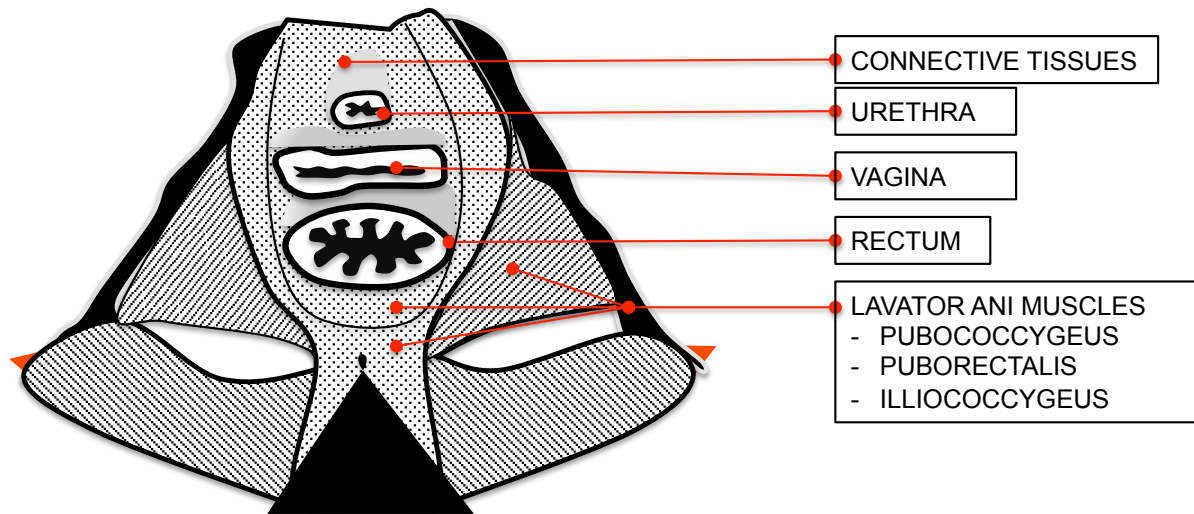


**Figure 6. Schematic Representation of the Pelvic Floor Musculature.** The levator ani muscles are the major muscle supports for the pelvic organs. They provide support in response to downward forces, and are subjected to large magnitudes of force during parturition.

Trauma to the levator ani may include detachment of individual muscle components from their insertion points along the pelvic sidewalls, avulsion, or denervation resulting in generalized atrophy. Peschers' et al. evaluation of levator ani muscle function before and after childbirth showed evidence of muscle strength reduction 3-8 days following vaginal birth, but muscle strength returned to normal values within two months for most women [52]. To determine if impaired levator ani muscle strength was associated with POP, DeLancey et al in a case control study, compared women with prolapse to women with normal pelvic support [53]. Women with prolapse were more likely (55% vs 16%) to have levator ani defects and to generate less force during maximum levator ani contraction. However, Diezt et al. showed no evidence of levator ani avulsion in 76% of women with POP [54]. The authors concluded that while childbirth is associated with POP, it is unclear whether it is due to delivery-related direct levator ani trauma. These findings support the idea that although a levator ani defect is characteristic of some cases of POP, ultimate onset may be a result of a levator ani defect in combination with another phenomenon perhaps occurring during childbirth. This theory is further supported by a more recent study by Berger et al., under the guidance of DeLancey, which showed the capability of levator ani defect (LAD) scores to be predictive of POP occurrence in as many as 70% of women presenting with symptoms, but it not predictive of the stage of POP [55]. The pelvic floor may have some degree of redundancy in its support system, which would allow a partial loss of function in the levator ani muscles to be compensated for by other pelvic supportive structures. VaBI induced levator trauma, in addition to defects in the vagina supportive tissue complex (VSTC), may prove to be more predictive of the eventual eversion and protrusion of the pelvic organs into the vaginal canal.



### 1.2.3 Vaginal Supportive Tissue Complex (VSTC)

However, to date, there has been a paucity of studies evaluating the impact of VaBI on the VSTC (endopelvic fascia (pubocervical and rectovaginal fascia), the cardinal ligaments (CL), uterosacral ligaments (USL), and arcus tendineus fascia pelvis (ATFP)) **(Figure 2)**. These supportive structures have been formerly defined by DeLancey based on level of regional vaginal support [56]. As defined, the uterosacral and cardinal ligaments, which are attached to the apical portion of the vagina, encompasses Level I support. The uterosacral ligament bridges the upper vagina and the sacrum, providing vertical support to the vaginal apex, while the cardinal ligaments attaches the upper vagina to the pelvic sidewalls, providing lateral support. The endopelvic fascia and ATFP, which are attached to the middle vagina, provide level II support. The endopelvic fascia is laterally attached to the vagina and condenses into the ATFP, which is composed of dense connective tissues. The ATFP functions to laterally anchor the endopelvic fascia to the levator ani muscles, which are attached to the pelvic sidewalls. With lateral support provided by the endopelvic fascia and the ATFP, this aids in maintaining the vagina in a suspended position, which in turn allows it to provide anterior support to the bladder and posterior support to the rectum. The endopelvic fascia, which is also attached to the lower one third of the vagina, provides level III support. However, at this level, the rectovaginal fascia, which is fused to the perineal body, inserts at the pelvic sidewall, hence also aiding in vaginal suspension. The uterosacral ligament, which comprises level I or apical support, decreased resilience following vaginal delivery in women, has been associated with apical decent. Site-specific breaks, weakening, and detachment of endopelvic fascia from the ATFP have been well

documented in patients with POP, and are the main restorative targets of pelvic reconstructive surgeries [57]–[60]. However, it remains to be shown how these site-specific defects in the VSTC occur, and if they are indeed a result of VaBI. It has been well established that these structures undergo significant remodeling during pregnancy, to limit injury during delivery [61]–[63]. Evidence of these adaptations suggests that they are essential for a successful delivery, and that prevention of injury to these structures are necessary for full restoration of vaginal support, postpartum. Hence, there is a need to further investigate the impact of VaBI on the vagina, as the vagina is likely subjected to large magnitudes of force, prior to transmission of those forces to the paravaginal attachments. Highly understudied, as shown, the vagina serves as a supportive structure in the pelvic floor. Hence impaired functionality could potentially lead to the development of POP.

### **1.3 VAGINAL STRUCTURAL ANATOMY**

#### **1.3.1 Anatomical Layers**

The vagina is made up of several distinct layers (epithelium, subepithelium, muscularis, and adventitia), which contribute to its ability to serve as a pelvic supportive structure (**Figure 7**). The inner lumen of the vagina is a non-cornified stratified squamous epithelium. This structure is layers of cells deep with an abundance of estrogen receptors which undergo cyclical changes in response to the level of circulating hormones, for example, thinning when estrogen levels are low and thickening when baseline levels are

restored [64], [65]. The thickness of the epithelium also naturally varies, along its length, with increasing thickness from proximal to distal. This results in the presence of longitudinal rugae that run the entire length of the vagina, becoming more prominent at the narrow introitus. Another possible source of the rugae is from underlying connective tissues in the subepithelium, and hence the presence or lack of can serve as an indicator of vaginal structural integrity. This dense connective tissue layer is the major resistance to forces applied to the vaginal wall. As alluded to in the preceding paragraphs, changes along the vertical axis also includes the thickness of the subepithelial layer, which is much thicker in the proximal vagina than it is in the distal vagina. Also embedded within this layer, are nerve plexuses as well as blood vessels. Immediately beneath the subepithelium is the vaginal muscularis, a fibromuscular layer, which contains inner circular and outer longitudinal smooth muscles interspersed with fibrous connective tissue, particularly elastin. Smooth muscle plays an essential role in active vaginal mechanics, and also aids in restoring the vaginal muscularis and the folding rugae. The adventitia, the most external elastic layer of the vagina, is shared with the bladder anteriorly, and the rectum posteriorly. The adventitia consists of smooth muscle bundles interspersed with loose connective tissues, nerves, and blood vessels. Overall, the thickness of these layers and the maintenance of their constituents are essential for maintaining vaginal mechanical integrity, as each layer unique mechanics is essential for vaginal function [66].

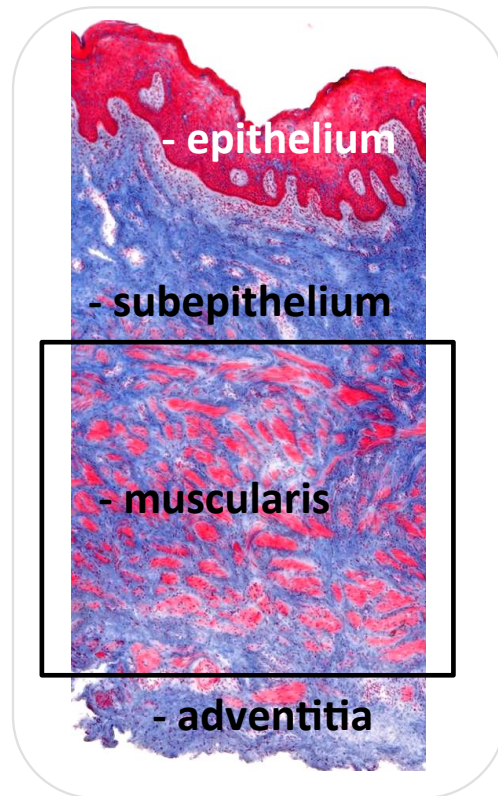


**Figure 7. Cross Section through the Vagina.** Shown are the layers of the vagina, which include the epithelium, subepithelium, muscularis, and the adventitia.

### 1.3.2 Mechanical Constituents

As shown below in **Figure 8**, several constituents (collagen, elastin and smooth muscle) within the respective layers of the vaginal wall contribute to the mechanical integrity of the vagina.

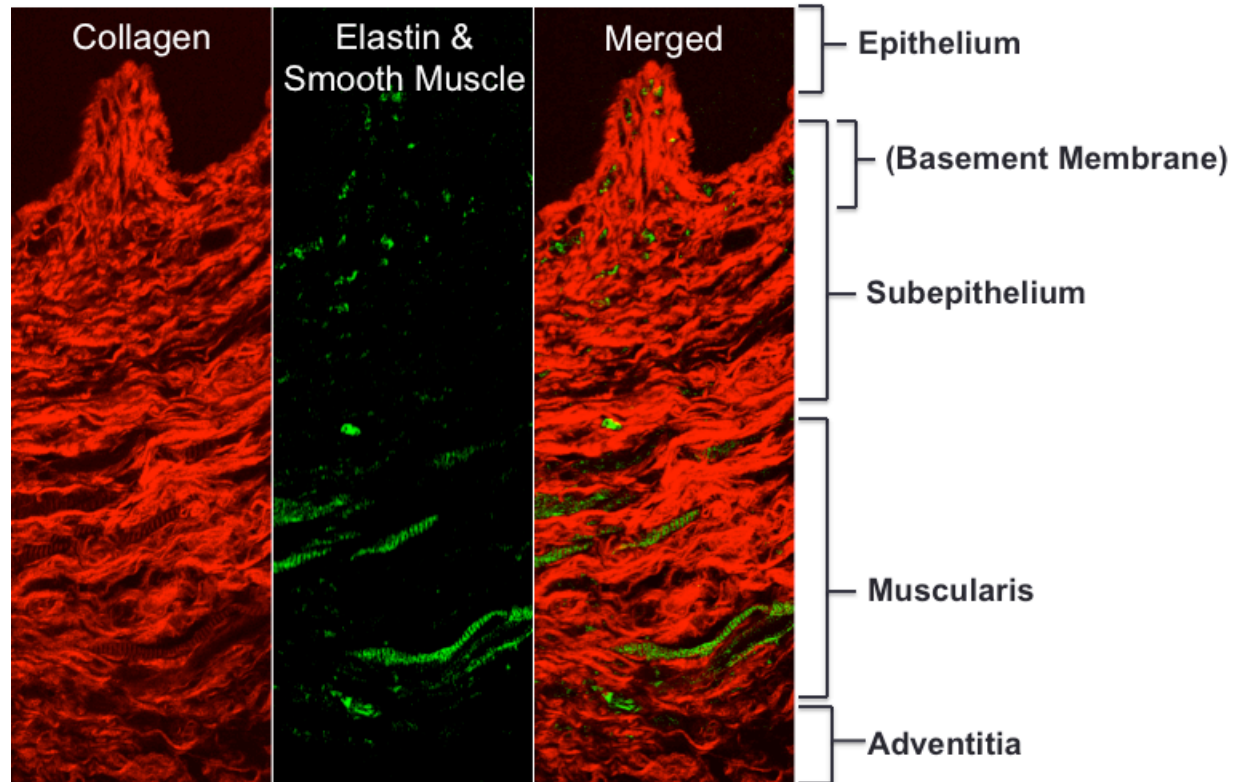


**Figure 8. Mechanical Constituents of the Vagina.** The vaginal layers contain collagen (red), elastin (green dots), and smooth muscle (green lines – actinin striations), which collectively, are the main contributors to the mechanical properties of the vagina.

Collagen provides the tensile strength and its type, ratio, density, and degree of crosslinking are important for the maintenance of the mechanical properties of the extracellular matrix, which is tissue-specific. The vagina is comprised of mostly fibrillar collagens (I: III: V), with a small amount of non-collagenous glycoproteins, elastin, hyaluronan and proteoglycans [67]–[69]. Collagen III is the predominant fibrillar collagen in the vagina, relative to stiffer organs like the aorta, which have a greater ratio of collagen

I:III [67]. The association of collagen I and collagen III with collagen V, is known to result in fibrils with controlled diameters, the level of which is important for the maintenance of the characteristic mechanics of the organ [70]–[72]. As demonstrated by Niyibzi and others, an increase in collagen III and V decreases the mechanical strength of the tissue by decreasing fiber size [73]. The degree of crosslinking of the collagen fibers following secretion into the extracellular space, also influences the mechanical properties of the resulting organ. Another important mechanical component of the vagina is elastin, which affords resiliency through its ability to recoil, returning the collagen fibers to their original configuration post-loading. Similar to collagen, elastin is present in the extracellular space in both an immature and mature form, with maturity and mechanical integrity typically defined by the degree of crosslinking. The length and amount of elastin could also change the mechanics of the vagina, and is associated with changes in the phenotype of smooth muscle, which synthesizes elastin [74], [75]. A loss of vaginal elastin can result in widening of the vaginal opening, which in turn, could alter the loading conditions of the attached connective tissues, and in turn pelvic organ support. The vaginal wall also contains smooth muscles, which provide active mechanics to the vaginal wall, allowing the vagina to rapidly change its diameter via contraction and relaxation, and maintain vaginal tone. The thickness of the inner circular and outer longitudinal smooth muscle layers vary along its length, with the proximal vagina containing denser and thicker muscle structures relative to the distal end, although the functional significance remains uncertain. As mentioned, these components are essential and their alteration are associated with pathologic conditions in many organs including the vagina.

### 1.3.3 Innervations

Embryologically, the vagina originates from the vertical fusion of the ascending sinovaginal bulb and the descending mullerian system, thus exhibiting gross structural and functional differences between the upper two-thirds and the lower one-third. As an example, innervation of the upper two-thirds of the vagina is supplied by autonomic nerve fibers from the inferior hypogastric plexus (utero vaginal plexus) while innervation of the lower one-third is supplied by both autonomic and somatic nerve fibers from the pelvic and pudendal nerve, as illustrated in **Figure 4** [76]. The presence of these nerve plexuses results in a rich supply of parasympathetic and sympathetic nerve innervations to all regions of the vagina, but with the parasympathetic innervation predominant in the upper two-thirds region and the sympathetic innervation dominant in the lower one-third region [40]. Innervation density also differs along the vertical axis, with increasing density from proximal to distal, resulting in low sensitivity at the vault and high sensitivity at the vaginal introitus [77]. These nerves fibers have been detected in the subepithelium, immediately below the muscularis and within thick-walled blood vessels. Intraepithelial varicosities have also been detected in the distal vagina (introitus) [77]. The muscularis region also contains nerve fibers, which innervate the smooth muscle within that layer. Smooth muscle within the upper two-thirds of the vagina is predominantly under parasympathetic and sympathetic control, with the exception of the 1-2 cm region encompassing the distal two-thirds of the vagina, which is partially innervated by somatic nerves, as discussed previously. The somatic innervations control the sphincter like circumferential striated muscle structure surrounding the distal end of the vagina [78]. These muscles are essential

for maintaining vaginal contraction, and have been shown to be essential for reproduction and parturition although as alluded to, they play a major role in maintaining vaginal support. Hence, their dysfunction has been linked to multiple pathologies, which could be due to alternation in their innervation [79]–[81]. As mentioned, VaBI has the potential to alter pudendal nerve innervation, and in turn, vaginal innervations. In addition, these muscles also contain receptors for cholinergic, adrenergic ( $\alpha_1$ ), and non-cholinergic and adrenergic (NANC) neurotransmitters released by the localized nerves, of which changes could also alter muscle function. The level of circulating hormones or changes in the loading environment resulting from changes in age, pregnancy status, and disease may subsequently influence innervation density due to the nervous system's role in organogenesis and tissue remodeling. However, more investigation into the influence of these factors on muscle innervation within the vagina, and its role in the pathogenesis of POP is highly warranted.

## **1.4 MARKERS OF VAGINAL REMODELING**

### **1.4.1 Biochemical and Immunohistochemical Markers**

To date, much effort has been directed towards understanding the remodeling of the major mechanical constituents (collagen and elastin) of the vagina during POP progression, and how their turnover may play a role in the pathogenesis of POP. Since smooth muscle synthesizes both elastin and collagen and maintains the active mechanics of the vagina, smooth muscle and its innervation have also begun to receive attention, albeit limited. If



the causative factors are not fully understood, preventative measures cannot be designed. This also means that despite excellent anatomical restoration following mesh repair for POP, remodeling of these major mechanical constituents may continue to ensue, likely leading to reported complications and mesh failure.

### *Collagen*

Studies investigating changes in vaginal tissue collagen content in women with POP relative to non-POP controls have shown higher collagen type III, a collagen type which is significantly less stiff than the also present, collagen type I [57], [82]. Changes in these ratios can have a significant impact on the resulting mechanics of the vagina, promoting a further loss of vaginal support, as these fibers have varying degrees of stiffness. There has also been evidence of a concomitant increase in the expression of matrix metalloproteinases (MMPS) associated with the proteolysis of these fibrillar collagens (MMP-1 & MMP-13) in the vagina supporting the loss of overall collagen content, which can alter vaginal mechanics [83], [84]. MMPs, which are produced by smooth muscle and fibroblasts, are synthesized intracellularly in their latent form, and then excreted into the extracellular space, where they become activated. Upon activation, MMPs can cleave various elements of the matrix, altering the balance of its composition [85][86]. In an effort to determine if the collagen fibers being synthesized are mechanically similar to those produced by women without POP, studies have attempted to evaluate the expression levels of lysyl oxidases (LOX), the crosslinking family of proteins. Increased crosslinking renders increased stiffness to the collagen fibers following synthesis and excretion into the

extracellular space, a process after which the fiber is referred to as mature. Of the few studies that have evaluated LOX expression in women with POP, the results showed a decline in lysyl oxidase like-1 (LOXL1) expression in women with POP [87], [88]. LOXL1 is associated with the crosslinking of collagen fibers, hence a decline would result in less stiff collagen fibers, however it remains uncertain as to the influence on the resulting vaginal mechanics. It is likely that parity and aging, which are major drivers for the manifestation of POP leads to destabilization of collagen synthesis, crosslinking, and degradation. Even more interesting are findings that this rapid remodeling process following childbirth is subdued in advanced stages of prolapse in post-menopausal women, without the amelioration of symptoms. These changes in collagen content may also be accompanied by changes in other tissue components, however how these factors collectively influences the pathogenesis of POP is unclear.

### *Elastin*

As noted, changes in other tissue components, including elastin expression in the vagina, has provided much insight into the pathogenesis of POP, and has prompted even more questions. Similar to collagen, both immature and mature elastin is found in vaginal tissue, and similar to collagen, mature elastin or crosslinked elastin exhibits increased stiffness relative to the immature or non-crosslinked elastin. In women with POP, both the expression of immature (tropoelastin) and mature elastin is down-regulated in the vagina and adjacent connective tissues [89]–[92]. MMP-9, a known gelatinase which degrades elastin was also unregulated, supporting the idea of a rapid remodeling process

characterized by increase degradation of elastin [69], [93]. Lysyl oxidase like-2 (LOXL2), which aids in the crosslinking of elastin is also known to be down regulated in women with POP, relative to controls, which again may result in inferior vaginal mechanics [87]. Fibulin 5, an extracellular matrix protein known to play a major role in elastin organization, has also been evaluated in women with POP, and the results showed a positive correlation between elastin and Fibulin 5 expression in the ECM [90]. The results also showed a correlation between the stage of prolapse and the degree of Fibulin 5 expression, further supporting their role in the pathogenesis of POP. However, similar to the changes in the expression of collagen, it remains unclear as to why these changes occur, and if they are the cause, or the effect of POP. This is indeed the case as the study showed no difference following vaginal birth or menopause, which as mentioned, are major risk factors of POP. Nevertheless, a more specific risk factor like VaBI may have the potential to increase elastin expression eventually leading to the development of POP, similar to the increased expression during pregnancy. However, a more direct association of these changes to VaBI is warranted.

### *Smooth Muscle*

Recent studies characterizing smooth muscles(SM) in women with POP have shown higher apoptotic rate of smooth muscle cells (SMCs), loss of innervation, as well as an overall disorganization and smaller fractional area of muscle fibers in the vaginal wall [94]–[97]. As confirmed by Northington et al, these histological changes are accompanied by functional changes. These changes can manifest as a loss of innervation to the muscle

bundles, a loss of receptors on the muscles, or a loss of the contractile components (actin fibers) within the muscles [98]. Following these changes, alterations in the forces generated by the muscle bundles can ensue, with the potential to alter tension on connective tissues and ligamentous attachments. This is due to the ability of smooth muscle to dynamically sense and respond to changes in force, as exhibited in other mechanical organs like the bladder, and arteries [80], [99], [100]. However, as expected, in the case of the vagina, these auto regulated muscles can respond to perturbations only after receiving the appropriate stimulation from their parasympathetic (M2,3-cholinergic) and sympathetic ( $\alpha$ 1-adrenergic) innervations. It can then be assumed that in women with POP, the vagina may lack this delicate balance of innervation or tensional stimulation, resulting in a negative remodeling response and the manifestation of POP. However, there has also been a lack of consensus in smooth muscle findings, particularly with regards to whether smooth muscle dysfunction is the cause or the effect of POP. The study by Boreham et al showed no correlation between changes in smooth muscle volume and POP stage of cycle, unlike with elastin and collagen [101]. The authors therefore inferred that these changes in smooth muscle must occur very early and may be influencing changes in elastin and collagen synthesis during POP progression. However, there has been no association to date between the onset of POP changes and any of the risk factors of POP, including VaBI.

### **1.4.2 Mechanical Parameters**

Changes in the above mentioned mechanical constituents have the ability to alter both the structural and mechanical properties of the vagina. This can result from either a loss in the active mechanical properties, the passive mechanical properties, or from both. The passive tissue mechanics, in general, reflect the properties of the acellular matrix components, including elastin and collagen, while active mechanics reflect the properties of smooth muscle. The passive and active mechanical properties hence represent distinct aspects of tissue function; and in order to fully understand remodeling of the vaginal mechanics, it is essential to evaluate both the active and passive mechanical properties. To date, however, studies evaluating changes in vaginal mechanics have predominantly focused on characterizing changes in the passive mechanics of the vagina, as changes in elastin and collagen content were assumed to be the only key pathogenic factors of POP [67], [102]–[104]. Rubod et al, after elongating tissues at varying deformation rates, revealed that the vagina normally exhibits a viscoelastic and a viscoplastic response [102]. The characterization of the mechanical properties of the vagina is essential, as these properties are normalized expression of a specimen's reaction to external forces. Therefore, they are excellent indicators of the bonds and state of the constituents of the tissues, making it an appropriate measure of tissue remodeling. Results from these studies have shown that the vagina of menopausal women with POP is stiffer than tissues from menopausal control women [103]. A very recent study, using tactile imaging, also showed that the vagina is less elastic in women with POP, a finding which could certainly influence the progression of POP, as well as how the vagina responds to surgical augmentation [67]. The increased

stiffness and loss of elasticity has been attributed to a decline in the ratio of collagen I/collagen III, however these changes could be a result of changes in elastin and smooth muscle. As previously stated, the possibility of this phenomenon has not been widely studied in the vagina, but findings from the cardiovascular literature support these assertions. Early studies suggest that a decrease in elastin with a corresponding decrease in smooth muscle, as found to be the case for women with POP, can lead to increased tissue stiffness. This conclusion is based on the intricate interaction between elastin and smooth muscle, and their ability to confer elasticity to resident structures through a delayed recruitment of collagen [105], [106]. However, more research is needed to understand how they are associated to risk factors for POP. Additionally, it needs to be specially determined how VaBI may lead to an alteration in these structures, and subsequently predisposes one to developing POP.

### **1.4.3 Animal Models**

As evidenced, human studies have provided much insight, but limitations associated with tissue acquisition and ethical limitations has left several gaps within our knowledge of the pathogenesis of POP. To improve our understanding, many investigators have experimented with animal models including primates, rodents, and sheep especially for mechanistic studies [107], [108]. Validation for use of these models generally involves investigation of the potential of the model to replicate the pathology as it occurs in humans, similarity of structure and function of the organ (s) involved relative to humans, the size of the organ (s) (which is influenced by the animal size), as well as tolerance to agents being

injected (eg. drugs, cells, etc, if applicable). For POP, the anatomical structures that are of major interest are the pelvic supportive structures, which have been associated with the development of POP. These structures include the levator ani muscles, connective tissue attachments, the vagina, and innervations of these structures. The cost of purchase, housing and surgical intervention can also influence ultimate use of a model, when several models meet the validation criteria for a study.

### *Rodents*

Rodent models (rats and mice), which are widely used for pelvic floor studies, have been reported by Moalli et al. to be an appropriate model for POP, due to analogous pelvic supportive structures to that of humans including the uterosacral ligament which attaches the upper vagina to the spine, at level I [109]. In rodents, the vagina is also supported by the endopelvic fascia and ATRF at level II, and is seen as a dense band of connective tissue extending from the pubic symphysis to the lateral bony pelvis. At level III in the rat, the connective tissue attachments at the distal vagina can also be observed. Observations of major lateral supports including the cardinal ligaments at level I have not been reported in the literature. Also, Moalli et al have also shown that the levator ani muscles, although present in rodents, primarily function to support the tail. Interestingly, these minor discrepancies can be advantageous for studies aiming to investigate the effects of the VSTC independent of the contribution of the levator ani muscles and cardinal ligaments. To date, the rodent model has also been successfully used to evaluate the impact of the effects of various risk factors of POP including simulated birth trauma, and molecular deficiencies on

the mechanical and biomechanical properties of pelvic structures, and their innervation [107][108]. However, the model is not without limitations. The shorter reproductive cycle and gestation period, multiple fetuses, quadrupedal posture, and small size limits its use. Additionally, the significantly shorter lifespan, variable healing response, and the absence of the manifestation of POP in rodents, renders other models more attractive for some studies.

### *Non-Human Primates*

Non-human primates' (NHP) (particularly the Rhesus Macaques and Squirrel Monkeys) similar reproductive cycles and gestation periods to humans, single fetuses, occasional bipedal posture, and large size indeed have made them a more attractive model for pelvic floor studies. Additionally, the primate model has also been shown to contain analogous level I, level II, and III support to that of humans [110]–[114]. At level II in the primate, the levator ani muscles consisting of the iliocaudalis, pubocaudalis, and puborectalis muscles, functions to support the pelvic organs similar to the iliococcygeus, puboccygeus, and puborectalis muscles in humans [112]. The primate model (Rhesus Macaques) has also been shown to contain the cardinal ligament, forming the uterosacral-cardinal ligament complex, a structure not found in rodents [114]. This model is highly preferred, as non-human primates also develop spontaneous prolapse related to childbirth [110]. Hence, this model has been successfully used to evaluate the effects of parity, hormone, and levator ani muscle integrity on the development of POP [107]. The effect of upright posture allows researchers to account for the effect of gravity on the pelvic floor,



making it ideal for studying the effects of strategies to improve pelvic organ support. Of recent, the primate model has also been successfully used for the evaluation of surgical prolapse mesh for pelvic organ support, as reported in this work. The primate model is considered the gold standard for pelvic floor studies, with Rhesus macaques proving more advantageous due to their larger size relative to squirrel monkeys. However the high cost, and inaccessibility of the animals limits widespread use.

### *Sheep*

The sheep (Ewe) model is a more cost-effective alternative to NHP models, as they also develop spontaneous prolapse. The manifestation of prolapse in the sheep is also known to be associated with increased intra abdominal pressure similar to what is clinically observed in humans. However, in contrast to humans, the presentation of symptoms of POP occurs closer to the time of delivery, making its manifestation different [115]. Nevertheless, it is adequate for evaluating changes associated with pregnancy and vaginal delivery independent of hormonal withdrawal that may predispose one to developing POP. Their unique and highly elevated intra-abdominal pressure may also lead to an altered loading environment within the pelvic floor that is absent in women, however, one could propose that the effects of the increased pressure may be negligible, as the supportive structures may be adequately designed to maintain support in the presence of this increased pressure. Additionally, being quadrupeds, the loading of the pelvic floor in the sheep differs from humans although similar pelvic supportive structures to humans, at level I, level II and level III of the vagina, have been observed. To date, the use of the sheep

model for POP is still relatively novel and highly limited relative to other models. However, it has been successfully used to evaluate the impact of parity on the development of POP, and the impact of prolapse mesh implantation for pelvic support [107]. Their limited use may be more a result of the cost-benefit relative to rodents, and the housing requirements needed for large studies.

## **1.5 MOTIVATION AND SPECIFIC AIMS**

### **1.5.1 Motivation**

The extended period of time period between childbirth, or more specifically VaBI, and the manifestation of POP symptoms (usually 20-30 years), makes it rather difficult to draw a direct causal relationship. If birth injury is indeed an inciting factor for developing POP, it must have the potential to induce a mechanically perturbed state in the pelvic floor, to continually induce a remodeling response that will manifest with time. However, to date, there is a paucity of studies that have investigated the potential of vaginal injury during delivery, to incite a degenerative remodeling response. Additionally, during delivery multiple structures can be impacted simultaneously, and as previously alluded to, the pelvic floor is a complex mechanical structure, and an injury impairing one structure, can disrupt the delicate balance of forces, leading to failure of the entire support system over time, making it difficult to determine the exact inciting factor.

The vagina is anchored to pelvic floor musculature to create a bridge of support for the bladder and urethra to sit upon, alteration in mechanical properties could in turn, alter

tension on its ligamentous supports, as well as its ability to support the pelvic organs. Hence, the vagina and its attachments have recently emerged as key supporting structures within the pelvic floor, and have also been identified as structures with a high likelihood of injury during delivery. The vagina and its attachments consist of collagen, elastin and smooth muscle cells (SMCs), work synergistically to maintain vaginal mechanical integrity, including tone and compliance. The literature suggests that changes in the mechanics of the vagina, i.e stiffness and elasticity, as seen with POP, are governed by the reported change in elastin and smooth muscle. However, there is no literature to support the timing of the onset of these changes and how they may be related to known risk factors of POP.

However, our previous characterization of an ideal adaptive remodeling process in rodents, which do not sustain vaginal injuries during delivery due to the small size of the fetal head relative to the vaginal opening, support an injury mechanism. The study results showed major adaptive changes in the active vaginal mechanics (smooth muscles) during pregnancy, but full postpartum recovery, suggesting that this recovery mechanism may be a key factor differentiating women that go on to develop prolapse, and those that do not. We therefore hypothesize that maternal birth injury causes a direct insult to vaginal SMCs, leading to a decline in vaginal tone. The rationale of which, is that the impairment of smooth muscle function (and indirectly elastin) will alter the load seen by the collagen, leading to mechanical stimulation of the resident fibroblasts, in favor of a degenerative remodeling process, perhaps manifesting as prolapse with time and age.

As noted, supporting studies have shown that women with POP have a higher apoptotic rate of SMCs, thus, contributing to a smaller fraction of smooth muscle in their vaginal wall, and a widened genital hiatus. The absence of adequate smooth muscle

support, paralleled with a widened genital hiatus in the vaginal walls of women with POP, further suggests a central role of SMCs in maintaining vaginal integrity. Hence, the goal of this thesis work was to evaluate the impact of VaBI on vaginal smooth muscle (VaSM) function, as this may play a key role in the pathogenesis of POP. More specially, this work i) evaluated the impact of a simulated vaginal injury on VaSM morphology, innervation, contraction, and receptor function ii) characterized the impact of a potential loss of smooth muscle function on vaginal mechanics, and iii) evaluated the ability of current treatment methods for POP to restore VaSM function (**Figure 9**).

### 1.5.2 Specific Aims

*Specific Aim 1: Evaluate the impact of a simulated injury in the rat on vaginal smooth muscle*

Rationale: As noted, VaBI has greatest association with the development of POP, and has been shown to negatively impact several pelvic floor structures. It is likely then that vaginal injury can directly impact the smooth muscle layers, as well as its innervation through the hypogastric and pelvic nerves.

Hypothesis: At 4 weeks post-injury, we expect to see less sensitivity, lower tension, and less force generation of VaSM in response to each of the receptor agonists, or nerve and muscle stimulants. These changes are expected to be evident to a greater degree, at 8 weeks, and would be indicative of degeneration of muscle innervation, contraction, and receptor function.

Significance: This aim provides a framework for the subsequent aims, due to its potential to show if smooth muscle is indeed impacted by birth injury, and if degeneration worsens with time. Evidence of recovery would, however, suggest that smooth muscle may not be an inciting factor and not be orchestrating the lingering effects of injury. This evidence of smooth muscle injury as well as a lack of recovery, but not necessarily evidence of POP is warranted in order to show the potential of VaBI to induce a degenerative remodeling response that may manifest as POP, with time.

*Specific Aim 2: Evaluate the impact of changes in smooth muscle function on vaginal biaxial mechanics*

Rationale: Based on the premise that smooth muscle acts as a dynamic shock absorber, and as a regulator of collagen fiber recruitment, a loss of its function, would lead to an alternation in tissue stiffness.

Hypothesis: Smooth muscle plays a protective role, thus after rendering the vagina passive, we expect to observe an increase in stiffness, and decreased areal strain, resulting from a more abrupt recruitment of collagen fibers.

Significance: Evidence of changes in smooth muscle function on vaginal mechanics would validate its role in inducing vaginal remodeling following injury during

delivery, as resident fibroblasts will be exposed to greater physiologic strains, which has the potential to induce increased production of matrix-degrading proteins and alteration in collagen production. These findings could have major clinical implications for both the evaluation and treatment of prolapse.

*Specific Aim 3: Assess the impact of surgical mesh implantation for POP on vaginal smooth muscle*

Rationale: Surgical mesh implantation for POP symptomatic management is associated with numerous complications including erosion through the vaginal wall. It is highly likely that with the migration of the mesh from the adventitia to the epithelium, the vaginal layers would be impacted, especially the smooth muscle layer.

Hypothesis: Mesh implantation will impair smooth muscle function contraction, innervation, and receptor function.

Significance: With the increased incidence of mesh complications and reoccurrences, if the study shows that smooth muscle is indeed impacted by mesh implantation, then efforts could be directed to redesign these meshes, in order to improve clinical outcomes.

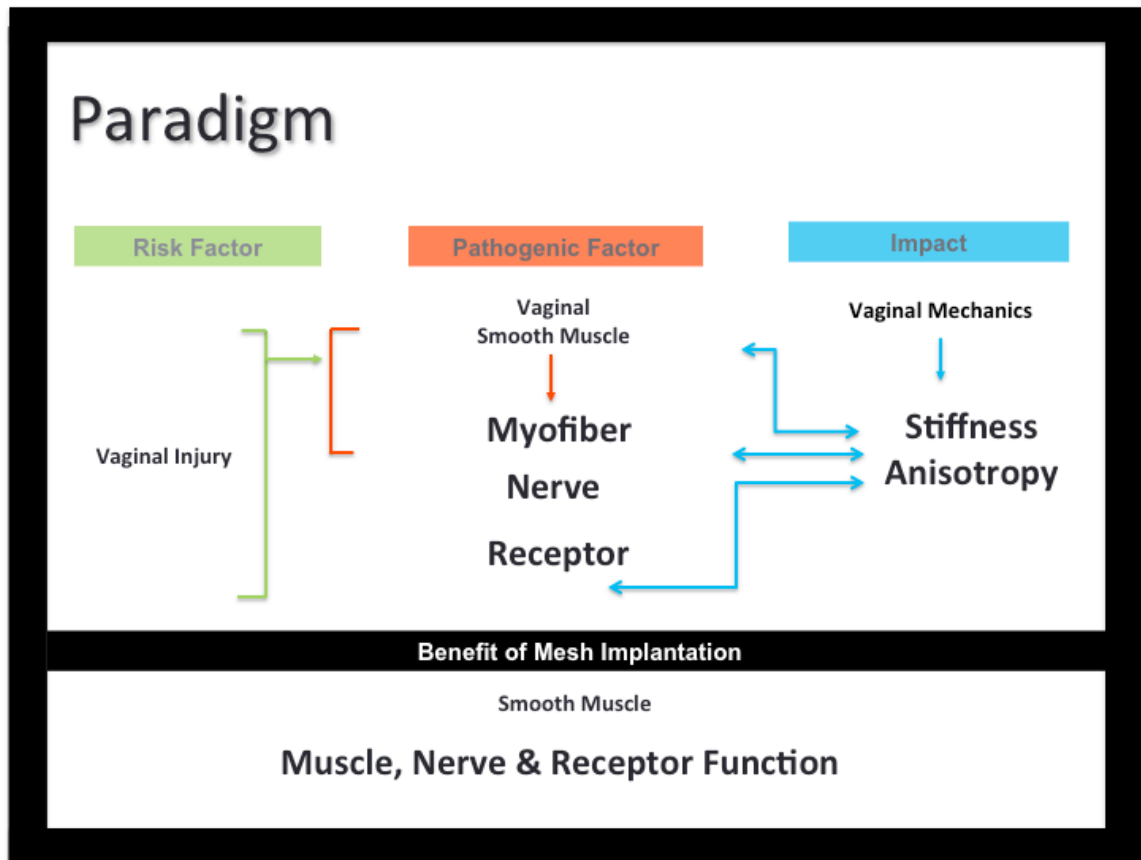


**Figure 9. Thesis Paradigm.** The goal of the thesis is to provide insight into the association between VaBI, and the development of POP. The focus of which, is on vaginal smooth muscle as a pathogenic factor of POP. Specially, the goal of this thesis is to 1) investigate the impact of a simulated vaginal birth injury on VaSM 2) characterize the impact of a potential loss of smooth muscle function on vaginal biaxial mechanics, and 3) evaluate the ability of surgical mesh, designed to restore the unsupported organs to their anatomical position, on VaSM function.

## **2.0 VAGINAL DELIVERY WITH INJURY ALTERS VaSM FUNCTION**

### **2.1 BACKGROUND**

Vaginal delivery is one of the most mechanically taxing events that the pelvic floor undergoes. Hence, the vagina and its supportive connective tissues undergo adaptive remodeling prior to delivery to minimize risk of injury, and to ensure a speedy recovery postpartum. Remodeling mechanisms that allow the tissue to withstand high degrees of deformation without damage and reduce pain include decreased number of cross-linked fibers of elastin and collagen, increase in smooth muscle volume, and a significant decline in local nerve terminals and nociceptors [116], [117]. These changes are usually accompanied by increased interstitial edema, and an increase in tissue water content, promoting tissue compliance and pliability [118]. However, the extent of remodeling varies by individual characteristics, and as such, some women would be more at risk of incurring more severe injuries than others. Approximately 78% of vaginal deliveries are known to be associated with injuries, and in some cases the post-partum recovery is far from ideal [119]. Despite the clear implications of VaBI as a risk factor, the exact mechanism remains elusive as the time lapse between childbirth and the manifestation of POP symptoms (usually 20-30 years) creates multiple confounders that limit the ability to prove causality.



Increased vaginal wall mobility, a condition usually associated with pregnancy, evident in women with POP has recently prompted conclusions that injuries during delivery may prevent the adaptive changes occurring during pregnancy from reverting to pre-pregnancy levels [117], [118]. As the degree of adaptive remodeling to accommodate passage of the fetus is usually indicative of the degree of successful postpartum recovery, our previously published study attempted to characterize an ideal adaptive remodeling process in rodents, as they do not sustain injuries during delivery. The results showed significant changes in the active mechanics (provided by smooth muscle) of the vagina during the course of pregnancy, while significant changes in the passive mechanics (provided by collagen, elastin, glycosaminoglycans, proteoglycans etc.) were observed post partum[22]. Additionally, the results also showed full post partum recovery of the active mechanics, but not the passive mechanics. Taken together, the results suggest an important role of smooth muscle remodeling in maternal adaptations, as well as their need for full recovery post partum. It could then be inferred that smooth muscle adaptive remodeling and full recovery post partum, as is seen in rodents, may be the key factor differentiating women that go on to develop prolapse, and those that do not.

Therefore, the objective of this study was to utilize both pharmacologic and immunohistochemical techniques to functionally and histologically assess the degree of smooth muscle recovery following a simulated vaginal birth injury in the rodent. The rodent model of simulated birth trauma has been widely used for mechanistic studies of stress urinary incontinence (SUI), and replicates many of the characteristics of SUI conditions in women, including impaired urethral smooth muscle function. Following injury, responses of the vaginal tissue strips to KCl and electrical field stimulation (EFS)

will serve as our general indicators of changes to the muscle myofiber and nerve innervations, while responses to agonists of muscarinic- and  $\alpha_1$ -adrenergic receptors, known to be dominant within the vagina, will serve as our indicators of adrenergic or cholinergic receptor changes. Histological analysis will be used to evaluate gross muscle morphology and nerve innervations, offering more rigorous characterization, as functional changes may precede histological changes or vice-versa.

Evidence of a lack of full recovery and a persistent decline in smooth muscle innervation and contraction would begin to illustrate how maternal birth injury, occurring in a subset of women, may potentially limit the ability of smooth muscle to fully recover post partum. More generally, this study has the potential to provide data that can aid in elucidating the association between vaginal delivery and the development of POP, as a loss of vaginal smooth muscle function could compromise vaginal support of the pelvic organs. Ultimately, studies like these could serve as guidelines for the design of more feasible clinical studies needed to equip clinicians with relevant information to develop more preventative treatment measures for POP, and other related pelvic floor dysfunctions.

## **2.2 PROTOCOLS**

### **2.2.1 Birth Injury Model**

3-month old virgin, female rats (Long Evans, 230-280 g, Hilltop Lab Animals, Inc., Scottsdale, PA) were randomly assigned to 4-week injured (n=30), 8-week injured (n=30), and control (n = 30) groups. Following the Institutional Animal Care and Use Committee

(IACUC) guidelines, the rats underwent a simulated birth injury to mimic vaginal distress occurring commonly during a prolonged second stage of delivery. To induce the injury, a 16 Fr catheter was inserted into the vagina of the anesthetized rats, and inflated with 5ccs of water. This volume has been shown previously by our group to induce a grossly observable vaginal laceration [4]. While maintaining the volume, the rats were placed with their pubic symphysis at the edge of the table, and the catheter was then weighted with 130gm, which was allowed to hang freely for 3 hours (**Figure 10**). Rats were housed in a temperature and light-controlled room with free access to food, and at 4-and 8-weeks post-injury the rats were sacrificed.

### **2.2.2 Functional Analysis (Organ Bath)**

Immediately after sacrifice at 4-weeks and 8 weeks post injury, the vagina was excised from each rat, and placed into Krebs'-bicarbonate buffer (in mM/L: NaCl 118, NaHCO<sub>3</sub> 25, KCl 4.7, MgSO<sub>4</sub> 1.2, CaCl<sub>2</sub> 2.5, KH<sub>2</sub>PO<sub>4</sub> 1.2, and D-glucose 11). Approximately 5 x 7 mm circumferential vaginal strips were obtained from the proximal, middle and distal vagina, and suspended between two stationary clips in 20 ml tissue baths containing oxygenated Krebs'-bicarbonate buffer (95% O<sub>2</sub>5% CO<sub>2</sub> at 37°C). Contractile responses were monitored with a pressure transducer (Transbridge 4M, World Precision Instruments), and recordings were obtained, with Chart 5 software on a PowerLab system (sampling at 40 Hz, AD Instruments). Each tissue strip was adjusted to a tension of 0.5 g and allowed to equilibrate for at least 60 min, while changing the buffer solution every 20 min. To evaluate muscle-mediated contractions, the contractile response to increasing

concentrations of KCl (10, 20, 30, 40, 60, 80, and 120 mM) was then measured (n=7). These concentrations were chosen based on results from dose response curves in preliminary experiments, in which we found the greatest change in force between 10-40 mM KCl, with a plateau generally reached by 120 mM KCl. Once the response to a dose of KCl plateaued, the tissue was washed with Krebs solution 3 times (10 minutes for each wash), prior to application of the next KCl dose. Contractile responses were normalized to tissue dry weight and volume, and EC<sub>50</sub> values (the concentration required to produce 50% of the maximal contractile response) were calculated. The tissue exposed to KCl was subsequently used to evaluate nerve mediated contractile response. Electrical field stimulation (EFS) at frequencies of 1-64 Hz, intensity of 20 volts, and duration of 2 seconds (n=6) was applied using a S88, Grass Telefactor stimulator. Tissue samples were washed with Krebs solution 2 times (5 minutes for each wash) between trials. Contractile responses were again recorded, and normalized to tissue dry weight and volume. For analysis of receptor-mediated contractions, the vaginas (n=14) were prepared in the same manner as those used for the KCl/EFS trials. Prior to stimulation with each agonist, the tissue was exposed to 120 mM KCl, which was used for evaluating muscle myofiber integrity and for normalizing for variability in muscle contractility. After the response to the 120mM dose of KCl plateaued, the tissue was washed with Krebs solution 3 times (10 minutes for each wash). Carbachol (n=7), a mixed muscarinic-nicotinic acetylcholine receptor (MR) agonist or phenylephrine (n=7), an  $\alpha_1$ -adrenoceptor (AR) agonist, was then added to the organ bath in increasing concentrations ( $10^{-8}$  to  $10^{-4}$  M); non-cumulatively. After the response to a concentration plateaued, the tissue was washed with Krebs solution 3 times (10 minutes for each wash), prior to the application of the next dose.

### 2.2.3 Histochemical and Immunohistochemical Analysis (Nerve Labeling)

Histological and immunohistochemical assays were also performed on fresh circumferential segments (proximal, middle, and distal), obtained from each rat. Each segment was fixed in 4% paraformaldehyde overnight, and then exposed to graded concentrations of sucrose (cryoprotectant) before embedding into optimal cooling temperature (OCT) medium (Tissue-Tek, Miles Inc., Elkhart, USA). For histochemical analysis of gross morphology, and to measure vaginal perimeter, 10-20  $\mu$ m serial cryostat-sections of the vaginal wall were obtained. The sections were then processed for hematoxylin and eosin staining according to the methods of the Center for Biological Imaging (CBI, University of Pittsburgh). For immunohistochemistry, the 10 $\mu$ m sections were air-dried for 1 hour, permeabilized in .2% Triton X-100 for 10 min, and then incubated for 1.5 hours in 2% Bovine Serum Albumin(BSA). Using the indirect probing method, the sections were first incubated for 1 hour at room temperature, with primary antibody diluted in PBDT (1xPBS, .2% BSA, 2% Donkey Serum (Jackson Laboratories; no. 017-000-00), and .03% Triton) against PGP 9.5 (1:10000; rabbit polyclonal antibody: Accurate Chemical, Westbury, NY YBG78630507), TH (1:1000; rabbit polyclonal antibody: Sigma T8700), and VACHT (1:5000 rabbit monoclonal antibody: Sigma V5387). Following primary incubation, the sections were rinsed with PBS, and incubated for 1 hour at room temperature with Cy3-conjugated f(ab) donkey anti-rabbit IgG (1:100; Jackson Laboratories no. 711 165 152) diluted in PBDT. The sections were again washed in buffer, and mounted in *Fluoro-Gel* medium (EMS, Hatfield, PA 17985-10). In control experiments, no immunofluorescence staining was observed when the primary antiserum was omitted.

#### **2.2.4 Morphometric Analysis**

All images were captured using a Nikon microscope synced to a Nikon color digital camera, before being imported into Elements software (NIS-Elements AR 3.2) for quantification. To measure the length of the vaginal perimeter in the three regions of the vagina, 4x images of hematoxylin and eosin stained cross-sections of the vaginal wall were prepared, and manual tracings of the outlines of the muscularis layer were performed. For comparative analysis of vaginal thickness, measurements were obtained at all four quadrants of the wall, and an average value of the four locations was obtained for each section. All measurements were done by blind estimation in duplicate, resulting in a repeat variability ratio of .01. To evaluate fibers immunoreactive for PGP 9.5, TH, and VACHT in the three regions of the vagina, images were randomly captured at 10x magnification, in all four quadrants of the vagina. For analysis, all images were acquired, and the same threshold was applied. Pixels of binary images whose intensity did not exceed the threshold value were automatically removed and considered negative. The number of profiles per unit area of the vaginal wall for the four locations were measured (fractional area) and averaged for each section. Nerves in all layers of the vaginal wall were quantified, but to prevent bias, attempts were made to exclude vascular innervation. For normalization, the fractional area of VACHT and TH immunoreactive nerves were expressed as a percentage of total nerves (PGP 9.5 immunoreactive nerves).

### 2.2.5 Statistical Analysis

#### *Functional Assays*

Non-linear regression was used to analyze response curves using GraphPad prism 6.0 (GraphPad Software, San Diego, CA). The maximal effect (Emax), and the half-maximal effective concentration values were compared between groups using one-way analysis of variance Students t-test. Results were reported as means  $\pm$  error. Significance was set at  $P < 0.05$ .

#### *Histochemical and Immunohistochemical Assays*

Statistical analysis was performed using SAS statistical software, version 9.2 (SAS Institute Inc.). The mean value  $\pm$  error of all parameter for each of the three vaginal segments was calculated. Differences in nerve type, vaginal wall thickness, and perimeter of the segments, between groups were compared using one-way analysis of variance Students t-test. Significance was set at  $P < 0.05$ .

## 2.3 RESULTS

### 2.3.1 Histological Results

#### *Effects of birth injury on gross tissue morphology*

Evaluation of gross morphological changes showed the greatest difference between groups, in the proximal- and mid-vagina (**Table 1**).

**Table 1. Morphometric Analysis**

	Perimeter (mm)	Thickness (mm)
<b>Proximal</b>		
Control	15.620 ± 0.088	0.307 ± 0.008
4 WEEK INJ	15.437 ± 0.167	0.428 ± 0.013 <sup>a*</sup>
8 WEEK INJ	16.170 ± 0.146	0.376 ± 0.010 <sup>a*</sup>
<b>Middle</b>		
Control	18.198 ± 0.336	0.309 ± 0.009
4 WEEK INJ	22.201 ± 0.309 <sup>a*</sup>	0.325 ± 0.005
8 WEEK INJ	21.067 ± 0.394 <sup>a*</sup>	0.343 ± 0.009
<b>Distal</b>		
Control	16.570 ± 0.259	0.551 ± 0.014
4 WEEK INJ	18.906 ± 0.390	0.632 ± 0.016
8 WEEK INJ	17.373 ± 0.235	0.601 ± 0.012

*Values presented as Mean ± SEM ( n = 6, per group) \*indicates significant at P< .05 <sup>a</sup> relative to control <sup>b</sup> relative to 4 WEEK INJ*



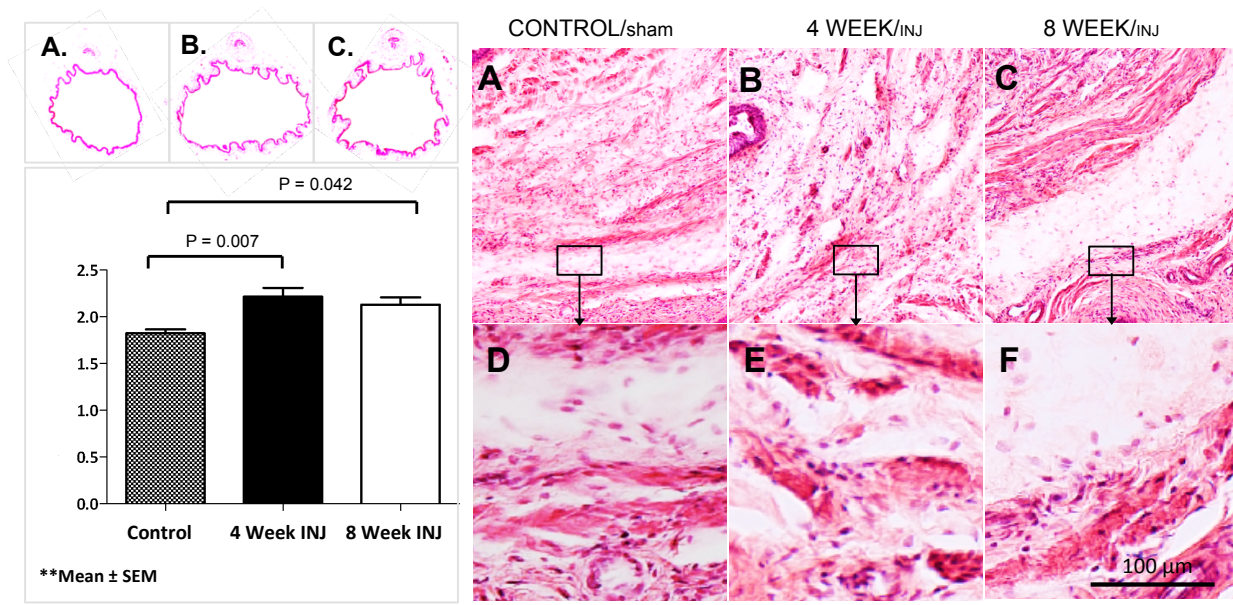


**Figure 10. Histological Results of Vaginal Cross-Sections.** (I) Representative outlines of the mid vaginal lumen of hematoxylinF and eosinF stained cross sections from control (A), 4 WEEK INJ (B), and 8 WEEK INJ (C) groups. Vaginal injury was associated with an increase in the vaginal lumen, observed in the 4 WEEK INJ group ( $P = 0.007$ ), with minimal recovery in the 8 WEEK INJ group ( $P = 0.041$ ). (II) Evaluation of morphology of the corresponding crossF sections from control (A), 4 WEEK INJ (B), and 8 WEEK INJ groups showed gross disorganization in the 4 WEEK INJ group (arrows), and increased fibrosis (arrows) in the 8 WEEK INJ group. (u = urethra, v = vagina, f = fascia) bar = 100  $\mu$ m

In the proximal vagina the thickness of the vaginal wall significantly increased from  $0.307 \pm 0.024$  mm to  $0.428 \pm 0.034$  mm ( $P = 0.010$ ) by 4 weeks post-injury, and at 8 weeks post injury the thickness had only marginally recovered relative to controls ( $0.376 \pm 0.025$  mm,  $P < 0.062$ ). In the mid vagina, the vaginal lumen increased from  $18.198 \pm 0.824$  mm to

22.201  $\pm$  1.011 mm at 4 weeks post injury, as illustrated by the representative outlines **(Figure 10 - Panel 1)**, corresponding to a 22.2% increase ( $P = 0.007$ ). Subsequent evaluation at 8 weeks also showed that the perimeter of the lumen had not fully recovered relative to controls ( $P < 0.042$ ). Hemotoxylin and Eosin staining performed to histologically assess the impact of these morphometric changes on gross tissue structure, showed at 4 weeks post injury, disorganization of connective tissues and smooth muscle bundles, most extensively in the mid vagina **(Figure 10)**. At 8 weeks post injury, there was less disorganization, but with increasing fibrosis **(Figure 10)**. Also at 8 weeks post injury, the location along the vagina where gross laceration had occurred did not recover, as there was less dense connectives tissues and muscles bundles relative to adjacent locations.

### 2.3.2 Functional Results

#### *Effect of VaBI on Musclegenic Contractions*

Our functional analysis began with the evaluation of myofiber function, as measured by the force generated following KCl-induced contractions ( $n = 7$ , per group) **(Figure 11)**.

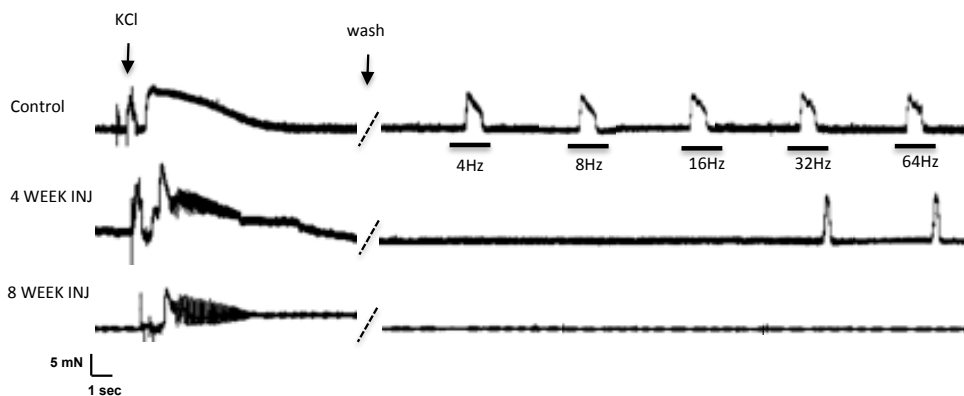


**Figure 11. Representative Tracings of EFS and KCl Responses.** Recordings of the contractile response of mid-vaginal segments to KCl (120 mM) and EFS (1- 64Hz), in control (A), 4 WEEK INJ (B), and 8 WEEK INJ (C) groups showed increased contraction in the control group, relative to the injured groups, with decreasing contractile magnitude with time post injury. There was also evidence of increased fatigue in the injured group as evidence by the oscillations following KCl administration.

The response curves showed concentration dependent contractions that were significantly different between the groups in the proximal and mid-vagina (**Figure 12**). In the proximal vagina, at 4 weeks,  $E_{max}$  was similar to controls but the  $EC_{50}$  had decreased in the proximal vagina relative to controls ( $P = 0.168$ ,  $P = 0.007$ ) (**Table 2**, **Table 3**). At 8-weeks the contractile force generated had become significantly higher, as evidence by an increase in  $E_{max}$  from  $1.198 \pm 0.213$  mN to  $2.618 \pm 0.824$  mN ( $P = 0.006$ ), with a persistent decrease in  $EC_{50}$  from  $-2.359 \pm 0.059$  M to  $-2.860 \pm 0.056$  M ( $P < 0.001$ ). In the middle vagina, at 4 weeks, the  $E_{max}$  also had not increased ( $P < 0.540$ ), but the  $EC_{50}$  had decreased from  $-2.45 \pm 0.048$  M to  $-2.59 \pm 0.056$  M ( $P = 0.056$ ). Subsequent evaluations at 8 weeks post injury

showed that the  $E_{max}$  had not increased ( $P < 0.540$ ), but the  $EC_{50}$  persistently declined  $-2.75 \pm 0.053$  M ( $P = 0.003$ ). Similar to the histological analysis, no differences were observed in the distal vagina. To determine if the effects varied with time post injury, comparisons between the 4- and 8-week groups were performed. The results showed no changes in  $E_{max}$ , but there was a significant increase in  $EC_{50}$  between the 4 and 8-week groups in the proximal and middle vagina ( $P = 0.001$ ,  $P = 0.069$ ), indicating a persistent increase in muscle hypersensitivity.

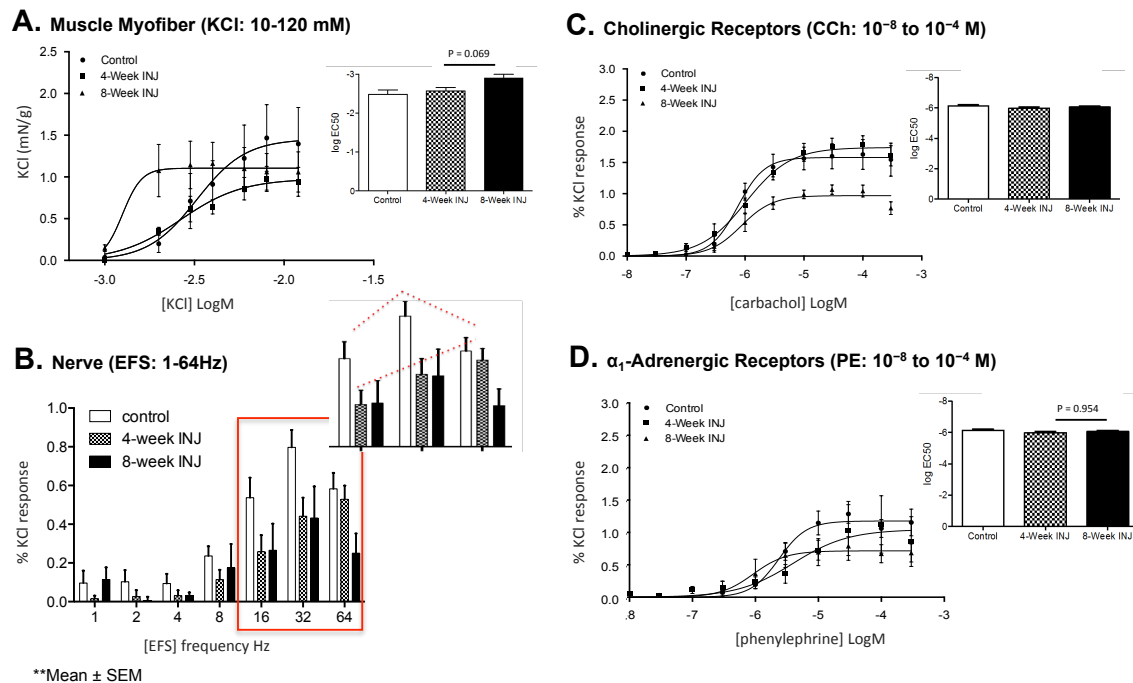


**Figure 12. Functional Response Curves.** Evaluation of the 4 WEEK INJ vs 8 WEEK INJ group showed an increase in  $EC_{50}$  ( $P = 0.001$ ,  $P = 0.069$ ) in response to KCl ( $n=7$ ), a decrease in  $E_{max}$  ( $P = 0.002$ ,  $P = 0.005$ ) in response to CCh ( $n=7$ ), a decline in the  $EC_{50}$  in the distal vagina ( $P = 0.011$ ) in response to PE ( $n=7$ ), and no further decline in EFS response following a decline in the 4 WEEK INJ group ( $P = 0.758$ ).

### *Effect of VaBI on Neurogenic Contractions*

To evaluate nerve function, the force generated following EFS-induced contractions were measured, as shown in Figure 1 ( $n = 7$ , per group). The response curves showed frequency dependent contractions that were significantly different between the groups in the proximal, mid- and distal vagina (**Figure 12**). In the proximal vagina, at 4 weeks post injury,  $E_{\max}$  was similar to control ( $P = 0.868$ ), but had declined at 8 weeks to  $0.471 \pm 0.381$  mN from  $0.804 \pm 0.241$  mN, albeit non-significantly ( $P = 0.085$ ) (**Table 2, Table 3**). In the mid-vagina, at 4 weeks there was significant decline in  $E_{\max}$  from  $0.822 \pm 0.204$  mN to  $0.533 \pm 0.180$  ( $P = 0.026$ ). Subsequently evaluation at 8 weeks showed a persistent decline ( $0.476 \pm 0.415$ ) mN but was variable, thus making differences undetectable ( $P = 0.091$ ). In the distal vagina, at 4 weeks post injury there was no decline in  $E_{\max}$  ( $P = 0.971$ ), but evaluations at 8 weeks post injury showed a persistent decline in  $E_{\max}$  from  $0.610 \pm 0.100$  mN to  $0.278 \pm 0.034$  mN ( $P = 0.023$ ). A more specific look at the  $E_{\max}$ , at 64 Hz, showed significant declines in the proximal, middle and distal vagina at 8 weeks relative to controls ( $P = 0.020$ ,  $P = 0.024$ ,  $P = 0.012$ ), indicating a persistent loss in nerve function. To again determine if the effect varied with time post injury, comparisons between the 4- and 8-week groups were performed. The results showed evidence of a decreasing trend in  $E_{\max}$  in the proximal and distal vagina ( $P = 0.034$ ,  $P = 0.032$ ), indicating a persistent loss of nerve function.

**Table 2. Maximum Contractile (E<sub>max</sub>) Response to KCl and EFS**

	KCl - E <sub>max</sub> (mN/mm <sup>3</sup> )	EFS - E <sub>max</sub> (% KCl)
<b>Proximal</b>		
Control	1.198 ± 0.079	0.804 ± 0.035
4 WEEK INJ	2.122 ± 0.224	0.824 ± 0.032
8 WEEK INJ	2.831 ± 0.200 <sup>b*</sup>	0.374 ± 0.043 <sup>ab*</sup>
<b>Middle</b>		
Control	1.537 ± 0.149	0.901 ± 0.054
4 WEEK INJ	1.033 ± 0.064	0.534 ± 0.030 <sup>a*</sup>
8 WEEK INJ	1.340 ± 0.091	0.246 ± 0.023 <sup>ab*</sup>
<b>Distal</b>		
Control	1.339 ± 0.084	0.610 ± 0.051
4 WEEK INJ	1.451 ± 0.133	0.489 ± 0.029
8 WEEK INJ	0.988 ± 0.076	0.278 ± 0.015 <sup>ab*</sup>

*E<sub>max</sub> determined from non-linear regression of the concentration-response curves - values presented as Mean ± SEM (n = 7)*  
*\*significant at P < .05 <sup>a</sup> relative to control <sup>b</sup> relative to 4 WEEK INJ*  
*abbreviations: KCl: Potassium Chloride, EFS: Electrical Field Stimul*

#### *Effect of VaBI on Muscarinic Receptor Mediated Contractions*

To evaluate muscarinic receptor function, the force generated following carbachol-induced contractions were measured (*n* = 7, per group). The response curves showed dose dependent contractions that were significantly different between the groups in the proximal, and distal vagina (**Figure 12**). In the proximal vagina, at 4 weeks post injury, E<sub>max</sub> decreased from 2.450 ± 0.390 mN to 1.443 ± 0.280 mN (*P* = 0.0193), but the EC<sub>50</sub> had was similar to control (*P* = 0.687) (**Table 3, Table 4**). Evaluation of the 8-week group showed that the E<sub>max</sub> had further decreased to 1.026 ± 0.023 mN (*P* = 0.010), but the EC<sub>50</sub> was still

similar to control ( $P = 0.869$ ). At 4 weeks post injury,  $E_{\max}$  in the proximal vagina had decreased from  $2.450 \pm 0.390$  mN to  $1.443 \pm 0.280$  mN ( $P = 0.019$ ), but the  $EC_{50}$  was similar to control ( $P = 0.687$ ). In the middle vagina, at 4 weeks post injury, the  $E_{\max}$  was similar ( $P = 0.331$ ) and the  $EC_{50}$  was also similar controls ( $P = 0.240$ ) and at 8 week  $E_{\max}$  had further declined, but did not reach significance ( $P = 0.060$ ) and neither did the  $E_{50}$  ( $P = 0.682$ ). In the distal vagina, at 4 weeks post injury,  $E_{\max}$  had also decreased from  $1.611 \pm 0.353$  to  $0.814 \pm 0.196$  % ( $P = 0.032$ ) but the  $EC_{50}$  had not decreased ( $P = 0.962$ ), and evaluation of the 8-week group showed a persistent decline in  $E_{\max}$  ( $0.788 \pm 0.181$  mN,  $P = 0.037$ ), but again there was no difference in the  $EC_{50}$  ( $P = 0.846$ ). Comparison of the 4-week vs 8-week group showed evidence of a decreasing trend in  $E_{\max}$  in the proximal and middle vagina ( $P = 0.002$ ,  $P = 0.005$ ), but with no corresponding change in  $EC_{50}$  ( $P = 0.772$ ,  $P = 0.804$ ), indicating a persistent decline in receptor density, but not in receptor sensitivity.

**Table 3. Half-Maximum Concentration (EC<sub>50</sub>) for KCl, CCh, and PE**

	KCl- pEC <sub>50</sub> (M)	CCh- pEC <sub>50</sub> (M)	PE- pEC <sub>50</sub> (M)
<b>Proximal</b>			
Control (n = 7)	-2.359 ± 0.019	-6.146 ± 0.021	-3.132 ± 0.275
4 WEEK INJ (n = 7)	-2.595 ± 0.019 <sup>a*</sup>	-6.078 ± 0.051	-4.523 ± 0.234
8 WEEK INJ (n = 7)	-2.860 ± 0.013 <sup>ab*</sup>	-6.155 ± 0.079	-3.616 ± 0.380
<b>Middle</b>			
Control (n = 7)	-2.454 ± 0.015	-6.089 ± 0.041	-1.765 ± 0.143
4 WEEK INJ (n = 7)	-2.595 ± 0.059 <sup>a*</sup>	-6.084 ± 0.047	-5.972 ± 0.119 <sup>a*</sup>
8 WEEK INJ (n = 7)	-2.756 ± 0.051 <sup>ab*</sup>	-6.033 ± 0.055	-5.949 ± 0.109 <sup>a*</sup>
<b>Distal</b>			
Control (n = 7)	-2.550 ± 0.030	-6.090 ± 0.036	-3.060 ± 0.460
4 WEEK INJ (n=7)	-2.515 ± 0.026	-5.969 ± 0.066	-6.034 ± 0.017 <sup>a*</sup>
8 WEEK INJ (n=7)	-2.536 ± 0.013	-6.011 ± 0.104	-6.342 ± 0.052 <sup>ab*</sup>

*EC<sub>50</sub> determined from non-linear regression of the concentration-response curves - values presented as Mean ± SEM (n = 7) \*indicates significant at P < .05 <sup>a</sup> relative to control <sup>b</sup> relative to 4 WEEK INJ - abbreviations: KCl: Potassium Chloride, CCh: Carbachol, PE: Phenylephrine Note: No sensitivity measure was obtained for EFS*

#### *Effect of VaBI on Adrenergic Receptor Mediated Contractions*

To evaluate  $\alpha_1$ -adrenergic receptor function, the force generated following phenylephrine-induced contractions was measured (n = 7, per group). The response curves showed dose dependent contractions that were significantly different between the groups in the middle, and distal vagina (**Figure 12**). In the middle vagina, at 4 weeks post injury, E<sub>max</sub> and EC<sub>50</sub> were similar to controls (P = 0.187, P = 0.609), but evaluation of the 8-week



group showed that the  $E_{\max}$  had decreased from  $1.366 \pm 0.190$  to  $0.825 \pm 0.420$  % ( $P = 0.030$ ), but there was no difference in the  $EC_{50}$  ( $P = 0.183$ ) (**Table 3, Table 4**). In the distal vagina, at 4 weeks post injury, the  $E_{\max}$  was similar to controls but the  $EC_{50}$  decreased relative to controls ( $P = 0.281$ ,  $P = 0.025$ ), and evaluation at 8 weeks showed similar trends ( $P = 0.229$ ,  $P = 0.025$ ). Comparison of the 4-week vs 8-week group showed evidence of a decreasing trend in  $E_{\max}$ , but significant declines were only evident in the  $EC_{50}$  in the distal vagina ( $P = 0.011$ ), indicating a persistent increase in receptor hypersensitivity.

**Table 4. Maximum contractile ( $E_{\max}$ ) response to CCh and PE**

	CCh - $E_{\max}$ (% KCl)	PE - $E_{\max}$ (% KCl)
<b>Proximal</b>		
Control	$2.450 \pm 0.147$	$0.753 \pm 0.044$
4 WEEK INJ	$1.470 \pm 0.036^{a*}$	$0.442 \pm 0.087$
8 WEEK INJ	$1.026 \pm 0.093^{ab*}$	$0.320 \pm 0.073^{a*}$
<b>Middle</b>		
Control	$1.706 \pm 0.080$	$0.777 \pm 0.026$
4 WEEK INJ	$1.805 \pm 0.045$	$0.896 \pm 0.065$
8 WEEK INJ	$1.107 \pm 0.026^{ab*}$	$0.825 \pm 0.070$
<b>Distal</b>		
Control	$1.611 \pm 0.113$	$0.967 \pm 0.031$
4 WEEK INJ	$0.851 \pm 0.063^{a*}$	$1.637 \pm 0.075^{a*}$
8 WEEK INJ	$0.788 \pm 0.073^{a*}$	$2.053 \pm 0.217^{a*}$

*$E_{\max}$  determined from non-linear regression of the concentration-response curves - values presented as Mean  $\pm$  SEM ( $n = 7$ )  
<sup>a</sup>indicates significant at  $P < .05$  <sup>a</sup> relative to control <sup>b</sup> relative to 4 WEEK INJ abbreviations: CCh: Carbachol PPE: Phenylephrine*

### 2.3.3 Immunohistochemical Results

#### *Effect of VaBI on Peripheral Nerve Density*

PGP 9.5, an enolase expressed in peripheral nerves, was used as a pan neuronal marker ( $n = 5$ , per group). Following labeling and quantification of the percent fractional area of PGP-IR nerves, there were significant differences in the middle and the distal vagina (**Figure 13, Table 5**). In the middle vagina, at 4 weeks post injury, the percent fractional area of PGP-IR nerves had decreased relative to controls ( $0.922 \pm 0.153$  to  $0.438 \pm 0.056$  %,  $P = 0.026$ ), and evaluation of the 8-week group showed a further decline to  $0.300 \pm 0.030$  ( $P = 0.006$ ). In the distal vagina, at 4 weeks post injury, the percent fractional area had also declined relative to controls ( $0.428 \pm 0.028$  to  $0.256 \pm 0.047$  %,  $P = 0.018$ ), and evaluation of the 8-week group showed that the innervation density had not recovered ( $0.206 \pm 0.036$ ,  $P < 0.001$ ). Comparison of the 4-week vs 8-week group showed evidence of a decreasing trend, but no significant difference in the percent fractional area in the middle and distal vagina ( $P = 0.090$ ,  $P = 0.406$ ).

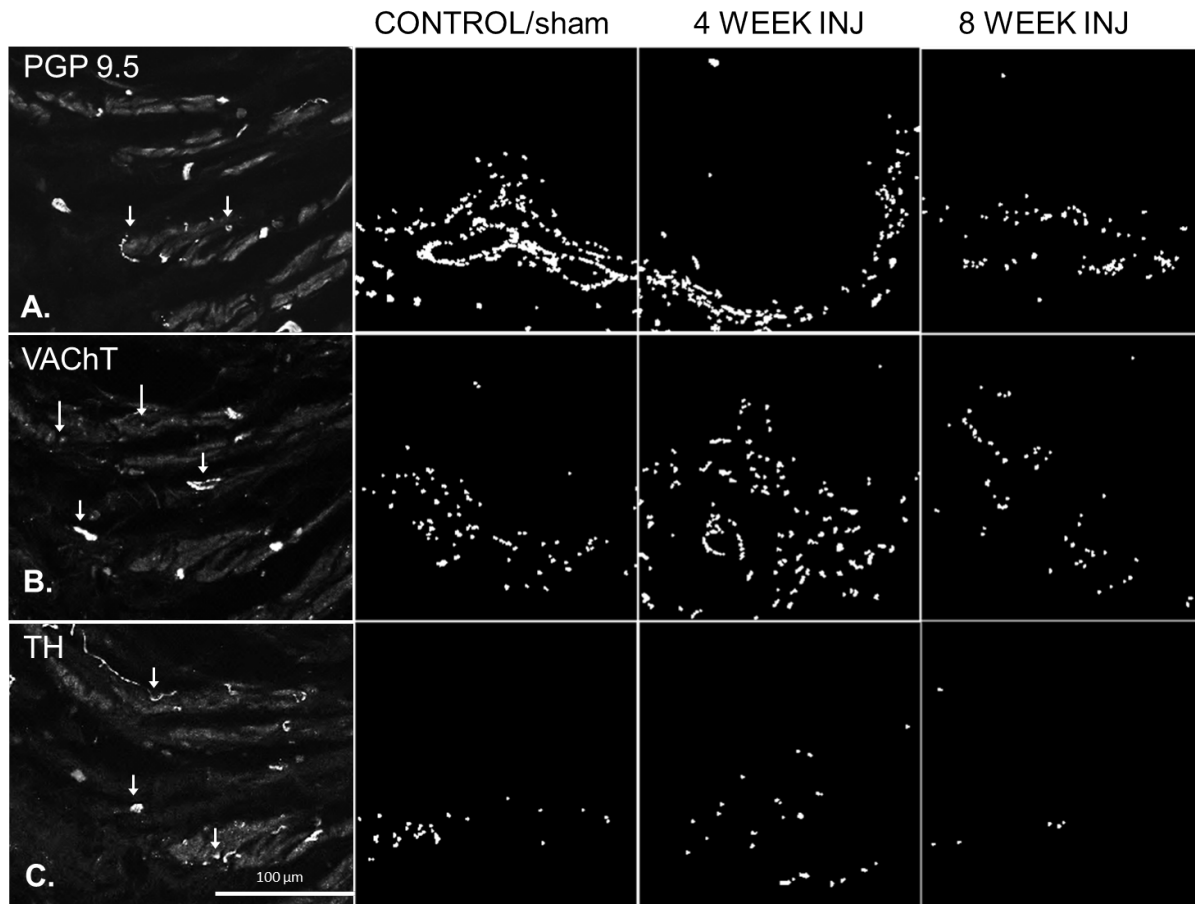


**Figure 13. Peripheral Nerve Labeling.** Evaluation of peripheral innervations (A) in addition to more specific evaluations of the cholinergic (B), and adrenergic innervations (C) of mid-vaginal segments from control 4 WEEK INJ and 8 WEEK INJ middle groups, showed a increased paucity of adrenergic nerve innervations with injury.

#### *Effect of VaBI Cholinergic Nerve Density*

Nerves labeling positive for a vesicular acetylcholine transporter (VAChT), which mediates acetylcholine storage by synaptic nerves was used as a marker of cholinergic

nerves. Following labeling and quantification of the percent fractional area of VACHT-IR nerves, the results showed significant differences in the proximal, middle and distal vagina (**Figure 13, Table 5**). In the proximal vagina, at 4 weeks post injury, the percent fractional area of VACHT -IR nerves had decreased relative to controls ( $0.818 \pm 0.115$  to  $0.203 \pm 0.042$  %,  $P < 0.001$ ), and evaluation of the 8-week group no recovery at  $0.205 \pm 0.030$  ( $P < 0.001$ ). In the middle vagina, at 4 weeks post injury, the percent fractional area had also declined relative to controls ( $0.520 \pm 0.043$  to  $0.195 \pm 0.027$  %,  $P < 0.001$ ), and evaluation of the 8-week group showed that the percent fractional area had not recovered ( $0.235 \pm 0.037$ ,  $P < 0.001$ ). In the distal vagina, at 4 weeks post injury, the percent fractional area had declined relative to controls ( $0.702 \pm 0.037$  to  $0.166 \pm 0.044$  %,  $P < 0.001$ ), and evaluation of the 8-week group showed no recovery ( $0.104 \pm 0.018$ ,  $P < 0.001$ ). Comparison of the 4-week vs 8-week group showed no significant difference in the percent fractional area in the proximal, middle or distal vagina ( $P = 0.972$ ,  $P = 0.443$ ,  $P = 0.264$ ).

#### *Effect of VaBI on Adrenergic Nerve Density*

Tyrosine hydroxylase (TH), which catalyzes the conversion of the amino acid L-tyrosine to dihydroxyphenylalanine (DOPA), was used as a marker for adrenergic nerves ( $n = 5$ , per group). Following labeling and quantification of the percent fractional area of TH-IR nerves, the results showed significant differences in the middle and distal vagina (**Figure 13 Table 5**). In the middle vagina, at 4 weeks post injury, the percent fractional area of TH-IR nerves had decreased relative to controls ( $0.407 \pm 0.051$  to  $0.214 \pm 0.052$  %,  $P = 0.046$ ), and evaluation of the 8-week group showed no recovery at  $0.156 \pm 0.065$  ( $P = 0.001$ ). In the

distal vagina, the percent fractional area at 4 weeks had also declined relative to controls ( $0.492 \pm 0.087$  to  $0.119 \pm 0.032$  %,  $P = 0.006$ ), and evaluation of the 8-week group also showed that the percent fractional area had recovered ( $0.065 \pm 0.016$ ,  $P < 0.001$ ). Comparison of the 4-week vs 8-week group showed declining trends, but no significant difference in the percent fractional area in the middle or distal vagina ( $P = 0.334$ ,  $P = 0.179$ ).

**Table 5. Innervation Density (% Fractional Area)**

	PGP 9.5 (pan neuronal)	VACHT (cholinergic)	TH (adrenergic)
<b>Proximal</b>			
Control	$0.536 \pm 0.070$	$0.818 \pm 0.054$	$0.500 \pm 0.039$
4 WEEK INJ	$0.305 \pm 0.016$	$0.203 \pm 0.017^{a*}$	$0.159 \pm 0.029$
8 WEEK INJ	$0.251 \pm 0.016$	$0.205 \pm 0.012^{a*}$	$0.136 \pm 0.013^{a*}$
<b>Middle</b>			
Control	$0.922 \pm 0.075$	$0.520 \pm 0.021$	$0.407 \pm 0.031$
4 WEEK INJ	$0.438 \pm 0.027^{a*}$	$0.195 \pm 0.013^{a*}$	$0.214 \pm 0.025^{a*}$
8 WEEK INJ	$0.300 \pm 0.016^{a*}$	$0.235 \pm 0.015^{a*}$	$0.156 \pm 0.007^{a*}$
<b>Distal</b>			
Control	$0.428 \pm 0.013$	$0.702 \pm 0.022$	$0.492 \pm 0.042$
4 WEEK INJ	$0.258 \pm 0.019^{a*}$	$0.166 \pm 0.018^{a*}$	$0.119 \pm 0.016^{a*}$
8 WEEK INJ	$0.206 \pm 0.013^{a*}$	$0.104 \pm 0.009^{a*}$	$0.065 \pm 0.006^{a*}$

*Values presented as Mean  $\pm$  SEM (n = 7) - significant difference <sup>a</sup> relative to control  
<sup>b</sup> relative to 4 WEEK INJ, significant at  $*P < .05$ , abbreviations: PGP 9.5: Protein Gene Product 9.5, VACHT: Vesicular Acetylcholine Transporter, TH: Tyrosine Hydrolase*

## 2.4 DISCUSSION

This study was designed to pharmacologically and immunohistologically assess smooth muscle recovery following a simulated birth injury in a rodent model. At 4 weeks and 8 weeks post injury, evaluations were performed to assess time-dependent changes in recovery, as evidence of a persistent change in smooth muscle morphology and function would illustrate how maternal birth injury, occurring in a subset of women, may potentially limit the ability of smooth muscle to fully recover, postpartum. The results showed changes in smooth muscle morphology, as well as myofiber, nerve and receptor function. Interestingly, morphological changes were observed to recover or stabilize with time, while changes in function steadily declined. More specifically, muscle and receptor function significantly declined with time, suggesting their potential role in modulating smooth muscle degeneration. The responses were also region specific, with the greatest impact of injury occurring in the proximal and middle vagina, but with the distal vagina rapidly declining by 8 weeks to the level of the proximal and middle vagina. The injury model utilized does not mimic the hormonal and mechanical adaptations that precede childbirth, and the regional differences may indeed be a function of the mode of injury, nevertheless the results show the gross potential of maternal birth injury to alter vaginal mechanics, when maternal adaptations are insufficient. Hence, the greatest contribution of this study could be the data that helps elucidate a potential link between birth injury and pelvic organ prolapse, as women with prolapse also have altered vaginal smooth muscle morphology and function.

These alterations in function are most evident in the anterior vaginal wall, which consists of a dense layer of circular and longitudinal smooth muscle bundles interlaced between layers of connective tissues. As such, the anterior vaginal compartment has an increased occurrence of prolapse, thus compromising support to the bladder and urethra [122]. Hence, much research has been geared toward the characterization of smooth muscle properties in vaginal tissues of the anterior wall in women with prolapse. A study by Boreham and el. analyzing smooth muscle morphometry in the anterior vaginal wall reported a decrease in thickness of the smooth muscle layer in women with prolapse relative to controls [101]. The observed changes were not related to age, race or stage of prolapse, hence the authors concluded that these changes may occur early in the pathogenesis of the dysfunction. Little is known, however, with respect to risk factors influencing the alteration in smooth muscle structure and function in prolapse vaginal tissues. What is known, however, is that these changes, in addition to the observed loss of tone and increased wall mobility, are both phenomena typically associated with pregnancy [123]. In preparation for delivery, smooth muscle cells dedifferentiate from a contractile (0.17 N/m) to a more undifferentiated and less contractile phenotype (0.09 N/m), characterized by increased migration and proliferation, thus increasing tissue growth and compliance [124]. According to Dietz et al, women with increased vaginal wall mobility before delivery are at less risk of incurring delivery related changes, a finding further supported Oliphant et al [125], [126]. These findings support the premise that smooth muscle in women with POP results from the disruption of the post partum recovery mechanisms following VaBI.

Injury to the smooth muscle can modulate its phenotype, as shown in a study evaluating injured arteries, which were injured similar to the method employed in this study [127]. The results showed a greater amount of synthetic smooth muscle cells in injured arteries, a phenomenon which is known to be a result of injury to the elastic lamellae. The injury induced increased matrix deposition and neointimal thickening of the arterial wall, but smooth muscle cells did eventually return to their contractile phenotype, restoring myofiber function. This study is one among several showing that strain induced injuries can cause smooth muscle modulation, and complementary studies have shown that these changes (i.e neointima formation) are necessary for equilibrating the stress field within the arterial wall following hemodynamic perturbations [128], [129]. These findings clearly attest to the potential of strain injuries to induce smooth muscle remodeling, but drawing further from these studies, one could infer that the observed increase in the thickness of the vaginal wall in the proximal vagina, and the increase in the perimeter of the vaginal lumen in the middle vagina, may be a result of smooth muscle phenotypic modulation in response to altered mechanical loading, following injury. One could also further infer, that in the absence of a response needed to equilibrate the stress field within the vaginal wall, a continuous remodeling response will ensue. However, for the vagina, the observed changes were short-lived, as our evaluations at 8 weeks showed a trend toward baseline. These findings suggest that the impact of mechanical perturbations may be compensated for, and hence may not be orchestrating the tissue degeneration.

However, changes in nerve function did persist, and hence may potentially orchestrate tissue degeneration. The pudendal nerve, arising from the S2-S4 nerve roots, supplies most of the anatomic pelvic structures and partially reversible pudendal nerve



injury occurs commonly with vaginal birth, as well as the pelvic and hypogastric nerves which innervates vaginal smooth muscle are also impacted [130]. Nerve injury is more likely with forceps delivery, multiparity, longer second-stage labor, third-degree perineal tear, and macrosomia [131]. Denervation within the pubococcygeus and anal sphincter muscles accompany 42% to 80% of vaginal deliveries, and these effects are likely also evident within the vagina. Snooks et al. also showed that denervation-reinnervation patterns become more pronounced with increased passage of time from delivery, supporting our functional and histological findings of persistent declines in cholinergic and adrenergic nerve function at 8 weeks relative to initial evaluations at the 4 weeks post injury [131]. The findings are limited to impact of injury on smooth muscle function in the circumferential direction since the circumferential direction is known to undergo the most significant deformation, but similar findings may be likely found in the longitudinal direction.

Correspondingly, evaluations of the receptors showed impact to cholinergic and adrenergic receptors in the proximal and middle vagina. Very few studies have evaluated the impact of prolapse on vaginal cholinergic and adrenergic receptor function, but recent studies by Northington et al. evaluating adrenergic receptor function; found that tissues from women with prolapse had a lower response to the adrenergic receptor agonist, phenylephrine relative to non-prolapse controls [98]. The difference was striking, and supports the idea that a loss of receptor function occurring after birth injury, may play a potential role in the pathogenesis of pelvic organ prolapse (POP). The functional and physiological significance of these receptors have not been widely studied in the vagina, but age related declines in M3 muscarinic receptors function in the bladder results in

decreased contractility, thus impairing voiding function [132]. The vagina is, however known to undergo age-related increases in cholinergic and adrenergic receptor innervation, perhaps as a compensation for a decline in vaginal receptor function [133]. Hence, a decline in receptor function in addition to a decline in nerve function as shown here following injury, could lead to a loss of tone within the vagina, thus comprising pelvic support. The semi-quantitative nature of immunolabeling techniques also renders it vulnerable to questions about reliability; however it suffices here, as only relative changes were evaluated.

Overall, our results showed progressive changes in myofiber and receptor function, with time post injury, which may be attributed to the observed loss of nerve function.. The lack of progressive histomorphologic findings suggests that changes in vaginal structure may be unreliable markers for early prognosis of POP, and-or may attest to the lower sensitivity of the histological assays relative, to functional assays. However, the functional assay did show a decline in nerve and receptor function with time, suggesting an increased role in orchestrating future changes in vaginal function. The impact was broad, severe, and region-specific, with the greatest impact observed in the middle vagina (20 -80% functional change). The injury model utilized, unfortunately, does not mimic the hormonally regulated maternal adaptations that precede a birth injury, and the regional differences may indeed be a function of the mode of injury, nevertheless the results show the potential of birth injury to alter vaginal smooth muscle function, when maternal adaptations are insufficient.

### **3.0 VaSM FUNCTION INFLUENCES VAGINAL BIAxIAL MECHANICS**

#### **3.1 BACKGROUND**

As reported in Chapter 2, vaginal smooth muscle contractile machinery, innervation, and receptor function are impaired following VaBI. Therefore, evidence of a strong relationship between smooth muscle function and vaginal mechanics would further validate the potential role of smooth muscle as a pathogenic factor of POP. It has been long established that pregnancy induces the differentiation of VaSM cells from a contractile (0.17 N/m) phenotype to a more immature or synthetic phenotype (0.09 N/m) [22]. These synthetic smooth muscles cells have no contractile tone, are migratory, and highly proliferative, enabling the vagina to increase its muscle content in order to accommodate passage of a large fetus with reduced risk of injury. These phenotypic changes can indeed alter vaginal mechanics. This is of particular relevance, as full recovery of smooth muscle to a contractile phenotype post-partum is essential for restoring vaginal tone. This is rather interesting, as after delivery in many women, the vagina is usually not fully restored. These changes can be observed as decreased vaginal tone, increased diameter, lower elasticity, in addition to other common characteristics of changes in the active muscle mechanics of the tissue [134].

The changes in vaginal properties following delivery, are interesting relative to the development of POP, as studies characterizing smooth muscle properties and density within prolapse and non-prolapse tissues have shown that women with POP have a lower amount of contractile smooth muscle cells compared to women presenting with symptoms of POP [94]. Additionally, studies evaluating vaginal smooth muscle protein at the transcriptional level showed alteration of SM-myosin heavy chain and caldesmon expressions, which are markers smooth muscle contractile potential [135]. However, there has been a lack of consensus in smooth muscle findings, especially with regards to whether smooth muscle dysfunction is the cause or the effect of POP. Limited sample sizes and challenges of human tissue acquisition for such studies contribute to the conflicting results. Notwithstanding, a definitive finding is that changes in smooth muscles are present within the vagina [136].

In arteries, smooth muscle acts as a shock absorber during phasic stroke volume in systole, thereby dampening the arterial pressure wave [137]. The active tension generated by smooth muscle also decreases compliance, and increases wall area, wall stiffness and stress. Smooth muscle also has a huge effect on arterial elasticity, due to its abundance in the wall, and comparable percentages (28% of wall area) have been determined for vaginal smooth muscle, further supporting its major role in maintaining vaginal mechanics [138], [139]. It has also been shown that elastin and collagen account for a larger percentage of wall area, and mechanics of the vaginal wall is likely highly dependent on these passive structures. However, impairment of the active components may have secondary effects on the passive components, with the potential to alter the loading environment, and induce tissue remodeling. It is not surprising then, that studies do find a degree of correlation

between collagen architecture and POP. If smooth muscle is in series with elastin and collagen in the vaginal wall, as has been postulated by Bank et al. **(Figure 16)**, a loss of smooth muscle function would cause more rapid recruitment, altering the mechanical properties of the vagina. These changes in mechanical properties could therefore promote a remodeling response that could manifest as POP.

This finding is expected because a myriad of diseases are associated with an alternation in the mechanical properties of the pathologic organs. For abdominal aortic aneurysms, a “rupture potential index,” defined as the locally acting wall stress divided by the local wall strength, was suggested for predicting the risk of abdominal aortic aneurysm rupture, to determine point of intervention, and evaluate surgical outcomes [140]. The utilization of these principles in the field of gynecology may also improve clinical outcomes, because POP does result in significant biomechanical changes in pelvic supporting structures. Currently, there is no data available that shows alterations in vaginal mechanics, resulting from a loss of smooth muscle function, and especially following VaBI. Thus, the goal of this work is to characterize the contribution of vaginal smooth muscle to parameters of vaginal wall stiffness, elasticity, and anisotropy; as these findings could have major clinical implications for both the evaluation and treatment of POP.

## **3.2 PROTOCOL**

### **3.2.1 Animals**

The Institutional Animal Care and Use Committee at the University of Pittsburgh approved the use of animals, in accordance with the National Institute of Health Guide for the Care and Use of Laboratory Animals. For the study, 10 virgin female rats at 3-month old virgin were obtained (Long Evans, 230-280 g, Hilltop Lab Animals, Inc., Scottsdale, PA) and pair housed in a temperature and light-controlled room with free access to food, until the day of sacrifice.

### **3.2.2 Biaxial Mechanical Tests**

#### *Tissue Preparation*

Immediately after sacrifice, the vagina was excised from each rat, and placed into Krebs'-bicarbonate buffer (in mM/L: NaCl 118, NaHCO<sub>3</sub> 25, KCl 4.7, MgSO<sub>4</sub> 1.2, CaCl<sub>2</sub> 2.5, KH<sub>2</sub>PO<sub>4</sub> 1.2, and D-glucose 11). The vagina was then cut along the length of the urethra, the longitudinal edge of the specimen was then cut to ensure that the urethra had been completely dissected. Approximately 10 ± 3.0 x 10 ± 3.00 mm vaginal strips were obtained from the posterior wall of the vagina. Specimen thickness was obtained using a custom, laser reflection system, and the width and length were measured by digital calipers [141]. Hooks with suture lines attached, were inserted with 4 hooks along each edge of the tissue

as shown, five markers were then centrally placed on the tissue, to limit edge effects as shown in **Figure 1**. The tissue was then placed into a 400 ml tissue bath containing oxygenated Krebs'-bicarbonate buffer (95% O<sub>2</sub>5% CO<sub>2</sub> at 37°C) for the duration of the test.

### *Testing Regimen*

The sample was loaded into the biaxial testing device – Bose Electroforce LM1 Testbench system (Bose Corporation, Minnesota, USA). The sample was allowed to equilibrate for 5 minutes and then a preloaded (0.1N) using a triangular loading waveform at frequency of 0.25 Hz. The markers were tracked, during the test, using a contrast based camera system (Bose 2-D DVE software) to obtain tissue strain (Green strain). The sample was then subjected to 10 cycles of preconditioning using a sine wave displacement curve of equi-biaxial Lagrangian stress (0.1 MPa) along the longitudinal and circumferential directions. Additional cycles were performed at ratios of (.5:1, .75:1, 1:1, 1:75, 1:5), with 1:1 indicating 0.1 MPa of equibiaxial stress, and data were recorded for analysis. (For simplicity, only data from 1:1 regimen is discussed. Data on additional regimens are reported in **Appendix II**.) The specimen was then brought to the predefined zero position, and 120 mM KCl solution was added to the bath to induce smooth muscle tonic contraction. The specimen was equilibrated for 5 minutes and then preloaded, preconditioned, and tested as described above. Following the muscle contractile regimen, Ca<sup>2+</sup> free Krebs solution supplemented with 4 mM of the calcium-chelating agent EGTA, was added to the bath to induce muscle relaxation and the protocol was repeated [142].

## Parameters

For analysis, stress-strain curves were generated based on the Green-Lagrangian strains calculated from the marker displacements. The strains were calculated for both the circumferential ( $\epsilon_{\text{Circ}}$ ) and axial ( $\epsilon_{\text{Axial}}$ ) direction, each during the 3 experimental conditions (baseline, contacted and relaxed). The maximum strain and maximum tangent modulus for the toe stiffness vs linear stiffness region of the curve were obtained. Also calculated were the areal strain, and the anisotropic index (Eqs.1 and 2).

$$\text{Areal Strain} = \epsilon_{\text{Circ}} * \epsilon_{\text{Axial}} + (\epsilon_{\text{Circ}} + \epsilon_{\text{Axial}}) \quad (1)$$

$$\text{Anisotropic Index} = 2 * \frac{\epsilon_{\text{Circ}} * \epsilon_{\text{Axial}}}{(\epsilon_{\text{Circ}} + \epsilon_{\text{Axial}})} \quad (2)$$

To separate the contribution of the active ( $\text{MTM}_a$ ) and ( $\text{MTM}_p$ ) passive properties to the tensile modulus of the vagina, total tension ( $\text{MTM}_T$ ) was defined similarly to that previously reported by both Gao et al. and Tremblay et al [106], [143]. Total tension for the current study was calculated following KCl application. Using this method, total tension in the tissue is defined as the summation of active and passive tension. Thus, following the application of EGTA all active tension should diminish, resulting in a total tissue tension of only the passive contributors *ie* collagen, elastin, GAGs etc. However, it is possible that not all of the active tension will be eliminated. Therefore the parameter  $f$  (*a value representing the percent change in the active mechanics of the tissues*) was used to account for the



functional contribution of smooth muscle (Eq. 3). All Statistical analysis was performed utilizing a one-way ANOVA, with a significance level of  $P < 0.05$ .

$$MTM_T = MTM_P + fMTM_A \quad (3)$$

### **3.2.3 Collagen, Elastin, and Smooth Muscle Imaging**

Multiphoton imaging was performed to visualize collagen, elastin, and smooth muscle, in non-stretched specimens. Images of injured specimens evaluated in Chapter 2, were also captured to determine the impact VaBI on these structures. For visualization, each segment was fixed in 4% paraformaldehyde overnight. Following the methods of Hill et al., the specimen was placed on a glass slide and imaging was performed using an Olympus FV1000 MPE (Tokyo, Japan) equipped with a Spectra-Physics DeepSee Mai Tai Ti-Sapphire laser (Newport, Mountain View, CA) [144]. The images were obtained at an excitation wavelength of 870nm, numerical aperture (NA) of 1.12, using a 25x MPE water immersion objective.

### **3.2.4 Statistical Analysis**

Statistical analysis was performed using SPSS statistical software (version 17.0; SPSS Inc., Chicago, IL). The average parameter estimates for each muscle condition were compared using non-parametric one-way analysis of variance (ANOVA). Significance was set at  $p < 0.05$ .

### 3.3 RESULTS

#### 3.3.1 Functional Results

The results suggest that the vagina can be characterized as hyperelastic and anisotropic, as has been previously reported (**Figure 14**).

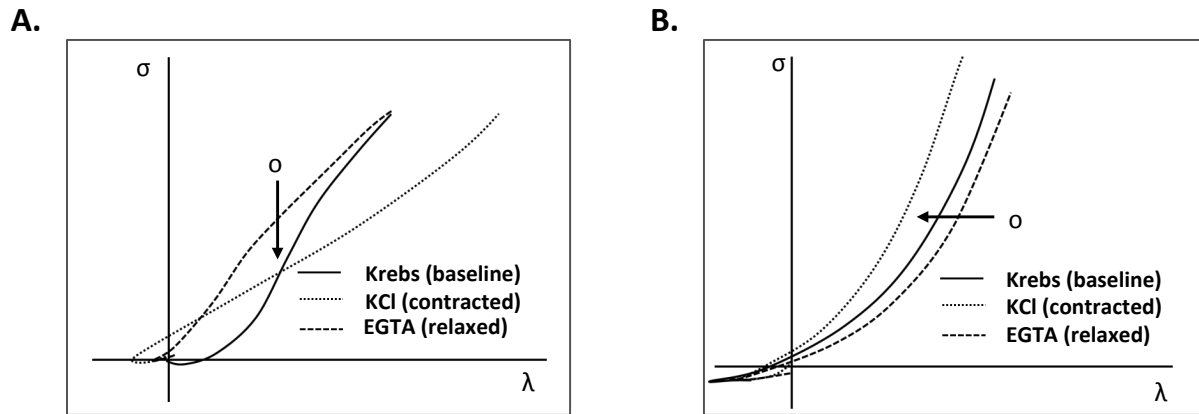


**Figure 14. Schematic Representation of the Stretch-Stress Curves.** Loading of the axial (A), and the circumferential (B) direction of the vagina resulted in distinct loading patterns when the muscle was at baseline, contracted, or relaxed. Of note, was the observation that contraction of the muscle resulted in a curve synonymous of a more gradual recruitment of collagen fibers in the axial direction.

As such, at baseline, the circumferential direction was significantly less stiff than the axial direction ( $P = 0.020$ ), and strained less ( $P = 0.034$ ) (Figure 15). The stress-strain curves in the circumferential direction appeared bilinear, with low and high stiffness linear regions,

while the axial direction had a single linear slope. On average, there were differences in the shape of the stress-strain curves, most significantly in the axial direction following contraction and relaxation of the vaginal smooth muscle, as shown in the representative outlines in **Figure 15**.

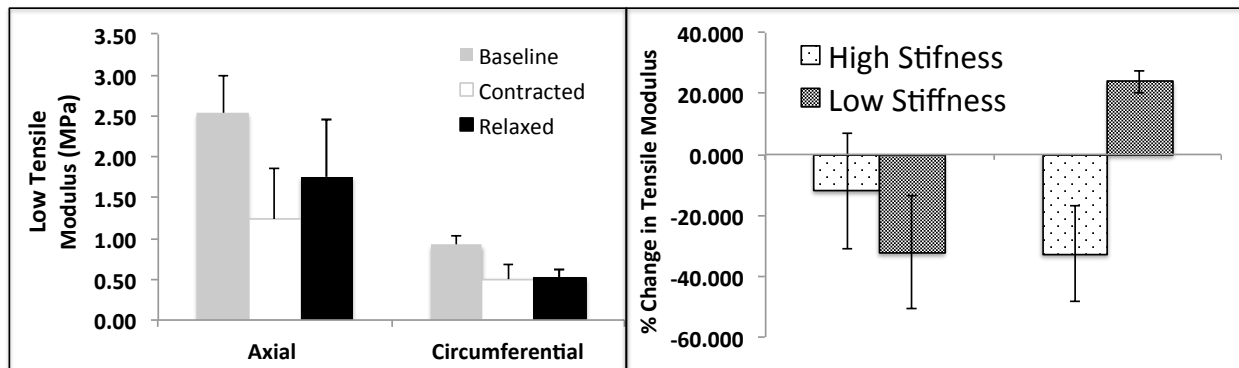


**Figure 15. Axial and Circumferential Tensile Modulus.** At the low-stiffness region, the vagina was significantly less stiff in the circumferential direction when smooth muscle was at baseline, contacted, and relaxed ( $P = 0.012$ ,  $P = 0.023$ ,  $P = 0.005$ ). (Panel 2) Smooth muscle contraction was associated with a trend toward a decrease in the tensile modulus in the high-stiffness region of the curve ( $P = 0.10$ ).

The effect of VaSM contraction was more evident in the toe-region, than at the high-stiffness region of the stress-strain curve (**Table 6**). In the high-stiffness region, VaSM smooth muscle contraction was associated with a trend toward a decrease in the tensile modulus in the axial direction, and an increase in stiffness in the circumferential direction, relative to the baseline condition

**Table 6. Biaxial Curves - Parameters**

	Baseline (Krebs)	Contracted (KCl)	Relaxed (EGTA)
E11 Low Tensile Modulus (MPa)	1.797 ± 0.460	1.678 ± 0.167	1.987 ± 0.454
E11 High Tensile Modulus (MPa)	1.944 ± 0.785	1.943 ± 0.799	2.236 ± 0.270
E11 Maximum Strain (%)	0.035 ± 0.004	0.027 ± 0.007	0.031 ± 0.010
E22 Low Tensile Modulus (MPa)	0.690 ± 0.058	0.571 ± 0.044	0.531 ± 0.139
E22 High Tensile Modulus (MPa)	2.640 ± 0.805	2.016 ± 0.581	1.710 ± 0.413
E22 Maximum Strain (%)	0.059 ± 0.004	0.063 ± 0.007	0.069 ± 0.017

*Parameter obtained from the stress-strain curves when smooth muscle was at baseline, contracted, and relaxed. The data are means ± SD; n = 5 \*indicates P < 0.05*

Specially, contraction of the VaSM caused a 36% (P = 0.74) percent decrease in the tensile modulus in the axial direction, and a 9% (P = 0.87) increase in the circumferential direction (**Figure 15**). Differences relative to the relaxed conditions were even more obscure, and no differences were observed in the maximum strain in the axial and the circumferential direction. As evident, from the Figure, the differences were not significant, as limitations of the testing system prevented the acquisition of data at low loads (load < 0.1 N). Previously, work by Bank et al et Gao et al showed that smooth muscle is most functional at low loads such as that used here (**Figure 16**) [105], [106]. Hence, the effect of smooth muscle was particularly evident by the significant difference in strains observed during our preload regimen. Specifically, following preloading of the tissue, the average strains in the baseline

vs contracted state significantly differed for E11 ( $13.6 \pm 4.8\%$  vs  $23.4 \pm 11.5\%$ ,  $P = 0.03$ ), and for the areal strain ( $0.29 \pm 0.13\%$  vs  $0.58 \pm 0.37\%$ ,  $P = 0.06$ ). The axial strains were large, thus rendering our baselines too high to observe any major significant effects of smooth muscle.

There was also very little difference observed in the areal strain or the anisotropic index (**Table 7**).

**Table 7. Biaxial Coupling - Parameters**

	Anisotropic Index	Areal Strain
Baseline (Krebs)	$0.78 \pm 0.414$	$0.10 \pm 0.04$
Contracted (KCl)	$0.91 \pm 0.289$	$0.12 \pm 0.06$
Relaxed (EGTA)	$0.99 \pm 0.272$	$0.11 \pm 0.02$

*Parameter obtained from the high-stiffness region of the stress-strain curves when smooth muscle was at baseline, contracted, and relaxed. The data are means  $\pm$ SD;  $n = 5$   
\*indicates  $P < 0.05$*

However, as shown in **Appendix II**, there was a trend at all loading regimens, toward increased areal strain and decreasing anisotropy following smooth muscle contraction. These changes were most evident when there was a significant difference in the stressing being applied to each axis (**Figure 29**). This supports the absence of any significant difference observed at the 1:1 loading regimen, as the ability of smooth muscle to distribute stress between the axes. The results in **Appendix II** also show a governing

role of strains in the circumferential direction on strains observed in the longitudinal direction, which may be indicative of the preferred orientation of the collagen and elastin.

### 3.3.2 Histological Results

Evaluation of the collagen, elastin, and smooth muscle in the vaginal muscularis showed smooth muscle bundles intricately connected to the surrounding collagen and elastin fibers (**Figure 16**). For validation of this method, vaginal tissues of VaBI injured rats, at 8 weeks post-injury were evaluated and showed less visible muscle bundles relative to controls (**Figure 17**).

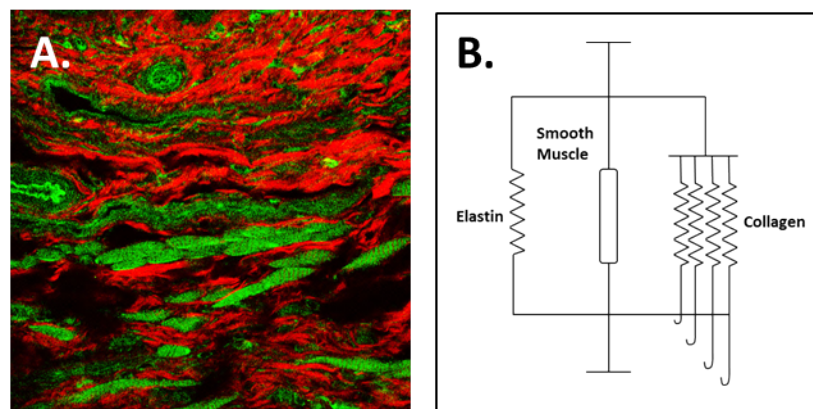


**Figure 16. Collagen, Elastin and Smooth Muscle Imaging.** Multiphoton imaging revealed resident collagen (red), elastin (green), and smooth muscle (green bundles) within the vaginal muscularis (**16-A**). These structures are intricately connected, and may function synergistically to regulate collagen recruitment in response to applied loads (**16-B**).

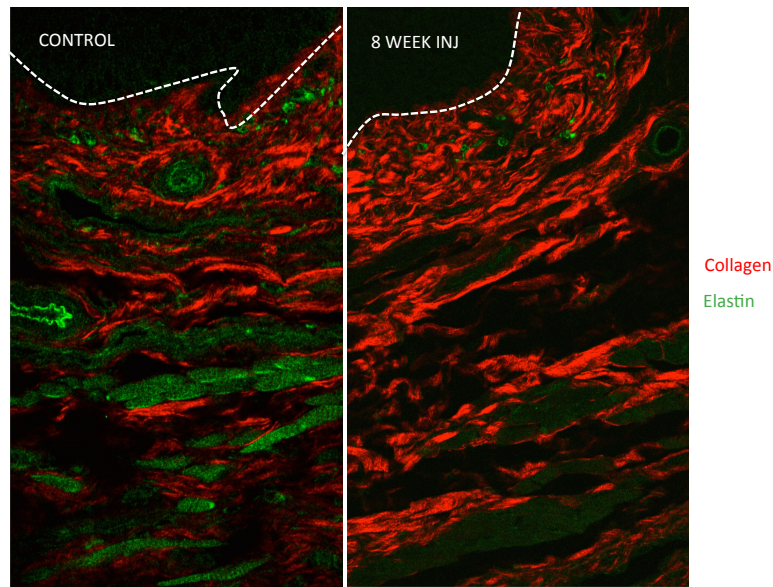


**Figure 17. Collagen, Elastin, and Smooth Muscle Imaging of the Injured Vagina.**

Multiphoton imaging of 8-weeks after VaBi in the rat revealed less visible smooth muscle (green bundles) within the vaginal muscularis, evidenced by the absence of  $\alpha$ -actinin,( an actin binding protein).

### 3.4 DISCUSSION

The evaluation of the mechanical properties of the vagina of both human and animal models is a very recent practice, and to date studies evaluating vaginal mechanics have been limited to uniaxial mechanics [22], [102], [107]. Data from uniaxial tests have proven useful for evaluating the effects of prolapse, pregnancy and parturition. However, there are inherent limitations of uniaxial tests including the loss of information pertaining to the interaction between the axes of the vagina in response the simultaneous axial loading,

which is more representative of in-vivo conditions. Uniaxial tests also provide very limited information about tissue properties especially when attempting to characterize changes in mechanics during periods of remodeling [145]. Therefore, for this work, we chose to perform equibiaxial mechanical tests to evaluate the role of smooth muscle in the vagina. This is particularly necessary here, as smooth muscle is oriented both axially and circumferentially within the vagina, and thus may have an individual impact on each axis, as well a combined or coupling effect. Additionally, with the focus being to investigate the mechanical role of smooth muscle, which to date has been poorly defined in the vagina; all tests were performed on viable specimens.

Stress-strain curves generated following load-control regimens were non-linear and biphasic, exhibiting a low-stiffness region and high-stiffness region, most evidently in the circumferential direction. The results showed a three-fold higher stiffness in the axial versus circumferential direction in the low stiffness region. However, there was no difference at the high stiffness region of the curve. Although it is assumed that strain in the circumferential direction must be larger than strains in the axial direction, especially during parturition, no previously published accounts were found. This degree of anisotropy was more evident when smooth muscle was at baseline level (ex-vivo resting tension) and when passivated (relaxation), versus when activated (tonic contraction), suggesting that anisotropy may be influenced by smooth muscle function. The large degree of anisotropy was more evident at the toe or low-stiffness region of the curve, than at the high-stiffness region of the curve, suggesting that collagen fiber recruitment or the rotation of the fibers may be influencing the anisotropic behavior [105], [106], [146]. This finding would be



remiss during uniaxial testing. However, our data is consistent with that reported by Feola et al. for the modulus ( $2.1 \pm 0.65$  MPa) following uniaxial testing of the axial direction [22].

The ultimate influence of smooth muscle modulation on the high stiffness modulus was indeed variable, and minimal effects on the high-stiffness modulus versus low-stiffness modulus were observed. Similar findings of decreasing influence of smooth muscle with increasing strain were reported by Tremblay et al [143]. Following smooth muscle tonic contraction, at the low-stiffness or toe-region of the stress-strain curves generated, there was a trend toward a decrease in stiffness in the axial direction and an increase in stiffness in the circumferential direction. This may perhaps be an attempt to redistribute stress along the loading axes, and/or a dampening effect by the smooth muscle. This dampening effect was most evident following the calculation of the percent contribution of smooth muscle, as there was a trend toward decreased stiffness in the high-stiffness region in both the axial and circumferential direction. At the low-stiffness region, smooth muscle decreased tonic contraction was associated with decreased stiffness in the axial direction and increased stiffness in the circumferential direction. As noted, the vagina is stiffer in the axial than circumferential direction, which further supports a protective dampening effect [147].

Tremblay et al did not observe this dampening effect, but did observe less influence of smooth muscle when tested arteries were at high-strains versus low-strains [148]. Although strain-control regimens were not performed here, it can be inferred that at high strains, smooth muscle tonic contraction would reduce wall stresses. As strain increases, there is increased force generation until an optimal length for smooth muscle contraction ( $L_0$ ) is attained, beyond which, smooth muscle force is known to rapidly decline [142]. This

phenomenon is commonly described as receptive relaxation, and is also evident in the bladder, as relaxation is required for adequate filling. Modeling by Rachev et al. showed that basal muscular tone also plays a role in maintaining more uniform stress distribution [149]. The baseline tension, also observed as residual stress, is commonly measured by the opening angle of a vessel [150]. It has been reported that smooth muscle contraction also affects the residual stress [149]. Skalak et al showed that the elimination of elastin and collagen of zero-stress slices, with elastase or collagenase, increased the opening angle by 53 and 70%, respectively, suggesting that smooth muscle must interact with these components to alter residual stresses [151]. At in-vivo resting condition, collagen and elastin are under compression by the retractive forces of smooth muscle. In the vagina, this external force provided by smooth muscle is required to facilitate vaginal folding to restore the diameter of the vagina. However following opening, there was a release of this compression or residual stress resulting in a relaxation of the vaginal folds. This is further supported by our multiphoton images, which showed significant interaction between the smooth muscle bundles, and the elastin and collagen fibers.

As noted in the results, the interaction between the smooth muscle and the elastin and collagen fibers proved most evident in the preload regimens, which interestingly, may represent the daily physiologic range. Smooth muscle tonic contraction was associated with a 50% higher areal strain relative to smooth muscle at baseline, following a .1N preload. These findings are supported by reports, which indicate that smooth muscle exhibits a highly compliant series elastic component, support these findings [152]. This is further supported by results from Gao et al which showed 80% of collagen being recruited at average strains of 1.61% in the duodenum of patients with systemic sclerosis, versus at

average strains of 2.97% for controls [106]. Gao and colleagues concluded that the results were due to the differences in smooth muscle contraction, as the average force generated by the duodenum of patients with systemic sclerosis was 45% less than controls; this assumption was validated by the replication of these findings in computational models for which the active smooth muscle component was modified. Further, Hill et al reported that the recruitment of collagen in passive tissues occurs at a finite strain [144], but in this study when smooth muscle was tonically contracted, the shape of the stress-strain curve suggests a more gradual collagen recruitment. However, more work is needed to validate this observation. In addition, it still remains to be proven if there is indeed collagen in series and collagen in parallel as proposed by Bank et al, as Gao et al obtained adequate fits of their data utilizing a model of only collagen in series [105], [106]. Our results could also likely be modeled with a single parallel component, as there may be no functional value of a less stiff collagen component in parallel with elastin. Smooth muscle contraction may simply be inducing increased crimp within the fibers, which may result in a more gradual recruitment or stiffening of the fibers when loaded **(Figure 16-B)**.

The current study provides the basis for future experimental techniques for the evaluation of smooth muscle mechanical role in the vagina, as well as sufficient premise for more studies aimed at further understanding how changes in smooth function could influence changes in the vagina. When combined with the preceding study in Chapter 1, which showed that smooth muscle functionality is persistently altered in following VaBI, it becomes a highly significant finding, as it builds substantial evidence for the potential role of smooth muscle injury in the pathogenesis of POP. This is indeed the case, as the potential for increased wall stresses and increased anisotropy or distribution of wall stresses,

following the loss of smooth muscle function could increase the propensity for vaginal remodeling. However, it is not without limitations, including the lack of significant findings, resulting from the relatively large pre-load applied to the tissue. Additionally, since it has been postulated that smooth muscle may govern the recruitment of collagen, our significant findings observed in the pre-load strains supports the lack of major significant findings as our baseline conditions may have surpassed the point at which smooth muscle is highly functional. Another limitation is that dynamic or simultaneous acquisition of collagen recruitment during loading was not obtained, which posed some disadvantages when attempting to associate collagen recruitment, tissue strain, and smooth muscle contraction. Future work could also involve evaluation of the intact organ.

## **4.0 PROLAPSE MESHES NEGATIVELY IMPACT VaSM FUNCTION**

### **4.1 BACKGROUND**

As shown in the preceding chapter, smooth muscle function is essential for maintaining vaginal mechanical function. With POP, being associated with changes in smooth muscle function, treatment methods for POP should at the very least, maintain smooth muscle function, if unable to improve it. However, mesh-related complications including exposure through the vaginal wall, erosion into an adjacent structure, and pain and infection are prevalent, and despite the introduction of light-weight ( $<45 \text{ g/m}^2$ ), large pore ( $>1 \text{ mm}^2$ ), monofilament polypropylene meshes into the market, roughly 10% of women who receive mesh have complications [15], [153], [154]. The prevalence of these complications recently prompted warnings from the US Food and Drug Administration (FDA), with the most recent public health notification appearing in 2011, warning that mesh-associated complications are not rare events and that more thorough investigations into mechanisms by which mesh may negatively impact the vagina are warranted [15].

Previous studies from our research group, have shown that implantation of mesh increases apoptosis, and decrease the thickness and contraction of smooth muscle in the underlying vaginal tissue [155]. Interestingly, the degree of impact varied with the specific mesh implanted, but these widely used meshes are typically marketed similarly, and used

interchangeably in clinical settings. These findings when paired with a previous study of ours which showed variability in the textile and mechanical properties of these meshes, suggest that the minor differences in mesh properties could be contributing to the different outcomes [19]. For example, the gold standard mesh, Gynemesh™ PS (Ethicon, Sommerville, NJ, USA), which exhibits the highest stiffness, highest weight and lowest porosity was associated with the greatest negative impact on smooth muscle relative to two lower stiffness meshes, UltraPro™ (Ethicon, Sommerville, NJ, USA) and Restorelle® (Coloplast, Minneapolis, MN). We therefore theorized that a high stiffness mesh may shield the underlying soft tissues from experiencing normal physiologic stress, thus inducing atrophy and thinning of the smooth muscle layer. This phenomenon, termed stress shielding, which has been widely studied, is based on a biomechanical principle (Wolff's Law) that the body undergoes structural remodeling in accordance to its functional demands, and in the absence of any mechanical demand, the tissues will begin to deteriorate [156][157]. Additionally, the high weight and low porosity likely result in a greater mesh burden, and increased likelihood of a heightened foreign body response with impaired tissue ingrowth and a poor functional outcome. As vaginal smooth muscle (VaSM) plays an essential role in maintaining vaginal function (eg. tone), and is compromised in women with prolapse, it is essential that its structure and function, at the very least, be preserved if not improved following surgery.

The results from the previously cited studies do suggest that lower stiffness and lighter weight meshes be used for prolapse procedures aiming to maintain VaSM structure and function, but the mechanism(s) remains unclear. Hence, to further investigate the mechanism and extent of the impact of mesh textile and mechanical properties on VaSM,

we evaluated the effect of mesh implantation on VaSM contraction, innervation, receptor function, and innervation density in the underlying grafted tissues and tissues adjacent to the mesh (non-grafted tissues). For the study design, the high stiffness mesh, Gynemesh™ PS (Ethicon;  $27.5 \pm 2.7$  N/mm), was evaluated relative to the two lower stiffness meshes, UltraPro™ (Ethicon;  $0.01 \pm 0.00$  N/mm) and Restorelle® (Coloplast;  $0.18 \pm 0.03$  N/mm). Additionally, UltraPro™ which is highly anisotropic, was implanted both with its blue line perpendicular (low stiffness direction,  $0.01 \pm 0.00$  N/mm) and parallel (high stiffness direction,  $0.26 \pm 0.09$  N/mm) to the long axis of the vagina. All meshes were implanted by abdominal sacrocolpopexy following hysterectomy, on cycling, parous Rhesus Macaques (*macacca mulatta*), without prolapse. This design ensured that the impact of mesh was being evaluated, independent of the degenerative effects of the disease (which could be variable), and following a procedure that has been shown with Level I clinical evidence to be associated with minimal complications [158].

Evaluation of the outcomes measures incorporated both functional and histological assessments of the grafted and non-grafted tissues. Specifically, smooth muscle contraction was measured by the force generated following muscle depolarization by a high potassium solution (KCl), innervation function was measured by the force generated following nerve stimulation, and receptor function was measured by the force generated following receptor depolarization by a non-selective muscarinic receptor (MR) and  $\alpha_1$ -adrenoceptor (AR) agonist. Innervation density was measured histologically as a percent of the fractional area of peripheral nerves labeled (cholinergic, adrenergic) within the smooth muscle layer. All outcome measures were analyzed as a function of mesh properties including porosity, weight, and stiffness. Results from the study will aid in determining whether the negative

impact of mesh on vaginal smooth muscle is the result of a loss of the muscle contractile elements, a loss of innervation, or a loss of receptor function, and if these changes are a function of mesh textile and mechanical properties. Additionally, the evaluation of both adjacent grafted and non-grafted tissues within the same animal will provide verification of the extent of the impact on the vagina.

## **4.2 PROTOCOLS**

### **4.2.1 Animals**

All animals (Rhesus macaques) used in this study were maintained and treated according to an experimental protocol approved by the Institutional Animal Care and Use Committee of the University of Pittsburgh (IACUC #1008675), and in adherence with the National Institutes of Health guidelines. Routine laboratory tests and regular examinations by veterinarians during a quarantine period were used to certify that these experimental animals were pathogen-free and in good physical condition. Animals were maintained in standard cages with water (*ad libitum*), and scheduled monkey diet supplemented with fresh fruits, vegetables and multiple vitamins, daily. A 12-hour light/dark cycle (7 AM – 7 PM) was used, and menstrual cycle patterns were recorded daily. Available demographic data of each NHP were collected prior to, and after surgery including age, weight, gravidity and parity. Researchers were blinded to all demographical data of each NHP until the completion of the study.



#### 4.2.2 Surgical Procedure

Following IACUC approval at the University of Pittsburgh, thirty-eight (38) cycling parous NHP (Rhesus macaques) were selected for sham or mesh implantation with the stiffer mesh Gynemesh™ PS (Ethicon;  $0.29 \pm 0.015$  N/mm, N=8) vs two lower stiffness meshes, Restorelle® (Coloplast;  $0.18 \pm 0.026$  N/mm; N=8) and UltraPro™ (Ethicon;  $0.009 \pm 0.0016$  N/mm, N=6). UltraPro™ which is a highly anisotropic mesh, was implanted in two directions, with its blue orientation lines perpendicular (UltraPro™ perpendicular – low stiffness direction,  $0.01 \pm 0.00$  N/mm), and with its blue orientation lines parallel to the long axis of the vagina (UltraPro™ parallel - high stiffness direction,  $0.26 \pm 0.09$  N/mm). Using a randomized procedure, each primate was assigned to a mesh group, or to the sham control group. All meshes were implanted via an abdominal sacrocolpopexy after hysterectomy, and the sham group (N=8) underwent the identical surgery without mesh. As previously published [155], [159], under general anesthesia, an abdominal hysterectomy was performed through a midline incision, without excision of the ovaries. The bladder was then dissected off the anterior vagina to the level of trigone, and the rectum dissected from the posterior vaginal wall to the level of the perineal body. A 5cm incision was made over the sacral promontory and carried down to the longitudinal ligament of the spine. After completion of these dissections, the surgeon was then informed by the unblinded biotechnician that it would be a sham operation, or handed a sterile piece of mesh to be implanted. For mesh implantation, 3 cm wide by 10 cm long straps of mesh were laid flat on the anterior and posterior wall, respectively, and secured in place with a continuous suture (2-0 Biosyn™; Synovis, St. Paul, MN, USA) along each lateral edge. The

two straps of mesh were then anchored into the sacral promontory with two delayed absorbable sutures, and any excess mesh was trimmed off prior to closing the peritoneum over the mesh. The abdominal muscle layer was closed with a single continuous suture, and three to five interrupted sutures were used to re-approximate the subcutaneous fat, followed by a continuous subcutaneous closure (4-0 polysorb). Postsurgical care inclusive of pain medication, oral intake and activity was carried out according to a standard postoperative protocol. Twelve weeks after surgery, the vagina was dissected, and immediately following acquisition, tissue blocks were obtained from a region of the anterior vagina underlying the mesh (grafted), and a region adjacent to the mesh (non-grafted). Additional steps were taken to ensure consistency of the biopsied site.

#### **4.2.3 Functional Analysis (Organ Bath)**

For the organ bath assay, grafted and non-grafted tissues were subsequently divided into four 2 mm wide x 7 mm long circumferential strips, each. Each strip was then carefully suspended between two wires using stationary clips, and then immersed in an organ bath (20 mL) containing oxygenated Krebs solution (95% O<sub>2</sub>-5% CO<sub>2</sub>), maintained at 37°C. Each segment was adjusted to a tension of 1 g and then allowed to equilibrate for 60 min. Contractile responses were monitored with a pressure transducer (Transbridge 4M, World Precision Instruments) attached to a load cell (Honeywell, Morristown, NJ, USA), and force measurements were recorded using Chart software (version 5) on a Power Lab system (sampling at 40 Hz, AD Instruments).

To evaluate muscle contractile function or specifically, myofiber function, muscle force generation following administration of 120 mM KCl was measured. This concentration was chosen based on results from dose response curves in preliminary experiments, in which we found the maximum force generated, to plateau following the administration of 120 mM KCl. Once the response to the dose plateaued, the tissue was washed with Krebs solution 3 times (10 minutes for each wash), prior to beginning the electrical stimulation experiments. To evaluate nerve function, muscle force generation to electrical field stimulation (EFS) at frequencies of 1-64 Hz, intensity of 20 volts, and duration of 2 seconds was applied using a S88, Grass Telefactor stimulator. These settings were based on preliminary experiments to ensure that they were low enough to activate the nerves, but not significant enough to activate the attached muscle fibers, thereby ensuring that the force generated was a result of the activated nerves synaptically activating the muscle fibers. Tissue samples were washed with Krebs solution 2 times (5 minutes per wash), between each stimulation. Contractile responses were recorded and normalized to the force generated following KCl (120mM) application, herein represented as a percentage of KCl response. For analysis of receptor-mediated function, muscle force generation to increasing concentrations of carbachol and phenylephrine ( $10^{-8}$  to  $10^{-4}$  M, non-cumulatively) were used to evaluate muscarinic receptor (MR) and  $\alpha 1$ -adrenoreceptor (AR) function, which are present within the vagina. After the application of each dose, and after the observed response had plateaued, the tissue was washed with Krebs solution 3 times (10 minutes for each wash), and the next dose was applied. Contractile responses were recorded and also normalized to the force generated following KCl (120mM) application. With 120 mM KCl proven to fully depolarize the smooth muscle, if only a

fraction of the muscles present had functional neurons or functional receptors, nerve depolarization or receptor depolarization would only yield a percentage of the contractile force generated by KCl, thus providing an opportunity to capture functional changes. Additionally, to ensure that the changes observed were not a result of changes in muscle function, the normalization to KCl response was necessary.

#### **4.2.4 Histochemical and Immunohistochemical Analysis (Nerve Labeling)**

For the histochemical and immunohistochemical assays, grafted and non-grafted tissues were fixed in 4% paraformaldehyde overnight, and then exposed to graded concentrations of sucrose (cryoprotectant). The tissues were washed in phosphate buffered saline (PBS), embedded into optimal cooling temperature (O.C.T) medium (Sakura Finetek USA, Inc., Torrance, CA, USA), and then cryosectioned at 10 $\mu$ m thickness, at an angle perpendicular to the long axis of the vagina. The sections were then processed for Masson's trichrome staining according to the methods of the Center for Biological Imaging (CBI, University of Pittsburgh). For immunohistochemical labeling, the sections were air-dried for 10 minutes, submerged into cold acetone for 20 minutes, and then washed with buffer. Permeabilization in 0.2% Triton X-100 for 10 min, followed by a wash in buffer, and then incubation for 1.5 hours in 2% Bovine Serum Albumin (BSA) was performed. Sections were incubated overnight at 4°C, with primary antibody diluted in PBDT (1xPBS, .2% BSA, 2% Donkey Serum (Jackson Laboratories; no. 017-000-00), and .03% Triton). Protein Gene Product (PGP 9.5), a neuron-specific ubiquitin which localizes to neuronal axons, was used to evaluate peripheral nerve density (1:10000; rabbit polyclonal antibody: Accurate

Chemical, Westbury, NY YBG78630507). Vesicular Acetylcholine Transporter (VACHT), which is localized within the soma and the axons of cholinergic neurons, and plays a role in the packaging and transporting of acetylcholine (ACh) into synaptic vesicles was used as a marker to evaluate cholinergic nerve density (1:5000 rabbit monoclonal antibody: Sigma V5387). Lastly, Tyrosine Hydroxylase (TH), a rate limiting enzyme that converts L-tyrosine to L-DOPA which is then converted to dopamine (a precursor of norepinephrine), was used to evaluate adrenergic nerve density (1:1000; rabbit polyclonal antibody: Sigma T8700). Following incubation with the primary antibodies, the sections were rinsed with PBS, and incubated for 4 hours at 4°C with Cy3 or FITC-conjugated f(ab) donkey anti-rabbit IgG (1:100; Jackson Laboratories no. 711 165 152) diluted in PBDT. The sections were again washed in buffer and cover-slipped with Fluoro-Gel medium (EMS, Hatfield, PA 17985-10). In control experiments, no immunofluorescence staining was observed when the primary antiserum was omitted.

#### **4.2.5 Morphometric Analysis**

All images were captured using a Nikon microscope synced to a Nikon color digital camera, before being imported into the Elements software (NIS-Elements AR 3.2) for quantification. To evaluate fibers immunoreactive (IR) for PGP 9.5, VACHT and TH in the three regions of the vagina, images were randomly captured at 10x magnification. For analysis, all images were acquired, and the same threshold was applied. Pixels of binary images whose intensity did not exceed the threshold value were automatically removed and considered negative. The numbers of profiles per unit area of the vaginal wall for the vaginal layers

was measured (fractional area) and averaged for each section. Nerves in all layers of the vaginal wall were quantified and evaluated separately, and vascular innervation shown by positive staining in the vascular structures was excluded.

#### **4.2.6 Statistical Analysis**

Statistical analysis of the functional (maximum force), and histological (% fractional area) parameters were performed using IBM SPSS statistical software (version 17.0; SPSS Inc., Armonk, NY). Differences between groups were evaluated using Kruskal Wallis one-way analysis of variance (ANOVA), and Bonferonni post-hoc tests. For additional analysis of UltraPro™ Perpendicular vs UltraPro™ Parallel, Mann Whitney U tests were used, and Regression and Correlation analysis were performed to evaluate the influence of mesh properties. For all measures, significance was set at  $P < 0.05$ .

### **4.3 RESULTS**

There was no significant difference in the age, weight and parity of the NHP groups (**Table 8**) prior to implantation with the three meshes, containing variable textile properties (**Table 9**).

**Table 8. Macaques Demographics**

	Mesh Groups					P-value
	Sham (n=7)	Gynemesh™ PS (n=7)	Restorelle® (n=7)	UltraPro™ perpendicular (n=6)	UltraPro™ parallel (n=7)	
Age (year)	15.0 (15.0,15.2)	13.5 (11.0,14.0)	13.0 (12.5,15.2)	13.0 (12.0,15.0)	13.0 (12.5,13.2)	≥ 0.132
Weight (gram)	8.5 (8.0,9.3)	7.9 (7.1,9.0)	9.4 (8.3,12.5)	7.3 (6.4,8.8)	8.2 (8.0,9.2)	≥ 0.426
Parity	6.0 (3.5,6.5)	4.0 (2.0,5.2)	5.0 (3.0,5.2)	3.0 (2.2,6.5)	4.0 (4.0,5.5)	≥ 0.782

*Values presented as Median (IQR)*

*Significance set a  $P < .05$*

However, upon explanation, the grafted region, shown as the boxed area in **Figure 18**, was distinct from the non-grafted region, and this grafted region was visually variable between groups. The mesh in the grafted region, had evidence of host tissue ingrowth (**Figure 18 [A-D]**), with the degree of incorporation varying according to the stiffness of the mesh implanted (**Figure 18. [E-H]**). Specifically, at the mesh-tissue interface, UltraPro™ perpendicular and Restorelle® had better tissue incorporation while Gynemesh™ PS and UltraPro™ parallel, in spite of having been implanted flat, appeared buckled, and surrounded by a connective tissue capsule (**Figure 1 [A-D]**).

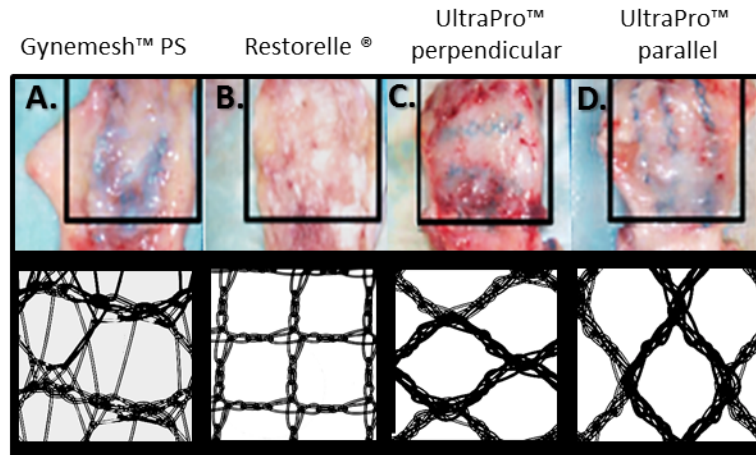


**Figure 18. Vaginal Explants.** 3 months post implantation explants from Gynemesh™ PS, Restorelle®, UltraPro™ perpendicular and UltraPro™ parallel (A-D). The half closest to the cervix, underlying the mesh was defined as the grafted region, and the lower portion adjacent to the mesh was defined as the non-grafted region. At the mesh-tissue interface of each mesh, there was evidence of host tissue ingrowth, with varying degree of incorporation as a function of mesh-type. Less stiff meshes, UltraPro™ perpendicular and Restorelle®, had better incorporation into the tissue, while the stiffer Gynemesh™ PS appeared buckled and surrounded by a connective tissue capsule (A).



### 4.3.1 Morphological Results

#### *Muscle Morphology*

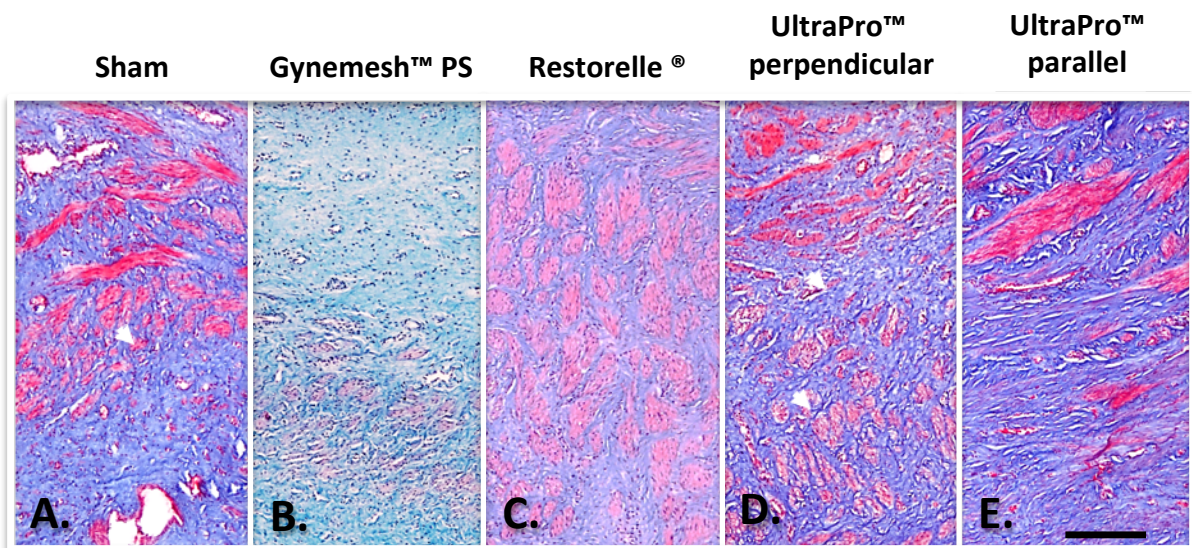


**Figure 19. Morphological Results.** Representative images showing gross smooth muscle morphology following Masson's trichrome staining of crossF sections of (A) sham operated; (B) Gynemesh PS, (C) Restorelle, (D) UltraPro™ perpendicular, and (E) UltraPro™ parallel tissue biopsies from the grafted region. Compared to Sham and UltraPro™ perpendicular, implantation with the higher stiffness meshes appeared to have more disorganized smooth muscle fibers. Additionally, following implantation with Gynemesh (B), there was increased thinning of the muscle layer relative to all the other meshes. Scale bar = 250  $\mu$ m.

### 4.3.2 Functional Results

#### *Muscle Mediated Contractions*

In the grafted region, evaluation of the contractile force generated following KCl administration showed that muscle function was significantly different between the groups ( $P < 0.001$ ) (**Figure 20**). Specifically, the grafted region of Gynemesh™ PS, UltraPro™ parallel (high stiffness), and Restorelle® generated significantly less force relative to sham ( $P < 0.001$ ,  $P < 0.001$ ,  $P = 0.015$ ), while there was no difference between sham and UltraPro™ perpendicular ( $P = 0.155$ ). As shown in Table 3, the decrease in contractile force following implantation of Gynemesh™ PS and UltraPro™ parallel was the greatest at 80% and 65%, respectively. When the contractile force generated by UltraPro™ parallel was compared to that of UltraPro™ perpendicular, the stiffer UltraPro™ parallel, generated less force, but this did not reach statistical significance ( $P = 0.078$ ). In the non-grafted region, there was no significant difference in contractile force generation between the groups ( $P = 0.085$ ), but UltraPro™ parallel again, in this region, generated less force than UltraPro™ perpendicular ( $P = 0.052$ ).

#### *Nerve Mediated Contractions*

In the grafted region, the contractile force generated following electrical stimulation showed that nerve function was significantly different between the groups ( $P < 0.002$ ) (**Figure 20**). Muscle contractile force following implantation with Gynemesh™ PS

was decreased by 91% relative to sham-operated controls ( $P = 0.008$ ). However, there no significant difference following implantation with the lower stiffness UltraPro™ perpendicular and Restorelle® ( $P = 0.187$ ,  $P = 0.155$ ). When we compared the contractile force generated by UltraPro™ parallel to that of UltraPro™ perpendicular, there was no significant difference observed ( $P = 0.143$ ). In the non-grafted region, there was also no significant difference in nerve function between the groups ( $P = 0.361$ ), and UltraPro™ parallel and UltraPro™ perpendicular were similar ( $P = 0.247$ ).

#### *Receptor Mediated Contractions*

In the grafted region, contractile force generated following the application of the muscarinic receptor agonist, carbachol, showed that receptor function was significantly different between the groups ( **$P = 0.008$ , Figure 20**). Of note, there was a 90% decline in the median contractile force generated following implantation with Gynemesh™ PS ( $P = 0.007$ ), while there was a 62% increase in the contractile force generated following implantation with Restorelle® ( $P = 0.037$ ). When the contractile force generated by UltraPro™ parallel to that of UltraPro™ perpendicular was compared, there was no significant difference observed ( $P \geq 0.999$ ). In the non-grafted region, there was no significant difference in cholinergic receptor function between the groups ( $P = 0.148$ ), and UltraPro™ parallel was not significantly different from UltraPro™ perpendicular ( $P = 0.647$ ). Contractile force generated following the application of the adrenergic receptor agonist, phenylephrine ( $10^{-8}$  to  $10^{-4}$  M, non-cumulatively), was not substantial while a robust response in our positive control (primate bladder) was observed.

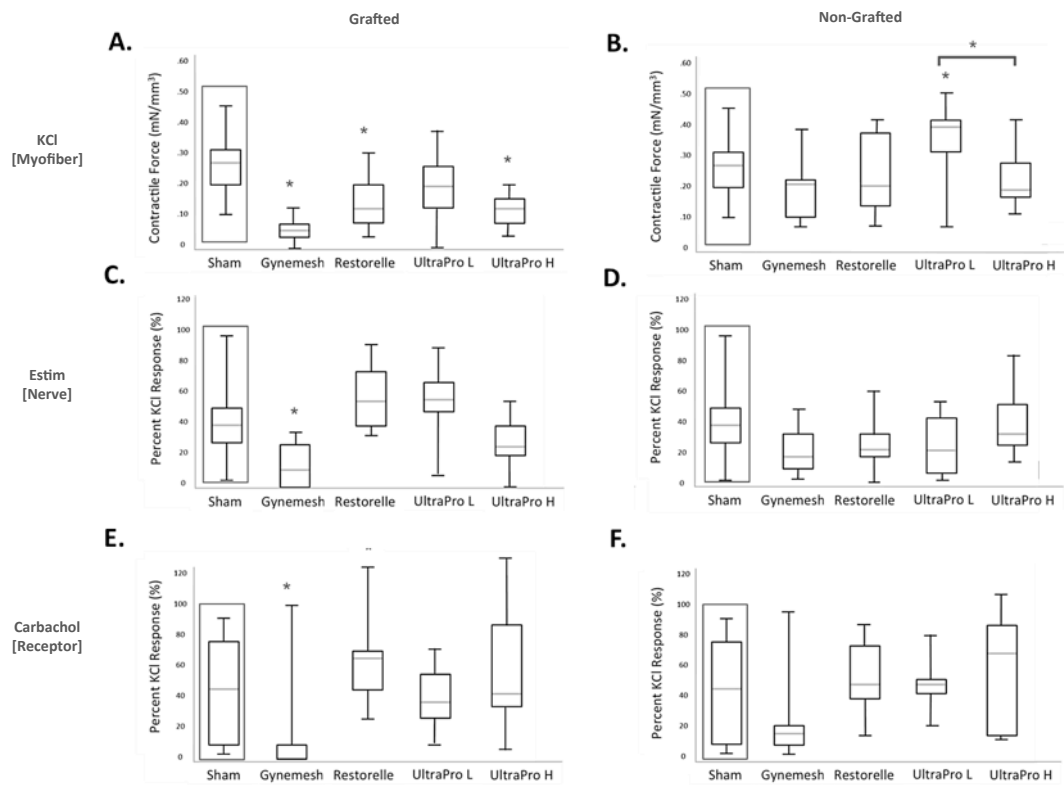


**Figure 20. Functional Response (Maximum Response).** Muscle mediated contraction significantly declined following implantation with Gynemesh PS, UltraPro™ parallel, and Restorelle® in the grafted region ( $P < 0.001$ ,  $P < 0.001$ ,  $P = 0.015$ ) (A), and UltraPro™ perpendicular was greater than UltraPro parallel ( $P = 0.052$ ) in the non-grafted region (B). Nerve mediated contractions significantly declined following Gynemesh™ PS ( $P = 0.008$ ) implantation in the grafted region (C). Cholinergic receptor mediated contractions significantly also declined following Gynemesh™ PS ( $P = 0.007$ ) in the grafted region (E).

### 4.3.3 Immunohistochemical Results

#### *Peripheral Nerve Density*

In the grafted region, peripheral nerve density as measured by labeling with the pan neuronal antibody, PGP 9.5, showed that nerve density was significantly different between the groups ( $P < 0.001$ ), with a decrease in the mesh implanted animals relative to sham-operated animals (**Figure 21 [A-D]**). Specifically, the grafted region of Gynemesh™ PS and UltraPro™ parallel had significantly less nerves relative to sham ( $P < 0.001$ ,  $P < 0.001$ ), while Restorelle® and the lower stiffness UltraPro® perpendicular were not significantly different from sham ( $P = 0.159$ ,  $P = 0.110$ ) (**Table 9**). When we compared nerve density in UltraPro™ parallel to that of UltraPro™ perpendicular, the less stiff UltraPro™ perpendicular had a greater density of nerves, but this did not reach statistical significance ( $P = 0.088$ ). In the non-grafted region, there was no significant difference in nerve density between the groups ( $P = 0.157$ ), and UltraPro™ parallel was not significantly different from UltraPro™ perpendicular ( $P = 0.684$ ).

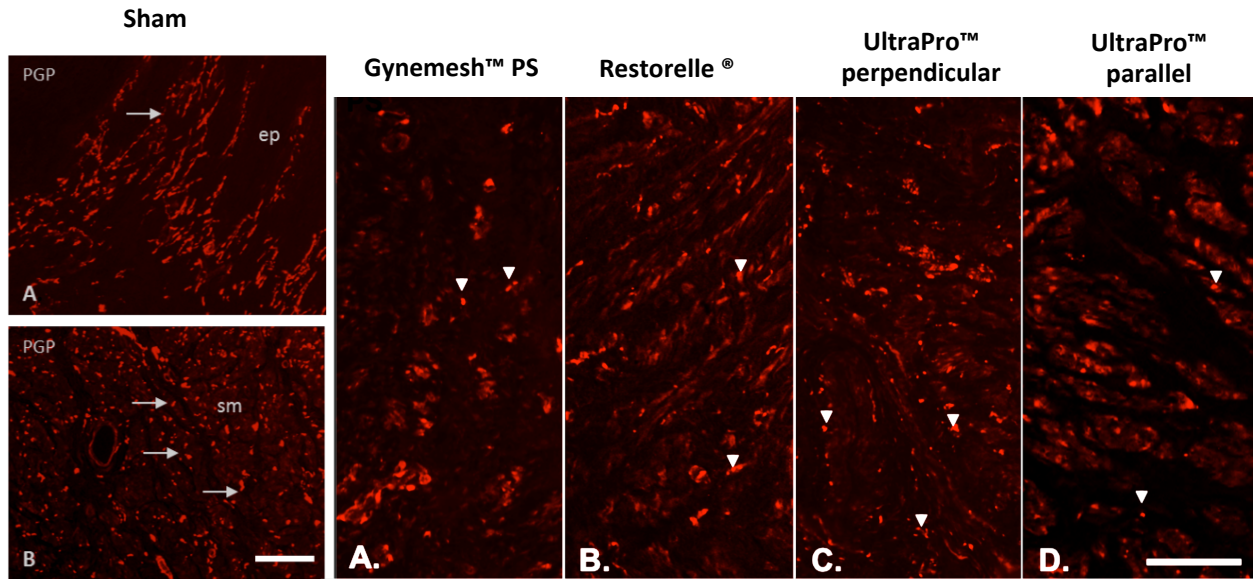


**Figure 21. Peripheral Nerve Labeling.** (Panel 1) PGP 9.5 immunolabeling (arrows: positive labeling) of cross-sections of tissue explants for the sham group, showed high levels of immunoreactivity (IR), indicative of the maintenance of peripheral nerve fibers following sham operation, localized immediately below the epithelial layer (ep) and within the smooth muscle (sm) bundles. Arrows: nerve fibers. Scale bar = 250  $\mu$ m (Panel 2) corresponding analysis of the smooth muscle layer following (A) Gynemesh™ PS, (B) Restorelle, (C) UltraPro™ perpendicular, and (D) UltraPro™ parallel showed decrease innervation density and altered innervation morphology, which was significantly different relative to Restorelle®, and UltraPro™ perpendicular ( $P < 0.001$ ,  $P < 0.001$ ,  $P < 0.001$ ), but not UltraPro™ H ( $P = 0.260$ ). Scale bar = 100  $\mu$ m.

**Table 9. Peripheral Nerve Density (%Fractional Area)**

	Peripheral Nerve Density (% Area)	
	Grafted	Non-grafted
Sham	0.53 (0.47, 0.58)	
Gynemesh™ PS	0.05 (0.04,0.05)*	0.41 (0.13,0.42)
Restorelle®	0.28 (0.19,0.30)	0.42 (0.33,0.50)
UltraPro™ perpendicular	0.25 (0.22,0.38)	0.30 (0.28,0.51)
UltraPro™ parallel	0.16 (0.15,0.17)*	0.30 (0.20,0.41)

*Values represented as mean ± standard deviation*

*\*Indicates significance relative to sham (P < .05)*

### *Cholinergic Nerves Density*

In the grafted region, cholinergic nerve density as measure by labeling with an antibody for the acetylcholine transporter, VACHT, showed that cholinergic nerve density was not significantly different from sham-operated animals ( $P < 0.093$ ). When we compared cholinergic nerve density following implantation with UltraPro™ parallel to that of UltraPro™ perpendicular, there was also no significant difference observed ( $P \geq 0.146$ ). Interestingly, in the non-grafted region, there was a significant difference between the groups ( $P = 0.009$ ). Cholinergic nerve density declined following implantation with Gynemesh™ PS, supporting the loss in nerve function, but the difference did not reach significance ( $P = 0.077$ ). Alternatively, an increase in cholinergic nerve density was

observed following implantation with the less stiff UltraPro™ perpendicular and Restorelle®, but again, the increase was not significant ( $P = 0.055$ ,  $P = 0.099$ ). However, when we compared the cholinergic nerve density in UltraPro™ parallel to that of UltraPro™ perpendicular, a significant difference was observed ( $P = 0.028$ ), which may explain the trend towards an increase in nerve density with the less stiff UltraPro™ perpendicular and Restorelle® (**Table 10**).

#### *Adrenergic Nerves Density*

In the grafted region, adrenergic nerve density as measured by TH was significantly different between the groups ( $P < 0.008$ ). Specially, the grafted region of Gynemesh™ PS and UltraPro™ parallel had significantly less nerves relative to sham ( **$P = 0.004$ ,  $P = 0.013$ , Table 10**), while Restorelle® and the less stiff UltraPro® perpendicular were not significantly different from sham ( $P = 0.848$ ,  $P = 0.121$ ). However, when we compared adrenergic nerve density in UltraPro™ parallel to that of UltraPro™ perpendicular, there was no significant difference ( $P < 0.464$ ). In the non-grafted region, there was also a significant difference in adrenergic nerve density between the groups ( $P = 0.005$ ). Similar to the grafted region, nerve density decreased following Gynemesh™ PS implantation and UltraPro™ parallel implantation ( $P = 0.004$ ,  $P = 0.011$ ), but there was no significant difference following implantation with Restorelle® or UltraPro™ perpendicular ( $P = 0.848$ ,  $P = 0.121$ ). Also, when we compared adrenergic nerve density in UltraPro™ parallel to that of UltraPro™ perpendicular, it was not significantly different ( $P < 0.223$ ).



### *Relationship Between Mesh Properties and Smooth Muscle Outcomes*

To determine if there was any association between mesh properties and the smooth muscle outcome measures (muscle contraction, innervation, receptor function, and nerve density), a correlation analysis was performed. The results showed that mesh stiffness was negatively correlated with all smooth muscle functional outcome measures, in both the grafted and non-grafted regions [Spearman  $\rho = -0.567$  ( $P = 0.001$ ),  $\rho = -0.718$  ( $P < 0.001$ ),  $\rho = -0.444$  ( $P = 0.018$ ), Spearman  $\rho = -0.398$  ( $P = 0.029$ ),  $\rho = -0.398$  ( $P = 0.029$ ),  $\rho = -0.398$  ( $P = 0.029$ )], respectively. Similar to mesh stiffness, mesh weight was also negatively correlated to all the smooth muscle outcome measures, but only in the grafted region [Spearman  $\rho = -0.427$  ( $P = 0.019$ ),  $\rho = -0.711$  ( $P < 0.001$ ),  $\rho = -0.605$  ( $P = 0.001$ )], while mesh porosity was positively correlated with smooth muscle outcomes in the grafted region [Spearman  $\rho = 0.427$  ( $P = 0.019$ ),  $\rho = 0.711$  ( $P < 0.001$ ),  $\rho = 0.606$  ( $P < 0.001$ )]. As shown, unlike mesh stiffness, the association with mesh weight and porosity on the functional outcomes was largely limited to the grafted region, and these trends were similar for the histological analysis.

To determine if mesh textile properties could indeed serve as predictors of these surgical outcomes of interest, we performed multiple regression analyses using mesh stiffness, weight, and porosity as the independent variables, and the smooth muscle functional outcomes (muscle contraction, innervation, receptor function, and nerve density) as the dependent variables. Results from the regression analysis showed that changes in smooth muscle contraction, in both the grafted and non-grafted regions, were a function of mesh stiffness ( $P = 0.030$ ,  $P = 0.009$ , respectively), while changes in nerve and

receptor function, evident in only the grafted region, were a function of the three textile properties combined ( $P = 0.001$ ,  $P = 0.022$ , respectively). We were also able to determine that mesh stiffness, alone, was a significant predictor of peripheral nerve density in the grafted region ( $P = 0.020$ ). However analysis of the specific nerve types showed that only in the non-grafted region was adrenergic [pore size, ( $P = 0.008$ )] and cholinergic [stiffness, ( $P = 0.010$ )] nerve density a function of mesh properties (mesh porosity and mesh stiffness, respectively).

**Table 10. Cholinergic and Adrenergic Nerve Density (%Fractional Area)**

	Cholinergic Nerve Density (% Area)		Adrenergic Nerve Density (% Area)	
	Grafted	Non-grafted	Grafted	Non-grafted
Sham	0.020 (0.025, 0.045)		0.20 (0.17, 0.25)	
Gynemesh™ PS	0.011 (0.010,0.020)	0.007 (0.005,0.012)*	0.01 (0.00, 0.03)*	0.08 (0.07, 0.11)*
Restorelle®	0.051 (0.042,0.054)	0.080 (0.047,0.091)	0.08 (0.06, 0.09)	0.23 (0.18, 0.30)
UltraPro™ perpendicular	0.052 (0.057,0.065)	0.096 (0.067,0.129)	0.14 (0.04, 0.17)	0.14 (0.13, 0.14)
UltraPro™ parallel	0.023 (0.005,0.048)	0.011 (0.016,0.022)	0.01 (0.00, 0.03)*	0.13 (0.09, 0.13)*

*Values represented as mean ± standard deviation*

*\*Indicates significance relative to sham ( $P < .05$ )*

#### 4.4 DISCUSSION

Synthetic polypropylene mesh, use for prolapse surgeries, was originally adopted by clinicians because of the long term anatomical support that it provides to the prolapsed vagina following failure of its fibromuscular support [13], [160]. As clinical successes associated with the use of mesh increased, widespread use of mesh ensued, as well as the advent of multiple mesh products onto the market. In 2010, the number of surgeries being performed annually had reached an estimated 100,000, and this figure is expected to double by 2050 [9]. However, the increased use of mesh has been paralleled by rising complication rates, which has prompted the need for studies aimed at elucidating possible sources of complication [161], [162]. Our initial studies investigating the impact of mesh implantation showed that mesh increases smooth muscle cell apoptosis, and decreases smooth muscle thickness and function in the underlying vagina and newly incorporated tissue [15], [155]. This current study, which uses detailed functional and histological analysis, expands upon our previous findings to further show the negative impact of mesh on vaginal smooth muscle contraction, innervation, receptor function, and innervation density. In addition, this study shows that the impact extends beyond the grafted tissues, and that the degree of impact is a function of the mesh properties, most notably, mesh stiffness. The results are intriguing, but also highly relevant as the meshes evaluated are all currently being used clinically, including Restorelle® (Coloplast), UltraPro™ (Ethicon), and the gold standard mesh, Gynemesh™ PS (Ethicon).

These meshes, which exhibit distinct textile and mechanical properties, are used interchangeably in clinical settings, but behaved very differently following implantation. As noted in the results, it was immediately apparent upon excision of the mesh implanted vaginas, that the less stiff UltraPro™ perpendicular and Restorelle® were better incorporated into the tissue than the stiffer Gynemesh™ PS, which appeared buckled and surrounded by a connective tissue capsule. This surprising finding is supported by recent studies, which show that less stiff implants do reduce macrophage activation, and elicit a less severe foreign body response (FBR), relative to their stiffer counterparts [163]. Although in-vivo studies are few, more data is available on in vitro models, which show that stiff substrates do indeed promote increased macrophage phagocytosis, migration, proliferation, differentiation, adhesion, and expression of the pro-inflammatory cytokine, TNF- $\alpha$  [164]–[166]. This suggests, that the stiffest and heaviest mesh implanted, Gynemesh™ PS, was the most vulnerable to eliciting an immense FBR, irrespective of surgical technique. These initial findings, although superficial, were in essence, indicators and possibly contributors to the more robust remodeling occurring within the tissues, as subsequent evaluations of the smooth muscle layer, also showed these mesh specific differences [167].

Of note, implantation with Gynemesh™ PS was shown to cause the most significant disruption of the smooth muscle bundles, and the greatest loss in muscle thickness, especially in the grafted region. This decline was also evident in the functional response to KCl, but again, to a greater degree in grafted region. UltraPro™ parallel, which has comparable stiffness to that of Gynemesh™ PS, had a similar degree of impact, while less stiff Restorelle® had less of an impact, and the least stiff mesh, UltraPro™ perpendicular,

had no negative impact. Interestingly, in the non-grafted region, UltraPro™ perpendicular exhibited the potential to cause an increase in the smooth muscle contractile response. As shown, the observed responses mirrored the stiffness profiles of the meshes, and upon statistical evaluation, mesh stiffness proved to be a significant predictor of smooth muscle function in both the grafted and non-grafted regions. Based on the principle of stress shielding, it can be postulated that the high stiffness meshes Gynemesh™ PS and UltraPro™ parallel likely shielded vaginal smooth muscle from sensing their normal physiologic loads, thus leading to disuse, and in turn, atrophy. This is similar to the case where the implantation of very stiff stents, which off-loaded the arterial wall, induced tortuosity, and in some cases, rapid and extensive atrophy of arterial smooth muscle, while less stiff stents caused increased proliferation and arterial occlusion [168]–[173].

This observed decline in myogenic contraction is indicative of a loss of myofiber integrity, but additional steps were also taken to evaluate the impact of mesh on nerve function. Upon evaluation, the results showed that the greatest change in neurogenic contraction occurred in the grafted region, following implantation of Gynemesh™ PS. The results also showed that the observed changes in neurogenic contraction were a function of not only mesh stiffness, but also of mesh weight and porosity. This is particularly important since women with POP have an overall paucity of peripheral nerves [174]. The results from the evaluation of nerve function suggests that mesh implantation could either be inducing changes in the amount of neurotransmitter binding to the receptors, changes in the number of nerves being stimulated, or both. Our analysis of muscle receptor function showed changes in the number of receptors were also occurring, as there was a significant impact of mesh implantation on muscarinic receptors in both the grafted and non-grafted regions.

Corresponding to the trends in nerve function, the greatest decrease in receptor function was observed following implantation with Gynemesh™ PS. As in the case of nerve function, the regression analysis also showed that changes in receptor function were governed by mesh stiffness, weight, and porosity, but only in the non-grafted region. The results in essence, show that Gynemesh™ PS, which has the greatest stiffness, weight, and least porosity was again more prone to eliciting the greatest negative impact on nerve function, and supports the likelihood that may have been via the upregulation of the muscarinic receptors.

As previously mentioned, however, changes in nerve function could also have been influenced by changes in nerve density. Results from the quantification of PGP 9.5-IR nerves showed that peripheral nerve density in the grafted region significantly declined following implantation with Gynemesh™ PS and UltraPro™ parallel, but not following implantation with UltraPro™ perpendicular and Restorelle® was significant. The regression analysis further showed that the decline in peripheral nerve density was a result of only mesh stiffness, and not mesh weight or porosity as was observed with nerve and receptor function. The results appear to be in support of the conclusion that the decline in peripheral nerve density may be the cause of, or the result of the previously reported decline in myofiber function, as myofiber function was also a function of mesh stiffness. Hence, more specific probing of dominant cholinergic showed that implantation with Gynemesh™ PS significantly decreased cholinergic nerve density in both the grafted and non-grafted regions, while implantation with UltraPro™ perpendicular and Restorelle® caused an increase in cholinergic nerve density, albeit non-significantly [175]–[178]. Taken together, the results support the conclusion that high stiffness meshes can have a negative

effect on cholinergic nerves, as in the case of Gynemesh™ PS, but that lower stiffness meshes may have the potential to maintain or increase nerve density.

The probing of cholinergic nerves were followed by subsequent analysis of adrenergic nerves, which showed that implantation with Gynemesh™ PS and UltraPro™ parallel significantly decreased adrenergic nerve density in both the grafted and non-grafted regions. The presence of a significant difference in both the grafted and non-grafted regions, suggest that adrenergic nerve density may be the most vulnerable to injury, and that it's loss may precede, and possibly orchestrate changes in the other smooth muscle components. This is further supported by a recent study by Northington et al., which showed that women with POP exhibit a complete loss of response to the  $\alpha_1$ -adrenoreceptor agonist, phenylephrine, relative to non-prolapse controls. Additionally, the study also found that the proportion of co-localized  $\alpha_1$ -adrenoreceptors and smooth muscle  $\alpha$  actin was significantly less in women with POP compared to non-prolapse controls [179]. Therefore perseverance of adrenergic nerve density following implantation with UltraPro™ perpendicular and Restorelle®, vs Gynemesh™ PS and UltraPro™ parallel, may explain the more favorable outcomes shown. Alternatively, the observed decline in adrenergic nerve density following Gynemesh™ PS and UltraPro™ parallel implantation may explain the gross negative impact on VaSM, by the influence of mesh stiffness.

Overall this study shows that mesh stiffness and weight are negatively correlated with smooth muscle outcomes, while porosity is positively correlated with muscle outcomes, supporting the transition as seen clinically, to light-weight and large pore meshes. It is possible that the impact of one of these negatively correlated mesh properties could prove tolerable, but a mesh exhibiting a combination of them, as shown in the case of

Gynemesh™ PS, could lead to a major negative impact on VaSM. It is unclear exactly how long this negative remodeling process takes place and complications like mesh exposures ensue. It is likely, however that for most meshes, it proceeds to a point where the forces equilibrate and the remodeling response reaches homeostasis, as most women do not experience a mesh exposure. However, this study's utilization of a non-human primate model, which is a highly acceptable model for pelvic floor disorders, findings can serve as a guide when designing future clinical studies to further evaluate sources of complications. Additionally, the results could prove useful when designing *de novo* meshes aiming to improve the occurrence of the post-operative degenerative effects following surgical mesh placement. Future work will involve more studies to explore the mechanisms of mesh impact, and methods to reduce stress shielding, in an effort to improve smooth muscle outcomes.



## **5.0 AFTERWORD**

### **5.1 SYNOPSIS**

Smooth muscle cells (SMCs) line the walls of hollow organs the like blood vessels, intestines, and remarkably, the vagina. These cells, which are modulated by environmental cues, involuntarily contract and are essential for maintaining the tone of the organs they occupy. Hence, their dysfunction has been linked to multiple pathologies [81], [127], [148], [180]–[182]. Pelvic Organ Prolapse (POP), a dysfunction characterized by the decent of the pelvic organs into the unsupported vagina, has also been linked to changes in smooth muscle thickness, structure and function. The studies characterizing these changes in the vaginal wall of women with prolapse, were unable to determine their onset, hence it is unclear whether these changes play of role in the progression of the dysfunction, or are the result of its progression. With the anticipated increase in the number of women presenting with POP, due to a rise in the aging population in the US, coupled with the increased incidence of complications from surgically implanted mesh used to restore support to the pelvic organs that recently prompted FDA warnings, there is an increased need to fully understand the mechanisms of POP development. In this thesis work, using principles rooted in pharmacology, mechanobiology, and biomechanics, we explore how vaginal birth injury, a major risk factor the development of POP, could induce changes in smooth muscle

function, and how these changes could play a role in the progression of the disorder. Additionally, we examined the ability of prolapse meshes currently being used clinically, to improve smooth muscle integrity.

### *Vaginal Delivery with Injury Alters VaSM Function*

The goal of the Aim 1 was to pharmacologically and immunohistologically assess the recovery of vaginal smooth muscle (VaSM) innervation, contraction and receptor function following a simulated maternal birth injury in a rodent model. For the study, sixty female Long Evans rats underwent a simulated maternal birth injury. At 4-weeks and 8-weeks post-injury vaginal tissues were harvested and divided into proximal, middle, and distal segments, and the force generated following KCl, phenylephrine (PE), carbachol (CCh), and electrical field stimulation (EFS)-induced contractions were evaluated. Histological evaluations of muscle morphology and peripheral nerve fiber density were also performed. In the proximal vagina the thickness of the vaginal wall significantly increased ( $P = 0.010$ ) by 4 weeks, and marginally recovered by 8 weeks post injury ( $P < 0.062$ ), however the location along the vagina where gross laceration had occurred did not recover. Comparison of the functional parameters between the 4 and 8-week groups also showed a significant increase in  $EC_{50}$  ( $P = 0.001$ ,  $P = 0.069$ ) in response to KCl in the proximal and middle vagina, a decrease in  $E_{max}$  ( $P = 0.002$ ,  $P = 0.005$ ) in response to CCh in the proximal and middle vagina, and a decline in the  $EC_{50}$  in the distal vagina ( $P = 0.011$ ) in response to PE. The results also showed a corresponding decrease in  $E_{max}$  in the proximal and distal vagina ( $P = 0.034$ ,  $P = 0.032$ ), with a persistent decline in the middle vagina in response to EFS ( $P =$

0.758). The results show a trend of increasing increase muscle hypersensitivity, decreasing density of cholinergic receptors in the proximal and middle vagina, and increasing adrenergic receptor sensitivity, perhaps as a result of a persistent loss of nerve function.

### *VaSM Function Influences Vaginal Biaxial Mechanics*

The next aim was to determine changes in the biaxial mechanical properties of the vaginal following a loss of VaSM function, as has been shown to be the case, following birth injury. For the study 6 virgin female Long Evans rats at 3-month old virgin were biaxially tested in the presence of a physiologic Krebs'-bicarbonate buffer, a high potassium muscle depolarizing solution (KCl), and a  $\text{Ca}^{2+}$  free Krebs'-bicarbonate supplemented with a calcium chelating solution (1 mM EGTA), to capture baseline (resting tension), activated (tonic contraction) and passivated (relaxed) smooth muscle states. For analysis, stress-strain curves were generated based on the Green-Lagrangian strains calculated from the marker displacements, for both the circumferential ( $\epsilon_{\text{Circ}}$ ) and axial ( $\epsilon_{\text{Axial}}$ ) direction. Multi-photon imaging of collagen, elastin and smooth muscle were also done, and the percent collagen crimp determined. The outcomes were analyzed using a one-way analysis of variance (ANOVA), with Bonferonni correction ( $P < 0.05$ ). The results showed that the vagina is hyperelastic and anisotropic, with the circumferential direction being significantly less stiff than the axial direction ( $P = 0.020$ ), and strained less ( $P = 0.034$ ). On average, there were differences in the shape of the stress strain curves, most impressively in the circumferential direction, where VaSM smooth muscle activation was associated with a 36% decrease in tensile modulus in the axial direction ( $P = 0.74$ ), and a 9% decrease in the

modulus in the circumferential direction ( $P = 0.87$ ). There was also very little difference observe in the areal strain or the anisotropic index. However, there was a trend during non-equibiaxial loading, toward increasing areal strain and decreasing anisotropy following smooth muscle contraction. The results also showed a governing role of strains in the circumferential direction on strains observed in the longitudinal direction, which may be indicative of the preferred orientation of the collagen and elastin. These findings show the potential of the loss of vaginal smooth muscle to cause an increase in tissue stress at low physiologic levels of strain, due to the absence of its protective ability to redistribute stress between the axes. These changes could cause resident cells to induce a catabolic response in an attempt to restore physiologic strains, resulting in tissue degeneration.

#### *Prolapse Meshes Negatively Impact VaSM Function*

The final aim was to evaluate the impact of polypropylene mesh on vaginal smooth muscle structure and function, and to evaluate these outcomes in the context of mesh textile and mechanical properties. For the study, thirty-eight parous Rhesus Macaques with similar age, parity and pelvic organ prolapse quantification (POP-Q) scores were implanted with mesh via sacrocolpopexy. Three months following implantation of the 3 polypropylene prolapse meshes with distinct textile and mechanical properties, mesh tissue explants were evaluated for smooth muscle contraction, innervation, receptor function, and innervation density. The maximum contractile force generated following muscle, nerve, and receptor stimulation, and for peripheral nerve density for each explant was recorded. The impact of Gynemesh™ PS (Ethicon; N=8), Restorelle® (Coloplast; N=8),

UltraPro™ parallel, and UltraPro™ perpendicular (Ethicon; N=6, N=8), were compared to sham-operated controls (N=8). The outcomes were analyzed by Kruskal-Wallis ANOVA, Mann Whitney U tests, and multiple regression analysis ( $P<0.05$ ). The results showed that muscle, nerve, and receptor mediated contractions were negatively impacted by mesh only in the grafted region ( $P<0.001$ ,  $P=0.002$ ,  $P=0.008$ ), while cholinergic and adrenergic nerve density were impacted in the grafted ( $P=0.090$ ,  $P=0.008$ ) and non-grafted ( $P=0.009$ ,  $P=0.005$ ) regions. The impact varied by mesh-property, as mesh stiffness was a significant predictor of the negative impact on muscle function and nerve density ( $P=0.030$ ,  $P=0.009$ ), while mesh density, weight and porosity (combined) were predictive of nerve and receptor function ( $P=0.001$ ,  $P=0.022$ ). Overall, this aim showed that mesh has an overall negative impact on vaginal smooth muscle, and that the effects are a function of mesh properties, most notably, mesh stiffness.

## 5.2 IMPLICATIONS

### *Basic Science Implications*

Stress is known to influence growth, adaptation and morphogenesis in many organs, and the vagina is no exception to this dogma. The vagina, a load bearing structure, suspends above the rectum and is kept in tension through its ability to dynamically contract against the levator ani muscles via its connective tissue attachments. In turn, the vagina provides support to the bladder, urethra, cervix and rectum. Hence, changes in the mechanical properties of the vagina or the vagina supportive connective tissues (VSTC),

could hamper its ability to adequately support these organs, thus compromising pelvic organ support. As mentioned, VaBI, which is one of the major risk factors of POP, has the potential to impact multiple mechanical components of the vaginal and the VSTC. However our initial investigation of changes in the passive mechanical components of the VSTC **(Appendix I)**, showed that the effects of injury on the passive components does not worsen with time post-injury, which may limit its effects as a pathogenic factor. However our investigation of VaBI on vaginal smooth muscle showed persistent loss of smooth muscle function with time-post injury. Hence, we further aimed to evaluate the impact of changes in smooth muscle function, as these persistent changes in vaginal smooth muscle mechanics could be driving a degenerative remodeling process and the eventual loss of pelvic organ support.

The results from chapter 3 indeed attest to the potential of changes in vaginal smooth muscle to alter vaginal wall mechanics, and the tension on connective tissues and ligamentous attachments. This is due to the ability of smooth muscle to dynamically sense and respond to changes in force, as exhibited in other mechanical organs like the bladder, duodenum and arteries [128], [183], [184]. As noted, a loss of smooth muscle contraction is associated with decreased compliance in the bladder, increased stiffening and decreased motility in the duodenum, as well as increased stiffening of the arteries. Shown in this work, is that a loss of smooth muscle function in the vagina, as evident following VaBI, could also result in increased stiffening of the vaginal wall, due to more rapid recruitment of collagen and elastin fibers. This rapid recruitment of collagen fibers, would then subject fibroblast and smooth muscle cells localized within the matrix to increased strains under physiologic loads. These cells interact with their matrix through distinct patterns of

signaling and migration, and can quickly detect changes in tensional homeostasis induced by changes in smooth muscle function [185]–[187]. The mechanostat set point of these cells are calibrated to the physiologic tensional homeostasis of the tissue, and catabolic mechanisms are activated when strain induced signals are below the set point, while anabolic mechanisms are activated when the signal is above the set point [188]–[190]. These catabolic and anabolic mechanisms are highly regulated by the balance between matrix metalloproteinases (MMPs) and their inhibitors (TIMPs). It is also possible that anabolic and catabolic mechanisms could persist due to failure to restore homeostasis, which is highly probable following VaBI, as smooth muscle contractile function continues to decline.

Not surprisingly, functional evaluation of the active mechanics of tissues from women show a decrease in smooth muscle contractility (when normalized to tissue area) in prolapse tissues relative to non-prolapse tissues [179]. Additionally, our finding that actinin, which aids in smooth muscle active tension development through binding of actin filaments and  $\beta$ -integrins, declines, offers even more substantial evidence towards the association of VaBI and the development of POP [191]. Also as previously mentioned, women with POP exhibit a decline in lysyl oxidase like-1 (LOXL1) expression. These changes in LOX expression, can alter the stiffness of the collagen fibers, hence it is another mechanism used by cells to restore mechanical homeostasis. Specifically, findings of a decline in LOX, supports the increased stress observed following smooth relaxation in chapter 2, as a decline in LOX expression would aid in lowering the stress environment in women with POP following a loss of smooth muscle. Interestingly, however, the application of surgical mesh for repair, leads to a subsequent alteration of the vaginal wall. As shown in

chapter 3, mesh stiffness significantly influenced smooth muscle outcomes, as the high stiffness meshes were associated with a greater loss of smooth muscle contractile function. The findings were theorized to be attributed to a stress-shielding phenomenon, similar to that observed in the cardiovascular literature [168]–[173]. This is further substantiated by Holzapfel et al. report of varying mechanical properties of the intima, media and adventitia of the coronary artery, which is comparable to the subepithelium, muscularis, and adventitia of the vagina [192]. The adventitia was found to be the least stiff, which is postulated to be essential as the adventitia engages under load, only after the media has been subjected to large strains, in order to prevent additional distention. Hence, it is likely that for the vagina, following the implantation of a stiff mesh onto the vaginal adventitia, the adventitia engages much earlier when subjected to loading thus shielding the muscularis from physiologic loads.

Numerous studies have in the cardiovascular and orthopedic fields have revealed this thin line between degenerative and regenerative remodeling, as a result of physiologic versus non-physiologic strain levels. An in vitro study on tendon cells by Yang et al. showed that for a load bearing structure like the tendon, strain magnitudes  $\leq 6\%$  can provide a protective effect, while strain magnitudes of  $\geq 8\%$  can prove detrimental with an increased expression of MMPs and other pro-inflammatory markers in an attempt to reorient and remodel the matrix to reduce strains [193]. Interestingly, a previous study from our laboratory also showed that vaginal fibroblast are mechanosensitive, with strain magnitudes of 8% and 16%, capable of increasing MMPs expression, relative to non-stretched controls [194]. Hence, a loss of smooth muscle function following VaBI, could indeed precede the eventual degenerative remodeling of the vagina leading to POP. The



results from this work also suggest that VaBI, may increase the odds of incurring a strain induced injury during a subsequent vaginal delivery, as the stress dampening effect provided by the smooth muscle function would be lacking. Additionally, as shown in Appendix I, VaBI is also associated with delayed or inadequately healing of the vagina supportive connective tissue complex (VSTC), which can also increase the risk of a subsequent injury. This supports clinical data showing that the odds of developing POP, increases with each subsequent delivery [29]. VaBI also did however; prevent post-partum recovery of the VSTC, which may be an alternate mechanism through which the vagina may be subjected to stress shielding. This would also, in turn, result in a time-dependent degenerative remodeling process that could manifest with time or hormonal withdrawal.

Overall this work provides major insights into the role of smooth muscle in the pathogenesis of POP, which is seldom evaluated. More broadly, this work has major implications for field of mechanobiology. The theoretical basis for this is that changes in active mechanics (smooth muscle) following VaBI can also lead to alteration of the passive mechanics (collagen and elastin), promoting the upregulation of MMPs, and a decline in TIMPS and LOX leading to decreased mechanical properties [197]. Additionally, with POP being significantly correlated with hormonal status, a factor, which can also influence the expression of these enzymes, it provides multiple avenues for which smooth muscle could influence tissue remodeling and the ultimate manifestation of POP. This theory also aligns well with our findings in Chapter 3, that a loss of smooth muscle can increase stiffness, hence the disruption of the matrix by an upregulation of these matrix degrading enzymes, and decreased expression of the crosslinking enzyme could be mechanisms to reduce the stiffness of the matrix, in order to lessen load transfer to resident cells.

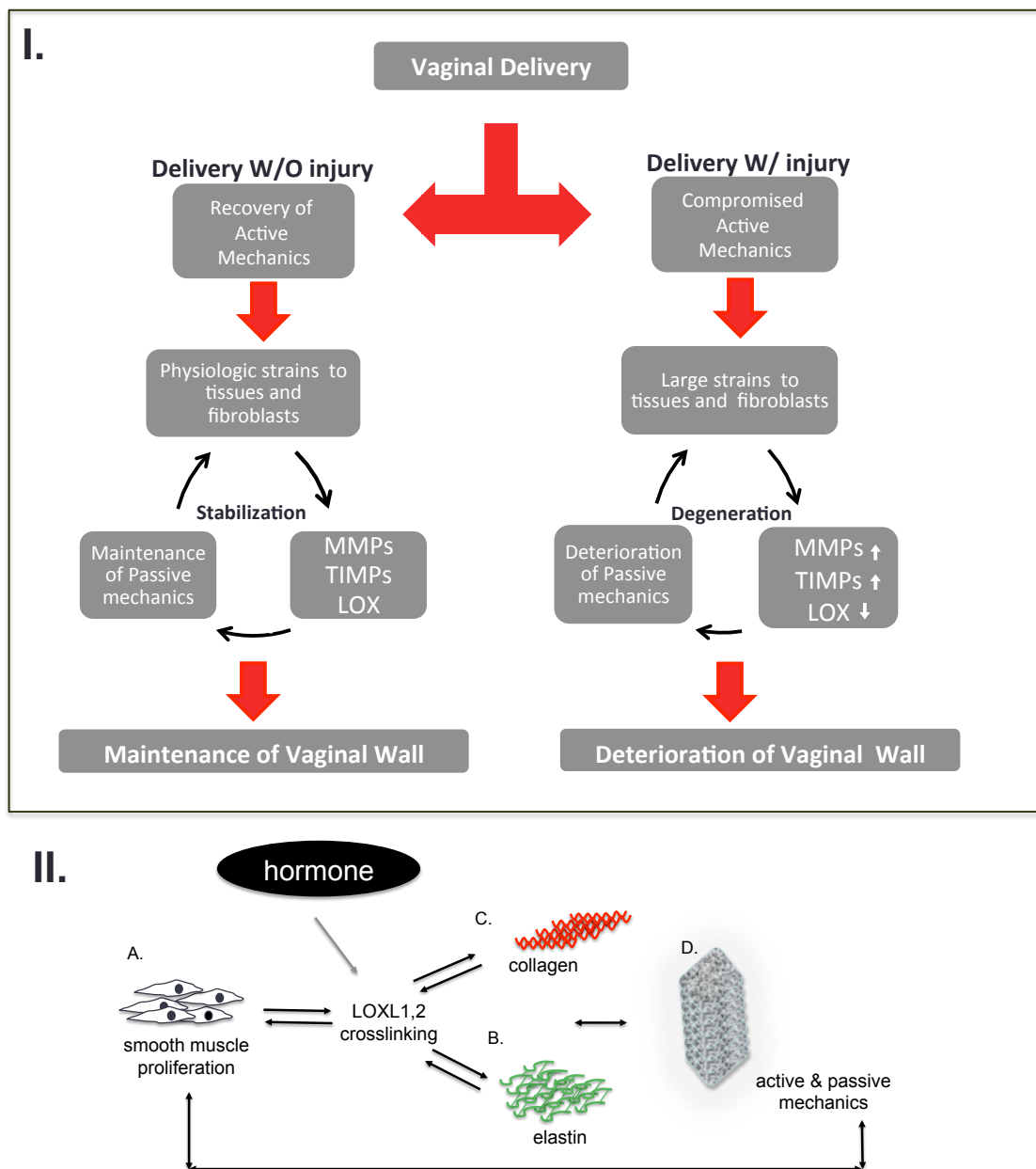


**Figure 22. Theoretical Framework.** VaBI can lead to a degenerative remodeling process, due to changes in the loading environment following the compromise of the active mechanics (smooth muscle) **(I)**. The underlying mechanism, of which is governed by the potential for changes in the active mechanics to alter changes in the passive mechanics **(II)**.

### *Clinical Implications*

Millions of women, in the United States and worldwide, presenting with POP have difficulty defecating and-or urinating, in addition to some degree of sexual dysfunction, which can result in decreased quality of life and depression [4], [5]. In the United States, the number of women who underwent surgery for POP was 28.9% in 2010, and with the expected increase in the elderly population; this figure is expected to double within the next 30 years [10] . As last reported in 1997, the direct annual cost for those that do seek surgical intervention, is over a billion dollars, and this figure is also expected to increase [11]. This rather exorbitant figure includes the cost of surgery performed for symptom management, and does not include strategies which address the underlying cause of the dysfunction, as it remains elusive. It is not surprising then, that within a few years, over 10% of repairs requires a second procedure, and is associated with complications that recently prompted FDA warnings [6], [23]–[25]. Hence, the studies which form the body of this thesis work is clinically relevant, as provide evidence to the support the role of smooth muscle as a pathogenic factor of POP, thus making it a potential target for clinical intervention for treatment and preventative strategies. Specifically, this work shows that vaginal injury during delivery, can lead to a steady decline in smooth muscle function, which can compromise vaginal support of the pelvic organs. In addition, it shows that surgically implanted meshes, designed to restore the unsupported organs to their anatomical position, have mechanical and textile properties that further promote a loss of VaSM.

The basis for this investigation is rooted in findings of numerous clinical studies showing the high association between vaginal delivery, and pelvic organ support. The findings, which were recently summarized in a publication by the International Continence Society (ICS), showed with Level I and Level II clinical evidence that vaginal delivery can impact the alignment, tone, attachment, and innervation of the vagina and its supportive tissue complex (VSTC) [198]. With only a percentage of women delivering vaginally, presenting with symptoms of prolapse, many clinical studies have focused on understanding the specific factors during delivery that may predispose a cohort of women to develop POP, especially with the rise in elective caesarian delivery to obviate the risk of POP [29], [32], [34], [47], [55], [199]. Injury emerged as a relevant predictor of a loss of pelvic organ support postpartum, as characterized by increased mobility. More specifically, these studies showed that rates of injury are increased with forceps delivery, multiparty, longer second-stage of labor, third-degree perineal tear, and macrosomia, but the exact mechanism remains elusive, and individual study results are conflicting. Hence, this work is essential as it aids in bridging the gap between vaginal injury during delivery, and the loss of pelvic organ support. More importantly, it identifies smooth muscle injury occurring during delivery, as a key pathogenic factor, irrespective of vaginal injury mode.

These findings paired with a study from Dietz et al. which showed that pelvic organ mobility antepartum was negatively associated with postpartum bladder ( $r = -0.52$ ), rectal ( $r = -0.60$ ), and cervical ( $r = -0.54$ ) descent, show the potential to design effective preventive measures [125]. Women at risk of incurring an injury during delivery could be easily identified, and offered alternate delivery options. . The correlation for the study was analyzed from outcomes obtained from evaluations at the third trimester of pregnancy and

2 months postpartum. These findings are further supported a study showing that the risk of incurring a sulcus tears, similar to the tear evaluated in this thesis work, are present even before pregnancy [37]. This is in contrast to, third and fourth-degree tears which are also preventable as they are related to physician management. The subset of women undergoing sulcus tears were also reported to have a trend toward less weight gain during pregnancy, fewer episiotomies, and lack of employment, and perhaps a lower socioeconomic status as there also had a trend towards lower mother-weight, mother-height, and birth weight. These findings have been further substantiated by more recent studies showing that body mass index, socioeconomic status are independently associated with POP, at a 95% confidence interval [200]. The assertion by the authors that the inadequate maternal adaptation may be related to lower social economic status through nutrition is indeed merited as changes in nutrition can influence hormonal levels, with down-stream effects.

It is known that diabetic women (type 1 and type 2), exhibiting high blood glucose levels have a 1.7 – 6.20 odds ratio of undergoing a c-section compared to women in the general population [201]. The elevated glucose levels have been shown to alter hormonal levels, which may increase in LOX and LOXL1 (elastin & collagen crosslinkers) mRNA expression, which can result in decreased antepartum mobility in addition to the inhibition of other necessary maternal adaptations [202]–[205]. This is further supported by studies, which show that the overexpression of LOX inhibits the phenotypic switch of smooth muscle from a contractile to a proliferative phenotype that is necessary for adaptations during pregnancy, as it allows for increased SMC proliferation and elastin synthesis [197]. It is possible that in the absence of adequate vaginal smooth muscle adaptation, it becomes

injured, initiating a cascade of degenerative events. The findings of this thesis suggest that these events could be a result of changes in the mechanical environment, nevertheless clinical analysis of antepartum pelvis organ mobility, nutrition, and increased physician training identified by Dietz and others, could serve as preventative measures **(Figure 22)**. In addition, the results from this work suggests that other preventative measure including lab tests similar to those utilized to predict cardiovascular risks, could prove beneficial for predicting the risk of birth injury, and hence prove beneficial for effectively selecting women who would benefit from a caesarean delivery. This lack of effective selection may be driving the conflicting results regarding the benefits of caesarean deliveries, as a caesarean may not be more beneficial relative to a vaginal delivery with following adequate maternal adaptations. The predictive biomarkers of interest could be similar to those being used to evaluate cardiovascular risk, as it is also characterized by increased smooth muscle proliferation and differentiation.

The finding from this work also suggest that smooth muscle could serve a marker for the evaluation of the efficacy of treatments methods for POP, and thus steps were taken to evaluate the impact of currently used meshes for POP. The results in Chapter 3, showed that meshes which were being used interchangeably, for POP repair, can compromise smooth muscle function, to varying degrees, with the single, most independent predictor of negative smooth muscle outcomes being increasing mesh stiffness. The results are not surprising, as the mechanical and textile requirements for gynecologic use have not yet been established, and to date, currently available meshes including the terminology “lightweight”, are all based on biomechanics parameters of the abdominal wall due to their class II classification so these light-weight meshes may indeed still be too heavy and stiff

for the vagina. Synthetic polypropylene meshes for prolapse surgeries was originally adopted by urogynecologic clinicians because of the long-term anatomical support that it provides to the prolapsed vagina following failure of its fibromuscular support [206]. As clinical successes associated with the use of mesh increased, widespread use of mesh ensued, as well as the advent of multiple mesh products onto the market. In 2010, the number of surgeries being performed annually had reached an estimated 100,000, and this figure is expected to double by 2050 [9]. However, recent reports indicate that the number of cases involving vaginal mesh erosion and or exposure ranges from 7-10%, with very little understanding as to the source of these complications [207]. These findings along with increased incidence of pain, dyspareunia, and reoccurrence prompted the FDA to release a warning in 2008, with a following in 2011, stating that mesh complications are not rare events.

Similar to mesh use for POP, at the onset, mesh use for hernia repair were published as having excellent outcomes, and so little emphasis was placed on mesh properties, but instead on surgical techniques. However, when synthetic mesh use for hernia repairs increased, as well as cases reporting complications following mesh procedures, numerous experimental studies and clinical observations began in 1995 to improve the understanding of the physiology and the mechanics of the abdominal wall in order to define the biomechanical requirements for successful integration into the host tissue [208]. Therefore, the new generation of lightweight and large pore meshes introduced for hernia repairs, had design criteria based on biomechanical studies showing that under normal physiologic load of 16 N, the abdomen undergoes 11-32% strain (normalized deformation) [209]. These mechano-physical requirements set the design criteria for abdominal hernia

meshes. Further, it was determined that the tensile strength of surgical meshes for abdominal wall placement for large vs small hernias be different, due to the differences in the support needed for each repair, as further surgical guidelines. Hence more work to understand the mechanics specific to the vagina, are needed to design optimally performing meshes, with design characteristics that can improve muscle outcomes. In 2011, the FDA warnings were followed by orders to tentatively reclassify urogynecologic meshes from class II to class III, medical devices requiring premarket approval (PMA), or notice of completion of a product development protocol (PDP). Therefore, the findings of this study are also chronologically relevant, and could begin to offer some preliminary guidelines, in an effort to meet the FDA's new requirements.

### **5.3 LIMITATIONS AND FUTURE DIRECTIONS**

This thesis aided in answering lingering scientific and clinical questions regarding the pathogenesis and treatment of POP, but there were limitations and unanswered questions.

Our investigation of the impact of birth injury on VaSM was evaluated following a simulated birth injury in non-pregnant rodents, which may vary from humans, and does not capture the hormonally induced mechanical adaptations present during delivery. More research is needed to therefore evaluate these outcomes in the presence of these adaptations. Evaluations were also limited to vagina, exclusive of its fibromuscular structures (i.e the paravaginal attachments), but these structures may have also sustained injuries, and may directly influence changes in pelvic floor support or via changes in VaSM.



Likewise, more studies are needed to evaluate the impact of injury on these structures, and to also determine the time-dependent changes. This is particularly important, as our findings did show evidence of compensation mechanisms to maintain muscle function, hence it is unclear when these compensatory physiologic mechanisms fail and a loss of support ensues. Our model of a simulated injury was similar to a sulcus seen clinically, hence studies designed to evaluate the association between POP and sulcus tears would be worthwhile. Additionally, evaluation of biomarkers of smooth muscle remodeling on patients antepartum and postpartum patients could also provide insights. Future work could also include intervention strategies used to clinically induce the necessary adaptive mechanisms, needed to prevent vaginal injury related to inadequate adaptations.

Our follow-up study evaluated the impact of changes in smooth muscle function on vaginal mechanics, anticipated following vaginal birth injury, was also conducted in *in vitro* conditions, and may not represent in-vivo conditions, although attempts were made to mimic in-vivo physiology. Additionally, this study provides an evaluation of the effect of severe loss in muscle function which may not be clinically relevant, nevertheless it does provide insights into soft tissue mechanics that are applicable to not only the vaginal wall, but vascular, duodenal, esophageal, and bladder mechanics, from which experiments in this thesis have been adapted. The evidence of the role of smooth muscle in strain distribution between the axial vs circumferential direction are also intriguing, and may explain how changes in smooth muscle can influence changes in the vagina. More studies designed to evaluate the impact of varying degrees of smooth muscle loss will assist in understanding the progression of the potential degenerative effects. Animal models that allow for the evaluation of only the influence of the loss of VaSM in-vivo, would be ideal. Such

evaluations would be preferable in a large animal model, as the rat vaginal smooth muscle thickness is relatively thin compared to the human vagina. It is possible that a loss of smooth muscle could have more, or less significant effect when evaluated in another model. The clinically relevant degree of loss of also needed, hence clinical studies designed to evaluate VaSM function, similar to those used to evaluate levator ani function are also warranted.

Our concluding study, which evaluated the impact of currently used prolapse meshes on vaginal smooth muscle, was evaluated following implantation in a primate model. The primate model does have its advantages, but the loading condition of the mesh, in the pelvic floor, does differ from humans, although minimally. Our results, which showed that mesh stiffness was the primary factor driving smooth muscle outcomes, may have therefore been influenced by the loading conditions. Studies evaluating the loading and tensioning of meshes are therefore needed. Additionally, the results also showed the most significant impact of mesh occurred in the underlying grafted region, with minimal changes in non-grafted region. It is also unclear if changes in nerve function precede changes in myofiber and receptor function, as there is literature in support of alternate mechanisms. More studies looking at the time-dependent progression of the degenerative effects of mesh in the unsupported non-grafted region, will help in better understanding mesh failure and recurrence. As is the limitation of all animals model, no measures of pain and discomfort were obtained following implantation, and clinical studies are indeed warranted. Findings of the influence of mesh stiffness on our smooth muscle outcomes suggest possible benefits of clinical standardization of mesh tensioning, and clinical studies designed to evaluating patient outcome should follow. However, not all processes

associated with mesh implantation can be standardized, but rigorous studies evaluating best practices, could also provide further insight. More, importantly, studies designed to aid in determining ex-vivo and in-vivo characteristics of mesh needed to perform optimally irrespective of minor variances in implantation techniques are warranted.

## **APPENDIX A**

### **VAGINAL DELIVERY WITH INJURY IMPAIRS VSTC RECOVERY**

#### **A.1 INTRODUCTION**

Maternal childbirth trauma has the greatest association with the development of pelvic floor dysfunctions (PFDs) later in life, which affect millions of women in the United States and worldwide [11], [119]. The odds ratio (OR) of developing pelvic organ prolapse (POP) is reported to be ~5.6 following a spontaneous vaginal delivery, and rising as high as 7.5 following operative vaginal delivery relative to a caesarean delivery. With only a percentage of women delivering vaginally presenting with symptoms of POP, many clinical studies have focused on elucidating specific factors that may predispose to developing POP, especially with the rise in elective caesarian deliveries in an attempt obviate the risk of developing PFDs [2], [6], [34], [210]. Recently, increased effort has been directed towards injury of the levator ani muscles. However, studies, including a recent study by Peschers et al., showed that 76% of women presenting with POP do not have levator avulsions [52], [54]. While vaginal delivery may be associated with POP, it may not be independently due to levator impairment, but perhaps levator impairment, concomitant with a loss of vaginal connective tissue support, allowing for visceral protrusion through the hiatus [211].

It is well established that mechanical failure of the vagina and supportive tissue-complex (VSTC) results in a loss of support to the bladder, uterus, and rectum, though very few clinical studies have been able to capture the impact of childbirth trauma on this highly complex network of supportive tissues. As anatomically structured, vaginal suspension is maintained by the VSTC, which is contiguous with the vaginal adventitia layer and inserts posteriorly into the levator ani muscles. It could be inferred that the VSTC is likely subjected to grave insult during traumatic deliveries, due to extreme deformations, prior to transmission of forces to the mechanically more sturdy levator ani muscles. Indeed, previous work showing that changes in the mechanics of these structures, evident in women with POP and also during pregnancy, are associated with the descent and increased mobility of the pelvic organs [125]. Unfortunately, limitations associated with tissue acquisition, as well as the level of control needed to make the association between childbirth trauma and altered VSTC support, precludes clinical associations.

In order to rigorously evaluate the effects of birth trauma on the VSTC, this study utilizes a previously established birth injury rodent model [116]. This model, which employs a balloon injury to the vagina, has been widely used for mechanistic studies of stress urinary incontinence (SUI), and has been shown to replicate many of the characteristics of SUI conditions in women [49]. Simulation of birth injury in rodents is also quite standard, as they do not naturally sustain an injury during delivery, presumed to be due to the small size of the fetal head relative to the vaginal diameter. This model further excels as the rodent levator ani muscles primarily function to control the tail, allowing for the investigation of the VSTC independent of contributions of the levator ani [212]. To quantify the impact of birth injury on the VSTC, we utilized an established mechanical

testing protocol, previously used to characterize changes in the mechanical properties of the VSTC during pregnancy and following hormonal withdrawal [196], [213].

Hence, the objective of this study was to evaluate the time-dependent impact of simulated maternal childbirth trauma on the vagina and supportive tissues complex in a rodent model (VSTC), as trauma-induced alteration of the VSTC could be a mechanism whereby childbirth leads to the eventual loss of pelvic organ support.

## **A.2 PROTOCOLS**

### **A.2.1 Animals**

Approval for this study was received from the Institutional Animal Care and Use Committee (IACUC) at the University of Pittsburgh. A total of 44 three-month-old female Lewis rats were used. 32 pregnant animals arrived at gestation day 21 and were randomly assigned to injured postpartum and control postpartum (n=8 for each of Control 4-week, Injured 4-week, Injured 8-week, Control 8-week) groups. To isolate the role of maternal adaptations, three-month old virgin female Lewis rats were also divided into control and injured groups (n = 6 for each Virgin group). Injured groups underwent a simulated maternal birth trauma, as described below, and each group was sacrificed at the corresponding time-points. All rats were housed in a temperature and light-controlled room with free access to food. Variables that could be influence by injury, including weight, pups/litter, genital hiatus (GH: measured from the middle of the external urethral meatus to the posterior

midline introitus), and total vaginal length (TVL: measured from posterior fornix to the introitus) were obtained prior to injury, and post-injury at the time of sacrifice of each rat.

### **A.2.2 Simulated Birth Injury**

A simulated birth injury was inflicted, using a previously established model, which is known to mimic the vaginal trauma that typically occurs during a prolonged second stage of labor. Within 2 hours of delivery (in the pregnant groups), each animal was anesthetized and a 16 Fr catheter was inserted and inflated with 10ccs of water. The catheter was placed in the vagina but not inflated in the control groups. This volume of water had previously been shown by our group to induce a grossly observable sulcus tear. While maintaining the volume, the rats were placed supine with their pubic symphysis at the edge of the table. A 130gm weight was then attached to the end of the catheter and allowed to hang freely for 3 hours. At the end of the 3-hour period, the balloon was deflated and the catheter was removed. Post-injury care including oral intake of pain medication was carried out according to a standard protocol.

### **A.2.3 Uniaxial Mechanical Tests**

Biomechanical Testing was performed as previously reported. Briefly, the vagina of each rat was dissected along the perineal body to isolate the distal 5 mm of the vagina from the rectum and adjacent tissues. The hind limbs were then disarticulated at the acetabulum, and the spine was disarticulated above the L1 vertebra, leaving the pelvis intact. To produce suitable rigidity for clamping, the spine was potted in polymethylmethacrylate

(PMMA), such that the spine and the pelvis were aligned. The PMMA secured spine was then mounted in a cylindrical clamp and a customized soft-tissue clamp was used to secure the distal 5 mm of the vagina. The cylindrical clamp was then fixed to the base of the materials testing machine (SmartTest EMS, Enduratec, Minnetonka, Minnesota; displacement resolution .025 mm), while the soft tissue clamp was attached to a load-cell (M-1000N, Interface, Scottsdale, Arizona; resolution 0.015 N) and fixed to the linear actuator. Before each test, specimens were preloaded to 0.15 N, and then preconditioned at an elongation rate of 25 mm/min between 0 and 2 mm for 10 cycles. Following preconditioning, the specimen was loaded until failure at 25 mm/min.

Failure modes were recorded and load-elongation data sampled at 50 Hz was imported into Excel for analysis (Excel, Microsoft Corp, Redmond, Wash). All load-elongation curves in this study were shaped similarly, with a defined toe, linear, and failure regions, corresponding to when the vagina and paravaginal attachments become engaged, distended and when one or more of these structures fail (**Figure 23**). The structural properties of the vagina supportive tissue complex (VSTC) were represented by the following parameters: linear stiffness (N/mm), ultimate load at failure (N), ultimate elongation (mm), and energy absorbed to failure (N\*mm). Linear stiffness, a measure of a specimen's ability to resist deformation with tension, was defined as the steepest positive slope measured over a moving 1 mm window of elongation for each specimen. Ultimate load at failure is a measure of the maximal sustainable force of the VSTC and was defined as the highest load on the load-elongation curve. Maximal elongation was the elongation that corresponded with the ultimate load and describes the maximum distance achieved before failing. Energy absorbed to failure was defined as the area under the load-elongation curve



up to the point of failure; this parameter is also influenced by the degree of crosslinking in collagen and elastin. The yield point, the point which marks the end linear region of the curve, was also compared between groups, as this point is usually indicative of permanent deformation of the tissue.

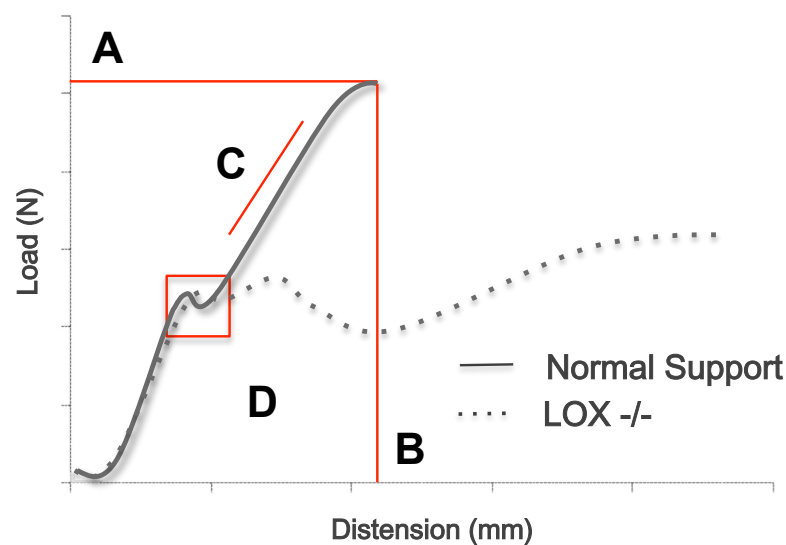


**Figure 23. Load-distension curves.** Typical curves generated from mechanically evaluating the VSTC in normal and LOX deficient mice (adapted from Alperin et al.), illustrating the potential of the mechanical tests to characterize differences in tissues resulting from pathologic conditions. Highlighted in the figure are the parameters obtained from each curve including maximum load (A), maximum distension (B), maximum stiffness (slope) (C), the energy absorbed (area under the curve). Also highlighted is the yield point or point of permanent deformation (boxed region) occurring in the tissues of LOX deficient mice at a lower load, as LOX deficient mice exhibit mechanically inferior tissues.

#### **A.2.4 Microanatomy and Histological Analysis**

To analyze the microanatomy of the vaginal wall and its connective tissue attachments to the pelvic sidewall, the pelvises of 10 rats were further dissected by dividing the pelvises along the horizontal axis. One half of the specimen was placed in 10% neutral buffered formalin for 24 hours. The pelvises were then cut in proximal, middle, and distal sections and placed in a decalcifying fixative (Cal-Ex™ II Fixative/Decalcifier, Fisher Chemical) for 48 hours. Following decalcification, the sections were embedded in paraffin blocks and sections were obtained at thicknesses of 5-7 $\mu$ m, followed by Masson's trichrome staining.

#### **A.2.5 Statistical Methods**

Statistical analyses were performed using SAS Version 9.4 (SAS Institute, Cary, NC). All parameters are described as mean  $\pm$  SD. Normality was assessed using skewness and kurtosis statistics as well as histograms. No significant departures from normality in the pre-test parameters (pups per litter, weight, GH, and TVL) or the mechanical parameters (load, stiffness, elongation, and energy absorbed), allowed for evaluation of differences between injured rats and control rats in each of the groups (4-week postpartum, 8-week postpartum, and virgin) using pairwise t-tests.

### A.3 RESULTS

**Table 11** displays characteristics of control rats vs. injured rats in each group (4-week postpartum, 8-week postpartum, and virgin) prior to conducting the mechanical tests. In the 4-week postpartum group, the injured rats trended towards lower weight ( $P=0.06$ ), larger GH ( $P=0.06$ ), and smaller TVL ( $P=0.08$ ). The 8-week postpartum group had slightly different trends, with the injured group trending toward higher weight ( $P=0.04$ ), with a smaller GH ( $P=0.07$ ). In the virgin group, the injured rats were significantly lighter ( $P<0.01$ ) with larger GH ( $P=0.04$ ) than the control rats.

**Table 11. Data Demonstrating the Baseline Number of Fetuses, Weight, GH, and TVL**

Group	N	Pups/Litter	Weight (g)	GH (cm)	TVL (cm)
4-Week PP Injured	8	5.88 ± 3.64	223.7 ± 9.90	0.84 ± 0.19 <sup>a</sup>	1.81 ± 0.26
4-Week PP Control	8	7.38 ± 3.38	234.6 ± 11.6	0.69 ± 0.12	2.00 ± 0.00
8-Week PP Injured	8	8.25 ± 3.24	249.2 ± 19.0	0.66 ± 0.40	1.94 ± 0.18
8-Week PP Control	8	6.29 ± 2.36	221.8 ± 14.8	0.50 ± 0.00	2.00 ± 0.00
Virgin Injured	6	N/A	198.9 ± 10.5	0.75 ± 0.22 <sup>a</sup>	2.00 ± 0.00
Virgin Control	6	N/A	221.8 ± 14.81	0.50 ± 0.00	2.00 ± 0.00

*Values presented as Median (IQR)- Significance set a  $P < .05$*

*<sup>a</sup> Relative to control matched controls*

Evaluation of the mechanical parameters in the 4-week postpartum injured group showed no difference in load bearing capacity ( $P=0.11$ ), stiffness ( $P=0.52$ ), elongation ( $P=0.39$ ), or the amount of energy absorbed ( $P=0.53$ ) by the VSTC before failure, relative to

the postpartum control group (**Table 12**). However, subsequent evaluation at 8 weeks injured group showed that the VSTC had 23% lower load-bearing capacity ( $P=0.03$ ), a 32% lower stiffness ( $P=0.02$ ), and a 40% greater elongation ( $P=0.02$ ) of the VSTC, relative to the postpartum control group (difference in load-bearing capacity shown in **Figure 24**).

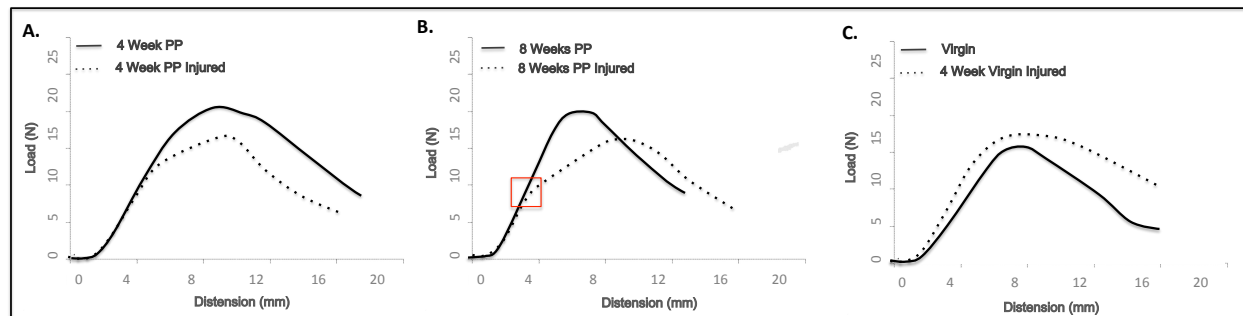


**Figure 24. Schematic of the Average Load-distension Curves.** The VSTC from Virgin (A), 4-week postpartum (B), and 8-week postpartum (C) control (solid lines) and injured groups (dotted lines). Distinct differences in the impact of injury on the virgin group vs the PP group can be observed. The curves also show increased stiffening of the VSTC with times PP in the absence of injury, but a lack of the recovery mechanism is observed in the presence of an injury. There was evidence of permanent deformation of the tissue occurring at 31% less load than controls in the 4-week postpartum injured group, and at 22% in the 8-week postpartum. This permanent deformation was appeared to be unique to VSTC in the postpartum group, as this did not occur in the virgin group.

**Table 12. Comparison of the Mechanical Properties of the VSTC**

	N	Load (N)	Stiffness (N/mm)	Elongation (mm)	Energy Absorbed (N*mm)
4-Week PP Injured	8	16.24 ± 1.89	3.49 ± 0.60	10.88 ± 1.96	93.06 ± 19.70
4-Week PP Control	8	17.73 ± 1.66	3.81 ± 1.26	9.86 ± 2.65	86.06 ± 24.10
8-Week PP Injured	8	14.59 ± 3.26	3.30 ± 1.19	10.68 ± 3.24	85.06 ± 37.58
8-Week PP Control	8	19.12 ± 3.06	4.87 ± 1.02	7.58 ± 0.92	68.85 ± 20.74
Virgin 4-Week Injured	6	16.51 ± 1.61	3.54 ± 0.90	9.70 ± 2.94	76.99 ± 29.87
Virgin Control	6	13.55 ± 1.50	2.95 ± 0.71	8.24 ± 1.08	51.51 ± 10.76
4-Week PP Injured vs 4-Week PP Control		P = 0.116	P = 0.521	P = 0.394	P = 0.535
8-Week PP Injured vs 8-Week PP Control		P = 0.032	P ≥ 0.015	P = 0.015	P = 0.196
4-Week PP Injured vs 8-Week PP Injured		P ≥ 0.197	P ≥ 0.230	P ≥ 0.814	P ≥ 0.776
4-Week PP Control vs 8-Week PP Control		P ≥ 0.276	P ≥ 0.083	P ≥ 0.038	P ≥ 0.148
Virgin vs Virgin 4 Week Injured		P ≥ 0.008	P ≥ 0.236	P ≥ 0.280	P ≥ 0.078

*Nomenclature - PP: Post Partum, Load: Maximum Load, Stiffness: Maximum Linear Stiffness, Elongation: Maximum Elongation –values represented as mean ± standard deviation  
Significance set a P < .05*

To determine if the significant decline of the mechanical properties of the VSTC observed in the postpartum injured vs. control group at 8 weeks following injury was a result of a time-dependent worsening of the injury or due to continuous recovery of the control group, comparison of the 4-week vs 8-week postpartum time-points for injured and control groups was performed. Although the results showed no significant difference in the 4 vs. 8 weeks postpartum injured group for any of the outcome measures, indicating no time-dependent worsening of the effects of injury, there was a 27% lower stiffness ( $P=0.010$ ) and 43% greater elongation ( $P=0.038$ ) in the 4 vs. 8 weeks postpartum control group. The results suggest that the time-dependent recovery occurring in the absence of injury may be prevented or delayed when significant injury is present (**Table 12**).

To further determine if the adaptive mechanisms occurring during pregnancy to afford vaginal distension at the time of delivery place the tissues at increased risk for injury if those adaptations are exceeded, we compared the impact of injury in the virgin vs postpartum group at 4 weeks post injury. Results from the evaluation showed that indeed the negative impact of injury in the postpartum group exceeded that observed in the virgin group (Figure 3). In the virgin group, the injured rats had significantly greater load-bearing capacity ( $P<0.01$ ), in contrast to the results showing no difference in load-bearing capacity in the 4-week postpartum group and significantly lower load-bearing capacity for injured rats in the 8-week postpartum group. In the virgin group, the increase in load was not accompanied by any decline in the stiffness ( $P=0.23$ ), elongation ( $P=0.29$ ), or the energy absorbed ( $P=0.09$ ).

Previous studies have shown that rodents do not typically sustain an injury to the VSTC during delivery. Not surprisingly, our results corroborate these findings showing no

significant correlations between the number of fetuses delivered and any of the mechanical outcomes in the absence of a simulated injury (load, stiffness, elongation and energy absorbed; correlation coefficients ranging from  $r=0.02$  to  $r=0.3$ ). However, in the presence of injury, there was a significant negative correlation between the number of pups and VSTC elongation ( $r=-0.59$ ) at 4 weeks and load-bearing capacity ( $r=-0.52$ ) at 8 weeks. Histological analysis also confirmed that the VSTC in the rat is indeed contiguous with the vagina, at level I, level II, and level III (**Figure 25**), suggesting that our mechanical tests which were performed by uniaxial pulling along the distal end of the vagina, did evaluate the integrity of these structures.

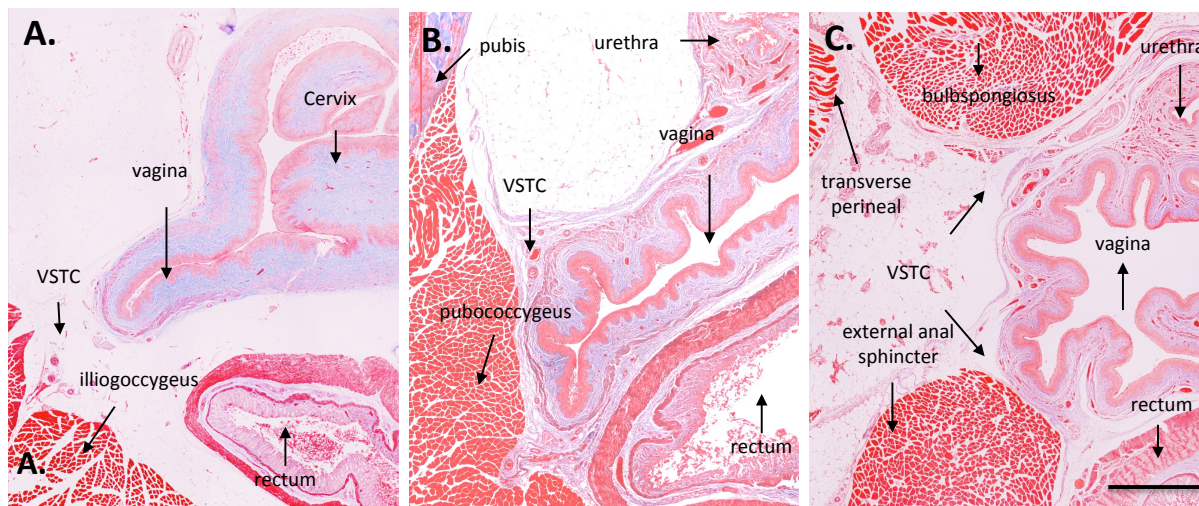


**Figure 25. Pelvic Cross-Sections.** Masson's trichome staining of paraffin embedded sections of the rat pelvis showing level I (A), level II (B) and level III (C) support. The vagina supportive tissue-complex (VSTC) in the rat are indeed contiguous with the vagina, and appears to be most dense.

## A.4 DISCUSSION

In women, observational data supports an association between traumatic vaginal delivery and POP. In this chapter, we aimed to evaluate the impact of simulated maternal childbirth trauma on the VSTC, in order to define the role of birth-related trauma in deterioration of the mechanical properties of the VSTC. In the absence of trauma, we observed a significant time-dependent postpartum recovery of the VSTC, with full recovery evident at 8 weeks postpartum. However, following simulated trauma, this time-dependent postpartum recovery was impeded as results showed that the load bearing capacity and stiffness of the injured group was significantly inferior to that of the control group at 8 weeks, in addition to exhibiting increased elongation. Injury was also associated with changes in the size of the genital hiatus and animal weight, although the significance is unknown. Nevertheless, the result suggests that injury impedes mechanical recovery of the VSTC, thus more easily deforming under a given load, presumably increasing susceptibility to failure over time and the development of POP.

During pregnancy, collagen (types I, II, V), which is a dominant biomechanical constituent of the VSTC, is known to increase in content, but the number of crosslinks within these fibers declines. This decrease in crosslinked fibers reduces the mechanical strength, allowing the fibers to undergo high degrees of deformation during delivery without fracturing, and ensuring rapid postpartum recovery[214]. The decline in crosslink density, is known to be due to a decline in the expression of lysyl oxidases (LOX), a cross linking enzyme. A robust study by Drewes et al. showed up to 80% decline in the expression of LOX during pregnancy in rodents [215]. LOX expression however began to



increase during labor, peaking at 24 hours after delivery, but rapidly declining by 48 hours postpartum below antepartum levels (remaining low for weeks postpartum). In this study, the significantly inferior mechanical response of the postpartum injured groups at 8 weeks after injury, characterized by increased deformation, elongation, and energy absorbed with loading, suggests inadequate LOX-induced crosslinking, as Alperin et al. reported similar mechanical properties in LOX  $-/-$  mice [195].

Such inadequate crosslinking may also provide a possible explanation as to why the impact of injury on the mechanical integrity of the postpartum group was more severe than the virgin group, following injury. It is likely that injury in the virgin group induced an elevated expression of LOX for weeks following injury, to facilitate wound contraction and scar formation [216]. In contrast, in the postpartum group, where LOX expression was below antepartum levels, the wound healing response may have been delayed, thus resulting in inferior mechanics of the VSTC [217]. If this is indeed the case, the lack of a significant difference between the 4-week postpartum control and 4-week postpartum injured group, suggests that LOX expression at 4 weeks postpartum may still be below antepartum levels, thus resulting in comparably inferior mechanics in both the postpartum injured and postpartum control groups. Following this progression, in thought, it could be inferred that a resurgence of LOX expression to, or above antepartum levels occurs at 8 weeks postpartum, explaining the superior mechanics of the VSTC in the 8-week versus 4-week postpartum control group.

Although more long-term data is needed to determine whether the postpartum injured group eventually recovers, our finding that healing of the VSTC is delayed is meaningful as it would render the VSTC more susceptible to damage and improper loading

during the early postpartum period. Indeed, we showed that the VSTC in the 8-week postpartum injured group began permanently deforming under 20-30% less load than the postpartum control group. Histological analysis also suggests that such a change in the mechanics of the VSTC could have a significant impact on vaginal suspension. Interestingly, Dietz et al. have shown that the odds of incurring a loss of postpartum pelvic organ support increases, with inadequate maternal adaptation [125]. Our results, which showed a negative correlation between number of pups/litter size and the resulting mechanical integrity following injury, support this mechanism, as more pups are likely associated with increased mechanical adaptation. This theory is further supported by studies showing an association of sulcus tears, similar to that imposed in this study, with inadequate maternal adaptation [37]. More data on the impact of mode of trauma on the development of POP are, however, warranted although the risk factors for sulcus tears and POP do align.

As reported, the findings of this study are noteworthy, however they should be interpreted in light of their limitations. One such limitation is the use of an animal model (rodent), whose recovery mechanism may be distinctively different from humans, although similar connective tissue supports were histologically observed. Postpartum injury-care, as well as postpartum exercise regimens may further result in distinct outcomes. In addition, our injury model was limited to sulcus tears, the effects of which may not apply to other types of lacerations. Further, as the trauma was simulated, tissue damage may be under or over exaggerated, Nevertheless this model is highly useful for the future evaluation of multiple modes of birth trauma, independently or combined with hormonal withdrawal for the elucidation of postpartum induced onset of POP. Future work will also evaluate the impact of a subsequent delivery (s) on the VSTC.

## **APPENDIX B**

### **SUPPLEMENTAL FIGURES – CHAPTER 3**

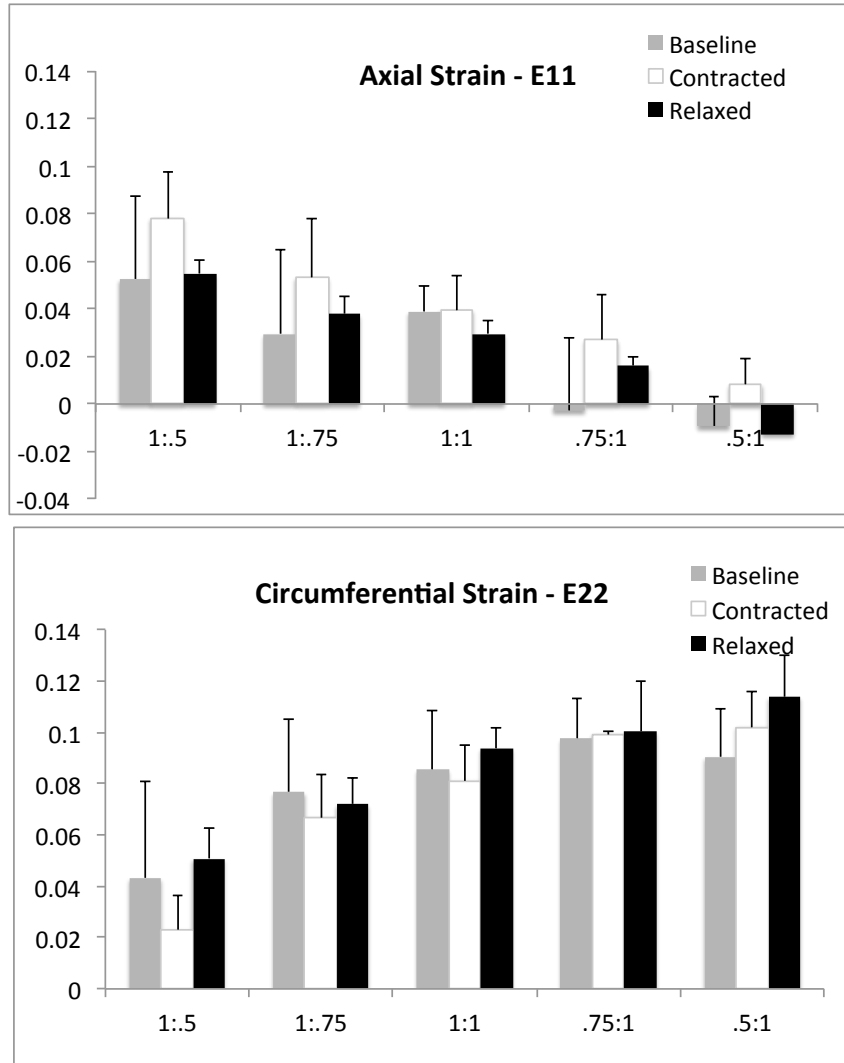


**Figure 26. Maximum Axial (E11) & Circumferential (E22) Strain.** Strains in the circumferential direction were, on average, greater than strains in the axial direction. Strains in the axial direction did not appear to be a function of the stress, but a function of circumferential strains. Increased strain in the circumferential direction was associated with decreased strain (or a shortening) in the axial direction (*Poisson* effect). Smooth muscle contraction enables the axial direction to maintain its geometry, thus limiting the *Poisson* effect (observed at .75:1 & .5:1 loading regimens).

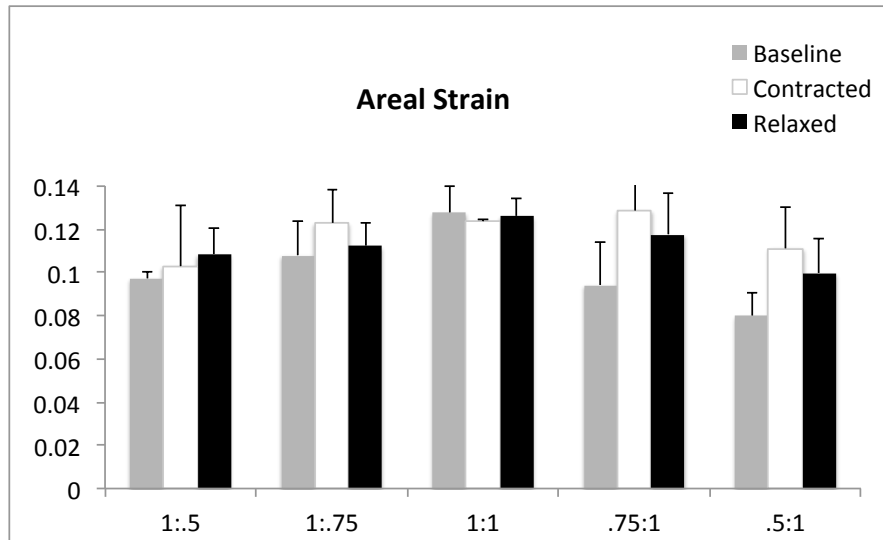


**Figure 27. Areal Strain.** Areal strain exhibited an increasing trend following smooth muscle contraction, relative to baseline and relaxed conditions. This trend is even more evident during .75:1 and .5:1 loading regimens, where smooth muscle contraction resulted in a greater increase in areal strain, likely due to the increase in the axial strain (**Figure 26**). As noted above, the observed increase in strain following smooth muscle contraction is likely associated with increased compliance and likely confers protection from vaginal injury.

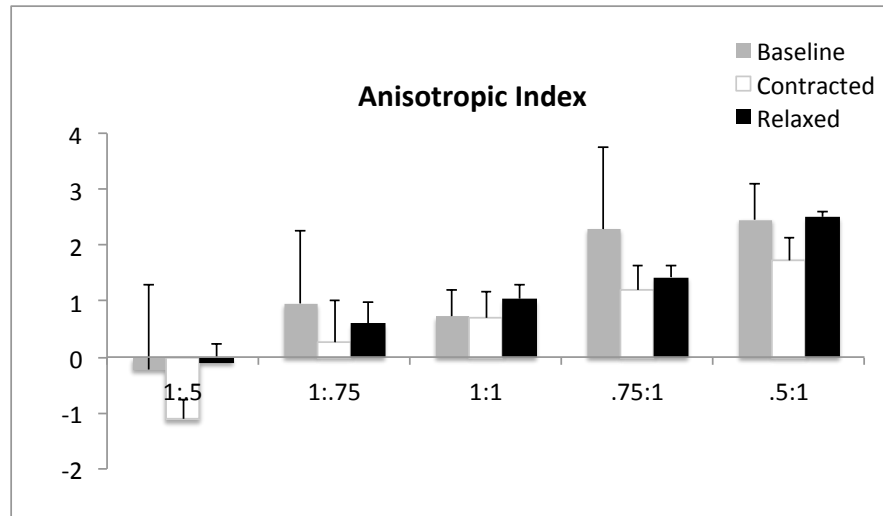


**Figure 28. Anisotropic Index.** Smooth muscle influences the anisotropic index, as previously noted. There was a trend toward decreased anisotropy with smooth muscle contraction, relative to when smooth muscle was at baseline or when relaxed. This decrease in anisotropy was even more evident when there is increased discrepancy between the magnitudes of the load applied to each axes (evident during .75:1 and .5:1 loading regimens). This finding further supports the theory of smooth muscles role in stress distribution [149].

## BIBLIOGRAPHY

- [1] G. M. Buchsbaum, "Urinary incontinence and pelvic organ prolapse.," *Minerva Urol. Nefrol.*, vol. 58, pp. 311–319, 2006.
- [2] V. L. Handa, L. Harvey, G. W. Cundiff, S. A. Siddique, and K. H. Kjerulff, "Sexual function among women with urinary incontinence and pelvic organ prolapse," *Am. J. Obstet. Gynecol.*, vol. 191, pp. 751–756, 2004.
- [3] S. A. Kingsberg and J. W. Janata, "Impact of pelvic floor disorders and prolapse on female sexual function and response.," *Urol. Clin. North Am.*, vol. 34, pp. 677–683, 2002.
- [4] J. E. Jelovsek and M. D. Barber, "Women seeking treatment for advanced pelvic organ prolapse have decreased body image and quality of life," *Am. J. Obstet. Gynecol.*, vol. 194, pp. 1455–1461, 2006.
- [5] C. Ghatti, J. L. Lowder, R. Ellison, M. A. Krohn, and P. Moalli, "Depressive symptoms in women seeking surgery for pelvic organ prolapse," *Int. Urogynecol. J.*, vol. 21, pp. 855–860, 2010.
- [6] A. L. Olsen, V. J. Smith, J. O. Bergstrom, J. C. Colling, and A. L. Clark, "Epidemiology of surgically managed pelvic organ prolapse and urinary incontinence," *Obstet. Gynecol.*, vol. 89, pp. 501–506, 1997.
- [7] I. Nygaard, M. D. Barber, K. L. Burgio, K. Kenton, S. Meikle, J. Schaffer, C. Spino, W. E. Whitehead, J. Wu, and D. J. Brody, "Prevalence of symptomatic pelvic floor disorders in US women.," *JAMA*, vol. 300, pp. 1311–1316, 2008.
- [8] I. Nygaard, C. Bradley, and D. Brandt, "Pelvic organ prolapse in older women: prevalence and risk factors.," *Obstet. Gynecol.*, vol. 104, pp. 489–497, 2004.
- [9] J. M. Wu, A. Kawasaki, A. F. Hundley, A. A. Dieter, E. R. Myers, and V. W. Sung, "Predicting the number of women who will undergo incontinence and prolapse surgery, 2010 to 2050," *Am. J. Obstet. Gynecol.*, vol. 205, 2011.

- [10] J. M. Wu, C. a Matthews, M. M. Conover, V. Pate, and M. Jonsson Funk, "Lifetime risk of stress urinary incontinence or pelvic organ prolapse surgery.," *Obstet. Gynecol.*, vol. 123, pp. 1201–6, 2014.
- [11] L. L. Subak, L. E. Waetjen, S. Van Den Eeden, D. H. Thom, E. Vittinghoff, and J. S. Brown, "Cost of pelvic organ prolapse surgery in the United States," *Obstet. Gynecol.*, vol. 98, pp. 646–651, 2001.
- [12] X. Jia, C. Glazener, G. Mowatt, D. Jenkinson, C. Fraser, C. Bain, and J. Burr, "Systematic review of the efficacy and safety of using mesh in surgery for uterine or vaginal vault prolapse," *International Urogynecology Journal and Pelvic Floor Dysfunction*, vol. 21. pp. 1413–1431, 2010.
- [13] C. Maher, B. Feiner, K. Baessler, E. J. Adams, S. Hagen, and C. M. Glazener, "Surgical management of pelvic organ prolapse in women.," *Cochrane database Syst. Rev.*, p. CD004014, 2010.
- [14] M. Jonsson Funk, A. L. Edenfield, V. Pate, A. G. Visco, A. C. Weidner, and J. M. Wu, "Trends in use of surgical mesh for pelvic organ prolapse," *Am J Obs. Gynecol*, vol. 208, p. 79 e1–7, 2013.
- [15] F. Daneshgari, "Words of wisdom. Re: FDA public health notification: serious complications associated with transvaginal placement of surgical mesh in repair of pelvic organ prolapse and stress urinary incontinence.," *Eur. Urol.*, vol. 55, pp. 1235–1236, 2009.
- [16] S. M. Jakus, A. Shapiro, and C. D. Hall, "Biologic and synthetic graft use in pelvic surgery: a review.," *Obstet. Gynecol. Surv.*, vol. 63, pp. 253–266, 2008.
- [17] T. Keys, L. Campeau, and G. Badlani, "Synthetic mesh in the surgical repair of pelvic organ prolapse: Current status and future directions," *Urology*, vol. 80. pp. 237–243, 2012.
- [18] H. P. Dietz, "Pelvic floor trauma in childbirth," *Australian and New Zealand Journal of Obstetrics and Gynaecology*, vol. 53. pp. 220–230, 2013.
- [19] A. Feola, S. Abramowitch, Z. Jallah, S. Stein, W. Barone, S. Palcsey, and P. Moalli, "Deterioration in biomechanical properties of the vagina following implantation of a high-stiffness prolapse mesh," *BJOG An Int. J. Obstet. Gynaecol.*, vol. 120, no. 2, pp. 224–232, 2013.
- [20] M. Jonsson Funk, A. L. Edenfield, V. Pate, A. G. Visco, A. C. Weidner, and J. M. Wu, "Trends in use of surgical mesh for pelvic organ prolapse," *Am. J. Obstet. Gynecol.*, vol. 208, 2013.



- [21] H. P. Dietz, P. Vancaillie, M. Svehla, W. Walsh, A. B. Steensma, and T. G. Vancaillie, "Mechanical properties of urogynecologic implant materials," *Int. Urogynecol. J. Pelvic Floor Dysfunct.*, vol. 14, pp. 239–243, 2003.
- [22] A. Feola, P. Moalli, M. Alperin, R. Duerr, R. E. Gandley, and S. Abramowitch, "Impact of pregnancy and vaginal delivery on the passive and active mechanics of the rat vagina," *Ann. Biomed. Eng.*, vol. 39, pp. 549–558, 2011.
- [23] M. A. Denman, W. T. Gregory, S. H. Boyles, V. Smith, S. R. Edwards, and A. L. Clark, "Reoperation 10 years after surgically managed pelvic organ prolapse and urinary incontinence," *Am. J. Obstet. Gynecol.*, vol. 198, 2008.
- [24] A. L. Clark, T. Gregory, V. J. Smith, and R. Edwards, "Epidemiologic evaluation of reoperation for surgically treated pelvic organ prolapse and urinary incontinence," *Am. J. Obstet. Gynecol.*, vol. 189, pp. 1261–1267, 2003.
- [25] S. Abbott, C. A. Unger, J. M. Evans, K. Jallad, K. Mishra, M. M. Karram, C. B. Iglesia, C. R. Rardin, and M. D. Barber, "Evaluation and management of complications from synthetic mesh after pelvic reconstructive surgery: A multicenter study," *Am. J. Obstet. Gynecol.*, vol. 210, 2014.
- [26] C. M. Kim, M. J. Jeon, D. J. Chung, S. K. Kim, J. W. Kim, and S. W. Bai, "Risk factors for pelvic organ prolapse," *Int. J. Gynaecol. Obstet.*, vol. 98, pp. 248–251, 2007.
- [27] M. C. P. Slieker-ten Hove, A. L. Pool-Goudzwaard, M. J. C. Eijkemans, R. P. M. Steegers-Theunissen, C. W. Burger, and M. E. Vierhout, "Symptomatic pelvic organ prolapse and possible risk factors in a general population," *Am. J. Obstet. Gynecol.*, vol. 200, pp. 184.e1–e7, 2009.
- [28] G. Rortveit, Y. S. Hannestad, A. Kjersti Daltveit, and S. Hunskar, "Age- and type-dependent effects of parity on urinary incontinence: The Norwegian EPINCONT study," *Obstet. Gynecol.*, vol. 98, no. 6, pp. 1004–1010, 2001.
- [29] J. Mant, R. Painter, and M. Vessey, "Epidemiology of genital prolapse: observations from the Oxford Family Planning Association Study," *Br. J. Obstet. Gynaecol.*, vol. 104, pp. 579–585, 1997.
- [30] G. M. Buchsbaum, E. E. Duecy, L. A. Kerr, L.-S. Huang, M. Perevich, and D. S. Guzick, "Pelvic organ prolapse in nulliparous women and their parous sisters," *Obstet. Gynecol.*, vol. 108, pp. 1388–1393, 2006.
- [31] A. Tsunoda, M. Shibusawa, G. Kamiyama, M. Kusano, Y. Shimizu, and T. Yanaihara, "The effect of vaginal delivery on the pelvic floor," *Surg. Today*, vol. 29, pp. 1243–1247, 1999.

- [32] R. E. Allen, G. L. Hosker, A. R. Smith, and D. W. Warrell, "Pelvic floor damage and childbirth: a neurophysiological study," *Br. J. Obstet. Gynaecol.*, vol. 97, pp. 770–779, 1990.
- [33] H. P. Dietz and P. D. Wilson, "Childbirth and pelvic floor trauma," *Best Practice and Research: Clinical Obstetrics and Gynaecology*, vol. 19, pp. 913–924, 2005.
- [34] V. L. Handa, T. A. Harris, and D. R. Ostergard, "Protecting the pelvic floor: Obstetric management to prevent incontinence and pelvic organ prolapse," *Obstetrics and Gynecology*, vol. 88, pp. 470–478, 1996.
- [35] R. G. Rogers, L. M. Leeman, N. Borders, C. Qualls, A. M. Fullilove, D. Teaf, R. J. Hall, E. Bedrick, and L. L. Albers, "Contribution of the second stage of labour to pelvic floor dysfunction: A prospective cohort comparison of nulliparous women," *BJOG An Int. J. Obstet. Gynaecol.*, vol. 121, pp. 1145–1153, 2014.
- [36] M. Heit, K. Mudd, and P. Culligan, "Prevention of childbirth injuries to the pelvic floor.," *Curr. Womens. Health Rep.*, vol. 1, pp. 72–80, 2001.
- [37] M. C. Klein, P. a. Janssen, L. MacWilliam, J. Kaczorowski, and B. Johnson, "Determinants of vaginal-perineal integrity and pelvic floor functioning in childbirth," *Am. J. Obstet. Gynecol.*, vol. 176, no. 2, pp. 403–410, 1997.
- [38] R. K. Marahatta and A. Shah, "Genital prolapse in women of Bhaktapur, Nepal.," *Nepal Med. Coll. J.*, vol. 5, pp. 31–33, 2003.
- [39] J. Ferdous, A. Ahmed, S. K. Dasgupta, M. Jahan, F. A. Huda, C. Ronsmans, M. Koblinsky, and M. E. Chowdhury, "Occurrence and determinants of postpartum maternal morbidities and disabilities among women in Matlab, Bangladesh," *J. Heal. Popul. Nutr.*, vol. 30, pp. 143–158, 2012.
- [40] F. Giuliano, O. Rampin, and J. Allard, "Neurophysiology and pharmacology of female genital sexual response.," *J. Sex Marital Ther.*, vol. 28 Suppl 1, pp. 101–121, 2002.
- [41] A. H. Sultan, M. A. Kamm, and C. N. Hudson, "Pudendal nerve damage during labour: prospective study before and after childbirth.," *Br. J. Obstet. Gynaecol.*, vol. 101, pp. 22–28, 1994.
- [42] M. S. Damaser, C. Broxton-King, C. Ferguson, F. J. Kim, and J. M. Kerns, "Functional and neuroanatomical effects of vaginal distention and pudendal nerve crush in the female rat.," *J. Urol.*, vol. 170, pp. 1027–1031, 2003.
- [43] S. J. Snooks, M. Setchell, M. Swash, and M. M. Henry, "Injury to innervation of pelvic floor sphincter musculature in childbirth.," *Lancet*, vol. 2, pp. 546–550, 1984.

- [44] S. J. Snooks, M. Swash, S. E. Mathers, and M. M. Henry, "Effect of vaginal delivery on the pelvic floor: A 5-year follow-up," *Br. J. Surg.*, vol. 77, pp. 1358–1360, 1990.
- [45] C. A. Wong, B. M. Scavone, S. Dugan, J. C. Smith, H. Prather, J. N. Ganchiff, and R. J. McCarthy, "Incidence of postpartum lumbosacral spine and lower extremity nerve injuries," *Obstet. Gynecol.*, vol. 101, pp. 279–288, 2003.
- [46] S. J. Snooks, P. R. Barnes, M. Swash, and M. M. Henry, "Damage to the innervation of the pelvic floor musculature in chronic constipation," *Gastroenterology*, vol. 89, pp. 977–981, 1985.
- [47] M. Gyhagen, M. Bullarbo, T. F. Nielsen, and I. Milsom, "Prevalence and risk factors for pelvic organ prolapse 20 years after childbirth: A national cohort study in singleton primiparae after vaginal or caesarean delivery," *BJOG An Int. J. Obstet. Gynaecol.*, vol. 120, pp. 152–160, 2013.
- [48] E. H. Sze, G. B. Sherard 3rd, and J. M. Dolezal, "Pregnancy, labor, delivery, and pelvic organ prolapse," *Obs. Gynecol.*, vol. 100, pp. 981–986, 2002.
- [49] K. D. Sievert, M. Emre Bakircioglu, T. Tsai, S. E. Dahms, L. Nunes, and T. F. Lue, "The effect of simulated birth trauma and/or ovariectomy on rodent continence mechanism. Part I: functional and structural change," *J. Urol.*, vol. 166, pp. 311–317, 2001.
- [50] H. P. Dietz, "Pelvic floor trauma following vaginal delivery," *Curr. Opin. Obstet. Gynecol.*, vol. 18, pp. 528–537, 2006.
- [51] R. M. Laterza, L. Schrutka, W. Umek, S. Albrich, and H. Koelbl, "Pelvic floor dysfunction after levator trauma 1-year postpartum: a prospective case-control study," *International Urogynecology Journal*, 2014.
- [52] U. M. Peschers, G. N. Schaer, J. O. DeLancey, and B. Schuessler, "Levator ani function before and after childbirth," *Br. J. Obstet. Gynaecol.*, vol. 104, pp. 1004–1008, 1997.
- [53] J. O. L. DeLancey, D. M. Morgan, D. E. Fenner, R. Kearney, K. Guire, J. M. Miller, H. Hussain, W. Umek, Y. Hsu, and J. A. Ashton-Miller, "Comparison of levator ani muscle defects and function in women with and without pelvic organ prolapse," *Obstet. Gynecol.*, vol. 109, pp. 295–302, 2007.
- [54] H. P. Dietz and J. M. Simpson, "Levator trauma is associated with pelvic organ prolapse," *BJOG An Int. J. Obstet. Gynaecol.*, vol. 115, pp. 979–984, 2008.
- [55] M. B. Berger, D. M. Morgan, J. O. DeLancey, "Levator ani defect scores and pelvic organ prolapse: is there a threshold effect?," *Int. Urogynecol J*, vol. 25, pp. 1375–79, 2014.

- [56] J. O. DeLancey, "Anatomic aspects of vaginal eversion after hysterectomy," *Am. J. Obstet. Gynecol.*, vol. 166, pp. 1717–1724; discussion 1724–1728, 1992.
- [57] M. Alperin and P. A. Moalli, "Remodeling of vaginal connective tissue in patients with prolapse," *Curr. Opin. Obstet. Gynecol.*, vol. 18, pp. 544–550, 2006.
- [58] B. L. Shull, "Pelvic organ prolapse: Anterior, superior, and posterior vaginal segment defects," *Am. J. Obstet. Gynecol.*, vol. 181, pp. 6–11, 1999.
- [59] M. D. Barber, A. G. Visco, A. C. Weidner, C. L. Amundsen, and R. C. Bump, "Bilateral uterosacral ligament vaginal vault suspension with site-specific endopelvic fascia defect repair for treatment of pelvic organ prolapse," in *American Journal of Obstetrics and Gynecology*, 2000, vol. 183, pp. 1402–1411.
- [60] C. L. Amundsen, B. J. Flynn, and G. D. Webster, "Anatomical correction of vaginal vault prolapse by uterosacral ligament fixation in women who also require a pubovaginal sling," *J. Urol.*, vol. 169, pp. 1770–1774, 2003.
- [61] R. B. Kurzels and D. H. Nichols, *Genital prolapse during pregnancy.*, vol. 24. 1980, pp. 46–47.
- [62] T. P., D. A., V. N., I. Z., B. S., P. P., T. N., L. V., G. G., and V. T. G.F., "Uterine prolapse in pregnancy: Risk factors, complications and management," *Journal of Maternal-Fetal and Neonatal Medicine*, vol. 27. pp. 297–302, 2014.
- [63] J. E. Monaco, "Orthopedic considerations in pregnancy," *Primary Care Update for Ob/Gyns*, vol. 3. pp. 197–200, 1996.
- [64] M. M. Cotreau, V. M. Chennathukuzhi, H. A. Harris, L. Han, A. J. Dorner, G. Apseloff, U. Varadarajan, E. Hatstat, M. Zakaria, A. L. Strahs, J. S. Crabtree, R. C. Winneker, and S. A. Jelinsky, "A study of 17 $\beta$ -estradiol-regulated genes in the vagina of postmenopausal women with vaginal atrophy," *Maturitas*, vol. 58, pp. 366–376, 2007.
- [65] C. M. Vaccaro, G. K. Mutema, A. N. Fellner, C. C. Crisp, M. V Estanol, S. D. Kleeman, and R. N. Pauls, "Histologic and cytologic effects of vaginal estrogen in women with pelvic organ prolapse: a randomized controlled trial," *Female Pelvic Med Reconstr Surg*, vol. 19, pp. 34–39, 2013.
- [66] K. R. Stenmark, N. Davie, M. Frid, E. Gerasimovskaya, and M. Das, "Role of the adventitia in pulmonary vascular remodeling," *Physiology (Bethesda).*, vol. 21, pp. 134–145, 2006.
- [67] L. Zhou, J. H. Lee, Y. Wen, C. Constantinou, M. Yoshinobu, S. Omata, and B. Chen, "Biomechanical properties and associated collagen composition in vaginal tissue of women with pelvic organ prolapse," *J. Urol.*, vol. 188, pp. 875–880, 2012.

- [68] Y. Wen, Y. Y. Zhao, S. Li, M. L. Polan, and B. H. Chen, "Differences in mRNA and protein expression of small proteoglycans in vaginal wall tissue from women with and without stress urinary incontinence," *Hum. Reprod.*, vol. 22, pp. 1718–1724, 2007.
- [69] W. Zong, S. E. Stein, B. Starcher, L. A. Meyn, and P. A. Moalli, "Alteration of vaginal elastin metabolism in women with pelvic organ prolapse," *Obstet. Gynecol.*, vol. 115, pp. 953–961, 2010.
- [70] D. E. Birk, J. M. Fitch, J. P. Babiarz, K. J. Doane, and T. F. Linsenmayer, "Collagen fibrillogenesis in vitro: interaction of types I and V collagen regulates fibril diameter," *J. Cell Sci.*, vol. 95 ( Pt 4), pp. 649–657, 1990.
- [71] M. Sun, S. Chen, S. M. Adams, J. B. Florer, H. Liu, W. W.-Y. Kao, R. J. Wenstrup, and D. E. Birk, "Collagen V is a dominant regulator of collagen fibrillogenesis: dysfunctional regulation of structure and function in a corneal-stroma-specific Col5a1-null mouse model," *Journal of Cell Science*, vol. 124. pp. 4096–4105, 2011.
- [72] R. J. Wenstrup, J. B. Florer, E. W. Brunskill, S. M. Bell, I. Chervoneva, and D. E. Birk, "Type V collagen controls the initiation of collagen fibril assembly," *J. Biol. Chem.*, vol. 279, pp. 53331–53337, 2004.
- [73] C. Niyibizi, S. Wang, Z. Mi, and P. D. Robbins, "Gene therapy approaches for osteogenesis imperfecta," *Gene Ther.*, vol. 11, pp. 408–416, 2004.
- [74] A. S. Narayanan, L. B. Sandberg, R. Ross, and D. L. Layman, "The smooth muscle cell. III. Elastin synthesis in arterial smooth muscle cell culture," *J Cell Biol*, vol. 68, pp. 411–419, 1976.
- [75] U. R. Rodgers and A. S. Weiss, "Cellular interactions with elastin," *Pathologie Biologie*, vol. 53. pp. 390–398, 2005.
- [76] Y. Cai, "Revisiting old vaginal topics: Conversion of the Müllerian vagina and origin of the 'sinus' vagina," *International Journal of Developmental Biology*, vol. 53. pp. 925–934, 2009.
- [77] M. Hilliges, C. Falconer, G. Ekman-Ordeberg, and O. Johansson, "Innervation of the human vaginal mucosa as revealed by PGP 9.5 immunohistochemistry," *Acta Anat. (Basel)*, vol. 153, pp. 119–126, 1995.
- [78] A. Shafik, "Vaginocavernosus reflex. Clinical significance and role in sexual act," *Gynecol. Obstet. Invest.*, vol. 35, pp. 114–117, 1993.
- [79] P. B. Dobrin, "and the Pathophysiology of Arterial Aneurysms," 2000.
- [80] R. R. Dmochowski, "Bladder outlet obstruction: etiology and evaluation," *Rev. Urol.*, vol. 7 Suppl 6, pp. S3–S13, 2005.

- [81] K. F. Chung, "The role of airway smooth muscle in the pathogenesis of airway wall remodeling in chronic obstructive pulmonary disease.," *Proc. Am. Thorac. Soc.*, vol. 2, pp. 347–354; discussion 371–372, 2005.
- [82] H.-Y. Chen, Y.-W. Chung, W.-Y. Lin, J.-C. Wang, F.-J. Tsai, and C.-H. Tsai, "Collagen type 3 alpha 1 polymorphism and risk of pelvic organ prolapse.," *Int. J. Gynaecol. Obstet.*, vol. 103, pp. 55–8, 2008.
- [83] T. Strinic, M. Vulic, S. Tomic, V. Capkun, I. Stipic, and I. Alujevic, "Increased expression of matrix metalloproteinase-1 in uterosacral ligament tissue from women with pelvic organ prolapse.," *Acta Obstet. Gynecol. Scand.*, vol. 89, pp. 832–834, 2010.
- [84] M. Dviri, E. Leron, J. Dreiherr, M. Mazor, and R. Shaco-Levy, "Increased matrix metalloproteinases-1,-9 in the uterosacral ligaments and vaginal tissue from women with pelvic organ prolapse.," *Eur. J. Obstet. Gynecol. Reprod. Biol.*, vol. 156, pp. 113–117, 2011.
- [85] W. Carver, M. L. Nagpal, M. Nachtigal, T. K. Borg, and L. Terracio, "Collagen expression in mechanically stimulated cardiac fibroblasts.," *Circ. Res.*, vol. 69, pp. 116–122, 1991.
- [86] L. E. Lanyon, A. E. Goodship, C. J. Pye, and J. H. MacFie, "Mechanically adaptive bone remodelling.," *J. Biomech.*, vol. 15, pp. 141–154, 1982.
- [87] M. Alarab, M. A. T. Bortolini, H. Drutz, S. Lye, and O. Shynlova, "LOX family enzymes expression in vaginal tissue of premenopausal women with severe pelvic organ prolapse.," *Int. Urogynecol. J. Pelvic Floor Dysfunct.*, vol. 21, pp. 1397–1404, 2010.
- [88] J. Klutke, F. Z. Stanczyk, Q. Ji, J. D. Campeau, and C. G. Klutke, "Suppression of lysyl oxidase gene expression by methylation in pelvic organ prolapse.," *Int. Urogynecol. J.*, vol. 21, pp. 869–872, 2010.
- [89] B. Chen, Y. Wen, and M. L. Polan, "Elastolytic Activity in Women with Stress Urinary Incontinence and Pelvic Organ Prolapse.," *Neurourol. Urodyn.*, vol. 23, pp. 119–126, 2004.
- [90] B. H. Zhao and J. H. Zhou, "Decreased expression of elastin, fibulin-5 and lysyl oxidase-like 1 in the uterosacral ligaments of postmenopausal women with pelvic organ prolapse.," *J. Obstet. Gynaecol. Res.*, vol. 38, pp. 925–931, 2012.
- [91] J. Klutke, Q. Ji, J. Campeau, B. Starcher, J. C. Felix, F. Z. Stanczyk, and C. Klutke, "Decreased endopelvic fascia elastin content in uterine prolapse.," *Acta Obstet. Gynecol. Scand.*, vol. 87, pp. 111–115, 2008.
- [92] C. Goepel, "Differential elastin and tenascin immunolabeling in the uterosacral ligaments in postmenopausal women with and without pelvic organ prolapse.," *Acta Histochem.*, vol. 110, pp. 204–209, 2008.

- [93] Y. J. Moon, J. R. Choi, M. J. Jeon, S. K. Kim, and S. W. Bai, "Alteration of elastin metabolism in women with pelvic organ prolapse," *J. Urol.*, vol. 185, pp. 1786–1792, 2011.
- [94] H. A. Inal, P. B. Kaplan, U. Usta, E. Ta??tekin, A. Aybatli, and B. Tokuc, "Neuromuscular morphometry of the vaginal wall in women with anterior vaginal wall prolapse," *Neurourol. Urodyn.*, vol. 29, no. 3, pp. 458–463, 2010.
- [95] M. K. Boreham, C. Y. Wai, R. T. Miller, J. I. Schaffer, R. A. Word, and A. Weber, "Morphometric properties of the posterior vaginal wall in women with pelvic organ prolapse," in *American Journal of Obstetrics and Gynecology*, 2002, vol. 187, pp. 1501–1509.
- [96] M. K. Boreham, R. T. Miller, J. I. Schaffer, and R. A. Word, "Smooth muscle myosin heavy chain and caldesmon expression in the anterior vaginal wall of women with and without pelvic organ prolapse," *Am J Obs. Gynecol*, vol. 185, pp. 944–952, 2001.
- [97] M. A. T. Bortolini, O. Shynlova, H. P. Drutz, R. A. Castro, S. Lye, and M. Alarab, "Expression of Genes Encoding Smooth Muscle Contractile Proteins in Vaginal Tissue of Women With and Without Pelvic Organ Prolapse," vol. 114, no. May 2011, pp. 109–114, 2012.
- [98] G. M. Northington, M. Basha, L. a. Arya, a. J. Wein, and S. Chacko, "Contractile Response of Human Anterior Vaginal Muscularis in Women With and Without Pelvic Organ Prolapse," *Reprod. Sci.*, vol. 18, no. 3, pp. 296–303, Mar. 2011.
- [99] M. R. Matrana and D. A. Margolin, "Epidemiology and pathophysiology of Diverticular disease," *Clin. Colon Rectal Surg.*, vol. 22, pp. 141–146, 2009.
- [100] P. Jeppesen, J. Sanye-Hajari, and T. Bek, "Increased blood pressure induces a diameter response of retinal arterioles that increases with decreasing arteriolar diameter," *Investig. Ophthalmol. Vis. Sci.*, vol. 48, pp. 328–331, 2007.
- [101] M. K. Boreham, C. Y. Wai, R. T. Miller, J. I. Schaffer, and R. A. Word, "Morphometric analysis of smooth muscle in the anterior vaginal wall of women with pelvic organ prolapse," *Am J Obs. Gynecol*, vol. 187, pp. 56–63, 2002.
- [102] C. Rubod, M. Boukerrou, M. Brieu, C. Jean-Charles, P. Dubois, and M. Cosson, "Biomechanical properties of vaginal tissue: Preliminary results," *Int. Urogynecol. J. Pelvic Floor Dysfunct.*, vol. 19, pp. 811–816, 2008.
- [103] M. Cosson, E. Lambaudie, M. Boukerrou, P. Lobry, G. Crépin, and A. Ego, "A biomechanical study of the strength of vaginal tissues: Results on 16 post-menopausal patients presenting with genital prolapse," *Eur. J. Obstet. Gynecol. Reprod. Biol.*, vol. 112, pp. 201–205, 2004.

- [104] V. Egorov, H. Van Raalte, and V. Lucente, "Quantifying vaginal tissue elasticity under normal and prolapse conditions by tactile imaging," *Int. Urogynecol. J. Pelvic Floor Dysfunct.*, vol. 23, pp. 459–466, 2012.
- [105] A. J. Bank, H. Wang, J. E. Holte, K. Mullen, R. Shammass, and S. H. Kubo, "Contribution of collagen, elastin, and smooth muscle to in vivo human brachial artery wall stress and elastic modulus," *Circulation*, vol. 94, pp. 3263–3270, 1996.
- [106] F. Gao, D. Liao, A. M. Drewes, and H. Gregersen, "Modelling the elastin , collagen and smooth muscle contribution to the duodenal mechanical behaviour in patients with systemic sclerosis," no. November 2008, 2009.
- [107] S. D. Abramowitch, A. Feola, Z. Jallah, and P. A. Moalli, "Tissue mechanics, animal models, and pelvic organ prolapse: A review," *European Journal of Obstetrics Gynecology and Reproductive Biology*, vol. 144, no. SUPPL 1. 2009.
- [108] A. Manuscript, "Animal models of female pelvic organ prolapse : lessons learned," vol. 7, no. 3, pp. 249–260, 2013.
- [109] P. A. Moalli, N. S. Howden, J. L. Lowder, J. Navarro, K. M. Debes, S. D. Abramowitch, and S. L. Woo, "A rat model to study the structural properties of the vagina and its supportive tissues," pp. 80–88, 2005.
- [110] R. J. Adams, J. A. Rock, M. M. Swindle, N. L. Garnett, and W. P. Porter, *Surgical correction of genital prolapse in three rhesus monkeys*, vol. 35. 1985, pp. 405–408.
- [111] K. W. Coates, H. L. Galan, B. L. Shull, and T. J. Kuehl, "The squirrel monkey: An animal model of pelvic relaxation," *Am. J. Obstet. Gynecol.*, vol. 172, pp. 588–593, 1995.
- [112] K. Akita, H. Sakamoto, and T. Sato, "Muscles of the pelvic outlet in the rhesus monkey (*Macaca mulatta*) with special reference to nerve supply," *Anat. Rec.*, vol. 241, pp. 273–283, 1995.
- [113] L. M. Pierce, M. Reyes, K. B. Thor, P. C. Dolber, R. E. Bremer, T. J. Kuehl, and K. W. Coates, "Immunohistochemical evidence for the interaction between levator ani and pudendal motor neurons in the coordination of pelvic floor and visceral activity in the squirrel monkey," *Am. J. Obstet. Gynecol.*, vol. 192, pp. 1506–1515, 2005.
- [114] A. Shahryarinejad and M. D. Vardy, "Comparison of Human to Macaque Uterosacral-Cardinal Ligament Complex and Its Relationship to Pelvic Organ Prolapse," *Toxicologic Pathology*, vol. 36. p. 101S–107S, 2008.
- [115] A. Sobiraj, "Ante partum vaginal prolapse in sheep--an unsolved problem," *Tierarztl. Prax.*, vol. 18, pp. 9–12, 1990.



- [116] J. L. Lowder, K. M. Debes, D. K. Moon, N. Howden, S. D. Abramowitch, and P. A. Moalli, "Biomechanical adaptations of the rat vagina and supportive tissues in pregnancy to accommodate delivery.," *Obstet. Gynecol.*, vol. 109, pp. 136–143, 2007.
- [117] Z. Liao and P. G. Smith, "Adaptive Plasticity of Vaginal Innervation in Term Pregnant Rats," *Reprod. Sci.*, vol. 18, no. 12, pp. 1237–1245, Dec. 2011.
- [118] A. Feola, M. Endo, and J. Deprest, "Biomechanics of the rat vagina during pregnancy and postpartum: A 3-dimensional ultrasound approach," *Int. Urogynecol. J. Pelvic Floor Dysfunct.*, vol. 25, pp. 915–920, 2014.
- [119] E. C. Samuelsson, A. Victor, G. Tibblin, and K. F. Svardsudd, "Signs of genital prolapse in a Swedish population of women 20 to 59 years of age and possible related factors," *Am. J. Obstet. Gynecol.*, vol. 180, pp. 299–305, 1999.
- [120] R. Prantil-Baun, W. C. de Groat, M. Miyazato, M. B. Chancellor, N. Yoshimura, and D. A. Vorp, "Ex vivo biomechanical, functional, and immunohistochemical alterations of adrenergic responses in the female urethra in a rat model of birth trauma.," *Am. J. Physiol. Renal Physiol.*, vol. 299, pp. F316–F324, 2010.
- [121] K. Jundt, I. Scheer, B. Schiessl, K. Karl, K. Friese, and U. M. Peschers, "Incontinence, bladder neck mobility, and sphincter ruptures in primiparous women.," *Eur. J. Med. Res.*, vol. 15, pp. 246–252, 2010.
- [122] S. L. Hendrix, A. Clark, I. Nygaard, A. Aragaki, V. Barnabei, and A. Mctiernan, "Pelvic organ prolapse in the Women ' s Health Initiative : Gravity and gravidity," pp. 1160–1166, 2002.
- [123] H. P. Dietz, A. Eldridge, M. Grace, and B. Clarke, "Does pregnancy affect pelvic organ mobility?," *Aust. New Zeal. J. Obstet. Gynaecol.*, vol. 44, pp. 517–520, 2004.
- [124] D. Barnett and D. H. Abbott, "Reproductive adaptations to a large-brained fetus open a vulnerability to anovulation similar to polycystic ovary syndrome," *American Journal of Human Biology*, vol. 15. pp. 296–319, 2003.
- [125] H. P. Dietz and A. B. Steensma, "Which women are most affected by delivery-related changes in pelvic organ mobility?," *Eur. J. Obstet. Gynecol. Reprod. Biol.*, vol. 111, pp. 15–18, 2003.
- [126] S. S. Oliphant, I. E. Nygaard, W. Zong, T. P. Canavan, and P. A. Moalli, "Maternal adaptations in preparation for parturition predict uncomplicated spontaneous delivery outcome," *American Journal of Obstetrics and Gynecology*, 2014.
- [127] D. A. Tulis, "Rat Carotid Artery Balloon Injury Model," vol. 139.

- [128] S. Q. Liu, L. Zhong, and J. Goldman, "Control of the shape of a thrombus-neointima-like structure by blood shear stress," *J. Biomech. Eng.*, vol. 124, pp. 30–36, 2002.
- [129] C. P. Regan, P. J. Adam, C. S. Madsen, and G. K. Owens, "Molecular mechanisms of decreased smooth muscle differentiation marker expression after vascular injury," *J. Clin. Invest.*, vol. 106, pp. 1139–1147, 2000.
- [130] M. Quinn, "Obstetric denervation-gynaecological reinnervation: Disruption of the inferior hypogastric plexus in childbirth as a source of gynaecological symptoms," *Med. Hypotheses*, vol. 63, pp. 390–393, 2004.
- [131] S. J. Snooks, M. Swash, M. M. Henry, and M. Setchell, "Risk factors in childbirth causing damage to the pelvic floor innervation," *Int. J. Colorectal Dis.*, vol. 1, pp. 20–24, 1986.
- [132] M. B. Siroky, "The aging bladder," *Rev. Urol.*, vol. 6 Suppl 1, pp. S3–S7, 2004.
- [133] G. Samsioe, "Urogenital aging--a hidden problem," *Am. J. Obstet. Gynecol.*, vol. 178, pp. S245–S249, 1998.
- [134] Y. Sekiguchi, Y. Utsugisawa, Y. Azekosi, M. Kinjo, M. Song, Y. Kubota, S. A. Kingsberg, and M. L. Krychman, "Laxity of the vaginal introitus after childbirth: Nonsurgical vaginal tissue restoration and improved sexual satisfaction with an office procedure of low-energy radiofrequency thermal therapy," in *Giornale Italiano di Ostetricia e Ginecologia*, 2013, vol. 35, pp. 328–334.
- [135] P. Takacs, M. Gualtieri, M. Nassiri, K. Candiotti, A. Fornoni, and C. A. Medina, "Caldesmon expression is decreased in women with anterior vaginal wall prolapse: A pilot study," *Int. Urogynecol. J. Pelvic Floor Dysfunct.*, vol. 20, pp. 985–990, 2009.
- [136] B. Chen and J. Yeh, "Alterations in connective tissue metabolism in stress incontinence and prolapse," *Journal of Urology*, vol. 186, pp. 1768–1772, 2011.
- [137] D. Bia, R. Armentano, D. Craiem, J. Grignola, F. Ginés, A. Simon, and J. Levenson, "Smooth muscle role on pulmonary arterial function during acute pulmonary hypertension in sheep," *Acta Physiol. Scand.*, vol. 181, pp. 359–366, 2004.
- [138] A. J. Bank, D. R. Kaiser, S. Rajala, and A. Cheng, "In vivo human brachial artery elastic mechanics: effects of smooth muscle relaxation," *Circulation*, vol. 100, pp. 41–47, 1999.
- [139] A. J. Bank, R. F. Wilson, S. H. Kubo, J. E. Holte, T. J. Dresing, and H. Wang, "Direct effects of smooth muscle relaxation and contraction on in vivo human brachial artery elastic properties," *Circ. Res.*, vol. 77, pp. 1008–1016, 1995.

- [140] J. P. Vande Geest, E. S. Di Martino, A. Bohra, M. S. Makaroun, and D. A. Vorp, "A biomechanics-based rupture potential index for abdominal aortic aneurysm risk assessment: Demonstrative application," in *Annals of the New York Academy of Sciences*, 2006, vol. 1085, pp. 11–21.
- [141] D. K. Moon, S. D. Abramowitch, and S. L. Y. Woo, "The development and validation of a charge-coupled device laser reflectance system to measure the complex cross-sectional shape and area of soft tissues," *J. Biomech.*, vol. 39, pp. 3071–3075, 2006.
- [142] J. T. Herlihy and R. A. Murphy, "Length-tension relationship of smooth muscle of the hog carotid artery," *Circ. Res.*, vol. 33, pp. 275–283, 1973.
- [143] D. Tremblay, R. Cartier, R. Mongrain, and R. L. Leask, "Regional dependency of the vascular smooth muscle cell contribution to the mechanical properties of the pig ascending aortic tissue," *J. Biomech.*, vol. 43, pp. 2448–2451, 2010.
- [144] M. R. Hill, X. Duan, G. a. Gibson, S. Watkins, and A. M. Robertson, "A theoretical and non-destructive experimental approach for direct inclusion of measured collagen orientation and recruitment into mechanical models of the artery wall," *J. Biomech.*, vol. 45, no. 5, pp. 762–771, Mar. 2012.
- [145] M. S. Sacks, "Biaxial mechanical evaluation of planar biological materials," *Journal of Elasticity*, vol. 61, pp. 199–246, 2000.
- [146] K. L. Billiar and M. S. Sacks, "Biaxial mechanical properties of the natural and glutaraldehyde treated aortic valve cusp--Part I: Experimental results," *J. Biomech. Eng.*, vol. 122, pp. 23–30, 2000.
- [147] K. Takamizawa, K. Hayashi, and T. Matsuda, "Isometric biaxial tension of smooth muscle in isolated cylindrical segments of rabbit arteries," *Am. J. Physiol.*, vol. 263, pp. H30–H34, 1992.
- [148] N. Choudhury, O. Bouchot, L. Rouleau, D. Tremblay, R. Cartier, J. Butany, R. Mongrain, and R. L. Leask, "Local mechanical and structural properties of healthy and diseased human ascending aorta tissue," *Cardiovasc. Pathol.*, vol. 18, pp. 83–91, 2009.
- [149] a Rachev and K. Hayashi, "Theoretical study of the effects of vascular smooth muscle contraction on strain and stress distributions in arteries," *Ann. Biomed. Eng.*, vol. 27, pp. 459–68, 1999.
- [150] J. Zhao, D. Liao, J. Yang, and H. Gregersen, "Biomechanical remodelling of obstructed guinea pig jejunum," *J. Biomech.*, vol. 43, pp. 1322–1329, 2010.
- [151] P. J. Zeller and T. C. Skalak, "Contribution of individual structural components in determining the zero stress state in small arteries," *J. Vasc. Res.*, vol. 35, pp. 8 – 17, 1998

- [152] P. B. Dobrin and T. R. Canfield, "Series elastic and contractile elements in vascular smooth muscle.," *Circ. Res.*, vol. 33, pp. 454–464, 1973.
- [153] C. E. Skala, K. Renezedder, S. Albrich, A. Puhl, R. M. Laterza, G. Naumann, and H. Koelbl, "Mesh-complications following prolapse surgery: management and outcome.," *Eur. J. Obstet. Gynecol. Reprod. Biol.*, 2011.
- [154] R. U. Margulies, C. Lewicky-Gaupp, D. E. Fenner, E. J. McGuire, J. Q. Clemens, and J. O. L. DeLancey, "Complications requiring reoperation following vaginal mesh kit procedures for prolapse," *Am. J. Obstet. Gynecol.*, vol. 199, 2008.
- [155] R. Liang, S. Abramowitch, K. Knight, S. Palcsey, A. Nolfi, A. Feola, S. Stein, and P. A. Moalli, "Vaginal degeneration following implantation of synthetic mesh with increased stiffness," *BJOG An Int. J. Obstet. Gynaecol.*, vol. 120, pp. 233–243, 2013.
- [156] P. Maquet, "Wolff's Law," in *Wolff's Law and Connective Tissue Regulation*, 1992, pp. 31–33.
- [157] H. M. Frost, "Wolff's Law and bone's structural adaptations to mechanical usage: an overview for clinicians.," *Angle Orthodontist*, vol. 64. pp. 175–188, 1994.
- [158] I. Nygaard, L. Brubaker, H. M. Zyczynski, G. Cundiff, H. Richter, M. Gantz, P. Fine, S. Menefee, B. Ridgeway, A. Visco, L. K. Warren, M. Zhang, and S. Meikle, "Long-term outcomes following abdominal sacrocolpopexy for pelvic organ prolapse," *JAMA*, vol. 309, pp. 2016–2024, 2013.
- [159] A. J. Feola, "IMPACT OF VAGINAL SYNTHETIC PROLAPSE MESHES ON THE MECHANICS," 2011.
- [160] X. Jia, C. Glazener, G. Mowatt, G. MacLennan, C. Bain, C. Fraser, and J. Burr, "Efficacy and safety of using mesh or grafts in surgery for anterior and/or posterior vaginal wall prolapse: Systematic review and meta-analysis," *BJOG: An International Journal of Obstetrics and Gynaecology*, vol. 115. pp. 1350–1361, 2008.
- [161] C. M. Maher, B. Feiner, K. Baessler, and C. M. A. Glazener, "Surgical management of pelvic organ prolapse in women: The updated summary version Cochrane review," in *International Urogynecology Journal and Pelvic Floor Dysfunction*, 2011, vol. 22, pp. 1445–1457.
- [162] D. Altman, T. Väyrynen, M. E. Engh, S. Axelsen, and C. Falconer, "Anterior colporrhaphy versus transvaginal mesh for pelvic-organ prolapse," *International Braz J Urol*, vol. 37. p. 675, 2011.

- [163] A. K. Blakney, M. D. Swartzlander, and S. J. Bryant, "The effects of substrate stiffness on the in vitro activation of macrophages and in vivo host response to poly(ethylene glycol)-based hydrogels," *J. Biomed. Mater. Res. A*, vol. 100, pp. 1375–86, 2012.
- [164] N. R. Patel, M. Bole, C. Chen, C. C. Hardin, A. T. Kho, J. Mih, L. Deng, J. Butler, D. Tschumperlin, J. J. Fredberg, R. Krishnan, and H. Koziel, "Cell Elasticity Determines Macrophage Function," *PLoS One*, vol. 7, 2012.
- [165] K. A. Beningo and Y. Wang, "Fc-receptor-mediated phagocytosis is regulated by mechanical properties of the target," *J. Cell Sci.*, vol. 115, pp. 849–856, 2002.
- [166] S. Féréol, R. Fodil, B. Labat, S. Galiacy, V. M. Laurent, B. Louis, D. Isabey, and E. Planus, "Sensitivity of alveolar macrophages to substrate mechanical and adhesive properties," *Cell Motil. Cytoskeleton*, vol. 63, pp. 321–340, 2006.
- [167] R. L. Heise, A. Parekh, E. M. Joyce, M. B. Chancellor, and M. S. Sacks, "Strain history and TGF- $\beta$ 1 induce urinary bladder wall smooth muscle remodeling and elastogenesis," *Biomech. Model. Mechanobiol.*, vol. 11, no. 1–2, pp. 131–145, Jan. 2012.
- [168] Z. S. Jackson, D. Dajnowiec, A. I. Gotlieb, and B. L. Langille, "Partial off-loading of longitudinal tension induces arterial tortuosity," *Arterioscler. Thromb. Vasc. Biol.*, vol. 25, pp. 957–962, 2005.
- [169] I. M. Bayer, S. L. Adamson, and B. L. Langille, "Atrophic remodeling of the artery-cuffed artery," *Arterioscler. Thromb. Vasc. Biol.*, vol. 19, pp. 1499–1505, 1999.
- [170] L. Deng, N. J. Fairbank, D. J. Cole, J. J. Fredberg, and G. N. Maksym, "Airway smooth muscle tone modulates mechanically induced cytoskeletal stiffening and remodeling," *J. Appl. Physiol.*, vol. 99, pp. 634–641, 2005.
- [171] L. H. Timmins, M. W. Miller, F. J. Clubb, and J. E. Moore, "Increased artery wall stress post-stenting leads to greater intimal thickening," *Lab. Invest.*, vol. 91, pp. 955–967, 2011.
- [172] S. J. Gunst, D. D. Tang, and A. Opazo Saez, "Cytoskeletal remodeling of the airway smooth muscle cell: A mechanism for adaptation to mechanical forces in the lung," *Respiratory Physiology and Neurobiology*, vol. 137, pp. 151–168, 2003.
- [173] N. A. Flavahan, S. R. Bailey, W. A. Flavahan, S. Mitra, and S. Flavahan, "Imaging remodeling of the actin cytoskeleton in vascular smooth muscle cells after mechanosensitive arteriolar constriction," *Am. J. Physiol. Heart Circ. Physiol.*, vol. 288, pp. H660–H669, 2005.

- [174] H. A. Inal, P. B. Kaplan, U. Usta, E. Ta??tekin, A. Aybatli, and B. Tokuc, "Neuromuscular morphometry of the vaginal wall in women with anterior vaginal wall prolapse," *Neurourol. Urodyn.*, vol. 29, no. 3, pp. 458–463, 2010.
- [175] A. Stenzl, "Neuroanatomy of the human female lower urogenital tract.," *International official journal of the Brazilian Society of Urology*, vol. 30, pp. 352–353, 2004.
- [176] M. Basha, E. F. Labelle, G. M. Northington, T. Wang, A. J. Wein, and S. Chacko, "Functional significance of muscarinic receptor expression within the proximal and distal rat vagina," *Am. J. Physiol. Regul. Integr. Comp. Physiol.*, vol. 297, pp. R1486–R1493, 2009.
- [177] A. Giraldi, P. Alm, V. Werkström, L. Myllymäki, G. Wagner, and K. E. Andersson, "Morphological and functional characterization of a rat vaginal smooth muscle sphincter," *Int. J. Impot. Res.*, vol. 14, pp. 271–282, 2002.
- [178] L. C. Skoczylas, Z. Jallah, Y. Sugino, S. E. Stein, A. Feola, N. Yoshimura, and P. Moalli, "Regional differences in rat vaginal smooth muscle contractility and morphology.," in *Reproductive sciences (Thousand Oaks, Calif.)*, 2013, vol. 20, no. 4, pp. 382–90.
- [179] G. M. Northington, M. Basha, L. a. Arya, a. J. Wein, and S. Chacko, "Contractile Response of Human Anterior Vaginal Muscularis in Women With and Without Pelvic Organ Prolapse," *Reprod. Sci.*, vol. 18, no. 3, pp. 296–303, Mar. 2011.
- [180] I. W. Mills, J. E. Greenland, G. McMurray, R. McCoy, K. M. Ho, J. G. Noble, and A. F. Brading, "Studies of the pathophysiology of idiopathic detrusor instability: the physiological properties of the detrusor smooth muscle and its pattern of innervation.," *J. Urol.*, vol. 163, pp. 646–651, 2000.
- [181] C. Reisenauer, T. Shiozawa, M. Oppitz, C. Busch, A. Kirschniak, T. Fehm, and U. Drews, "The role of smooth muscle in the pathogenesis of pelvic organ prolapse — an immunohistochemical and morphometric analysis of the cervical third of the uterosacral ligament," pp. 383–389, 2008.
- [182] T. Ramalingam, N. T. Durlu-kandilci, and A. F. Brading, "A Comparison of the Contractile Properties of Smooth Muscle from Pig Urethra and Internal Anal Sphincter," vol. 1331, no. November 2009, pp. 1326–1331, 2010.
- [183] Z. S. Jackson, A. I. Gotlieb, and B. L. Langille, "Wall tissue remodeling regulates longitudinal tension in arteries," *Circ. Res.*, vol. 90, pp. 918–925, 2002.
- [184] A. N. A. M. Herrera, R. F. O. R. T. H. E. D. E. G. R. E. E. Of, and D. O. F. Philosophy, "Airways Smooth Muscle Plasticity Correlation of Structure and Function," no. September, 2004.
- [185] F. Grinnell, "Fibroblast mechanics in three-dimensional collagen matrices," *J. Bodyw. Mov.*, vol. 12, pp. 191–193, 2008.

- [186] F. Grinnell, "Fibroblast-collagen-matrix contraction: growth-factor signalling and mechanical loading," in *Trends in Cell Biology*, 2000, vol. 10, pp. 362–365.
- [187] F. Grinnell, "Fibroblast biology in three-dimensional collagen matrices," *Trends in Cell Biology*, vol. 13, pp. 264–269, 2003.
- [188] S. P. A. Dvm, M. Lavagnino, M. E. Dvm, O. C. Ms, K. G. Ms, and M. A. Shender, "Loss of Homeostatic Strain Alters Mechanostat " " Set Point " " of Tendon Cells In Vitro," pp. 1583–1591, 2008.
- [189] D. G. Ezra, J. S. Ellis, M. Beaconsfield, R. Collin, and M. Bailly, "Changes in fibroblast mechanostat set point and mechanosensitivity: An adaptive response to mechanical stress in floppy eyelid syndrome," *Investig. Ophthalmol. Vis. Sci.*, vol. 51, pp. 3853–3863, 2010.
- [190] S. L. Bass, P. Eser, and R. Daly, "The effect of exercise and nutrition on the mechanostat," *Journal of Musculoskeletal Neuronal Interactions*, vol. 5, pp. 239–254, 2005.
- [191] W. Zhang and S. J. Gunst, "Dynamic association between alpha-actinin and beta-integrin regulates contraction of canine tracheal smooth muscle," *J. Physiol.*, vol. 572, pp. 659–676, 2006.
- [192] G. A. Holzapfel, G. Sommer, C. T. Gasser, and P. Regitnig, "Determination of layer-specific mechanical properties of human coronary arteries with nonatherosclerotic intimal thickening and related constitutive modeling," *Am. J. Physiol. Heart Circ. Physiol.*, vol. 289, pp. H2048–H2058, 2005.
- [193] G. Yang, H. Im, and J. H. Wang, "Repetitive mechanical stretching modulates IL-1  $\beta$  induced COX-2 , MMP-1 expression , and PGE 2 production in human patellar tendon fibroblasts," vol. 363, pp. 166–172, 2005.
- [194] W. Zong, Z. C. Jallah, S. E. Stein, S. D. Abramowitch, and P. A. Moalli, "Repetitive Mechanical Stretch Increases Extracellular Collagenase Activity in Vaginal Fibroblasts," *Female Pelvic Medicine & Reconstructive Surgery*, vol. 16, pp. 257–262, 2010.
- [195] M. Alperin, K. Debes, S. Abramowitch, L. Meyn, and P. A. Moalli, "LOXL1 deficiency negatively impacts the biomechanical properties of the mouse vagina and supportive tissues," *Int. Urogynecol. J. Pelvic Floor Dysfunct.*, vol. 19, pp. 977–986, 2008.
- [196] P. A. Moalli, K. M. Debes, L. A. Meyn, N. S. Howden, and S. D. Abramowitch, "Hormones restore biomechanical properties of the vagina and supportive tissues after surgical menopause in young rats," *Am. J. Obstet. Gynecol.*, vol. 199, 2008.

- [197] C. Rodríguez, J. Martínez-González, B. Raposo, J. F. Alcudia, A. Guadall, and L. Badimon, "Regulation of lysyl oxidase in vascular cells: Lysyl oxidase as a new player in cardiovascular diseases," *Cardiovascular Research*, vol. 79, pp. 7–13, 2008.
- [198] B. T. Haylen, R. M. Freeman, J. Lee, S. E. Swift, M. Cosson, J. Deprest, P. L. Dwyer, B. Fatton, E. Kocjancic, C. Maher, E. Petri, D. E. Rizk, G. N. Schaer, and R. Webb, "An International Urogynecological Association (IUGA)/International Continence Society (ICS) joint terminology and classification of the complications related to native tissue female pelvic floor surgery," *International Urogynecology Journal and Pelvic Floor Dysfunction*, vol. 23, pp. 515–526, 2012.
- [199] K. M. Luber, S. Boero, and J. Y. Choe, "The demographics of pelvic floor disorders: Current observations and future projections," in *American Journal of Obstetrics and Gynecology*, 2001, vol. 184, pp. 1496–1503.
- [200] P. J. Woodman, S. E. Swift, A. L. O'Boyle, M. T. Valley, D. R. Bland, M. A. Kahn, and J. I. Schaffer, "Prevalence of severe pelvic organ prolapse in relation to job description and socioeconomic status: A multicenter cross-sectional study," *Int. Urogynecol. J. Pelvic Floor Dysfunct.*, vol. 17, pp. 340–345, 2006.
- [201] K. E. Remsberg, R. E. McKeown, K. F. McFarland, and L. S. Irwin, "Diabetes in pregnancy and cesarean delivery," *Diabetes Care*, vol. 22, pp. 1561–1567, 1999.
- [202] K. Coral, J. Madhavan, R. Pukhraj, and N. Angayarkanni, "High Glucose Induced Differential Expression of Lysyl Oxidase and Its Isoform in ARPE-19 Cells," *Current Eye Research*, pp. 1–10, 2012.
- [203] T. Roth, F. Podestá, M. A. Stepp, D. Boeri, and M. Lorenzi, "Integrin overexpression induced by high glucose and by human diabetes: potential pathway to cell dysfunction in diabetic microangiopathy," *Proc. Natl. Acad. Sci. U. S. A.*, vol. 90, pp. 9640–9644, 1993.
- [204] S. Roy, E. Cagliero, and M. Lorenzi, "Fibronectin overexpression in retinal microvessels of patients with diabetes," *Investig. Ophthalmol. Vis. Sci.*, vol. 37, pp. 258–266, 1996.
- [205] J. Behmoaras, S. Slove, S. Seve, R. Vranckx, P. Sommer, and M.-P. Jacob, "Differential expression of lysyl oxidases LOXL1 and LOX during growth and aging suggests specific roles in elastin and collagen fiber remodeling in rat aorta," *Rejuvenation Res.*, vol. 11, no. 5, pp. 883–889, Oct. 2008.
- [206] Y. Barbalat and H. S. G. R. Tunuguntla, "Surgery for pelvic organ prolapse: A historical perspective," *Current Urology Reports*, vol. 13, pp. 256–261, 2012.



- [207] J. N. Nguyen, S. M. Jakus-Waldman, A. J. Walter, T. White, and S. A. Menefee, "Perioperative Complications and Reoperations After Incontinence and Prolapse Surgeries Using Prosthetic Implants," *Obstetrics & Gynecology*, vol. 119, pp. 539–546, 2012.
- [208] U. Klinge, J. Conze, W. Limberg, C. Brücker, A. P. Ottinger, and V. Schumpelick, "Pathophysiology of the abdominal wall," *Chirurg.*, vol. 67, pp. 229–233, 1996.
- [209] U. Klinge, B. Klosterhalfen, J. Conze, W. Limberg, B. Obolenski, A. P. Ottinger, and V. Schumpelick, "Modified mesh for hernia repair that is adapted to the physiology of the abdominal wall," *Eur. J. Surg.*, vol. 164, pp. 951–960, 1998.
- [210] I. H. Braekken, M. Majida, M. Ellström Engh, I. M. Holme, and K. Bø, "Pelvic floor function is independently associated with pelvic organ prolapse," *BJOG*, vol. 116, pp. 1706–1714, 2009.
- [211] J. A. Ashton-Miller and J. O. L. Delancey, "On the biomechanics of vaginal birth and common sequelae," *Annu. Rev. Biomed. Eng.*, vol. 11, pp. 163–176, 2009.
- [212] P. A. Moalli, N. S. Howden, J. L. Lowder, J. Navarro, K. M. Debes, S. D. Abramowitch, and S. L. Woo, "A rat model to study the structural properties of the vagina and its supportive tissues," *Am J Obs. Gynecol*, vol. 192, pp. 80–88, 2005.
- [213] M. Alperin, A. Feola, R. Duerr, P. Moalli, and S. Abramowitch, "Pregnancy-and delivery-induced biomechanical changes in rat vagina persist postpartum," *Int. Urogynecol. J. Pelvic Floor Dysfunct.*, vol. 21, pp. 1169–1174, 2010.
- [214] M. J. Buehler, "Nanomechanics of collagen fibrils under varying cross-link densities: Atomistic and continuum studies," *J. Mech. Behav. Biomed. Mater.*, vol. 1, no. 1, pp. 59–67, Jan. 2008.
- [215] P. G. Drewes, H. Yanagisawa, B. Starcher, I. Hornstra, K. Csiszar, S. I. Marinis, P. Keller, and R. A. Word, "Pelvic organ prolapse in fibulin-5 knockout mice: pregnancy-induced changes in elastic fiber homeostasis in mouse vagina," *Am. J. Pathol.*, vol. 170, no. 2, pp. 578–589, Feb. 2007.
- [216] H. Fushida-Takemura, M. Fukuda, N. Maekawa, M. Chanoki, H. Kobayashi, N. Yashiro, M. Ishii, T. Hamada, S. Otani, and A. Ooshima, "Detection of lysyl oxidase gene expression in rat skin during wound healing," *Arch. Dermatol. Res.*, vol. 288, pp. 7–10, 1996.
- [217] Y. K. I. Lau, A. M. Gobin, and J. L. West, "Overexpression of lysyl oxidase to increase matrix crosslinking and improve tissue strength in dermal wound healing," *Ann. Biomed. Eng.*, vol. 34, pp. 1239–1246, 2006.